ISSN 2960-9534
DOI https://doi.org/10.36073/2960-9534

JOURNAL OF THE GEORGIAN CERAMISTS' ASSOCIATION

INTERNATIONAL JOURNAL OF CERAMICS, COMPOSITES, SCIENCE AND ADVANCED TECHNOLOGIES

Scientific, technical and industrial illustrated, registered, referral magazine

Vol. 26. 1(51).2024

Guidelines for submitting an article to the journal

- It is necessary to submit, one hardcopy of the article, as well as an electronic versionin English language, to editorial office.
- The length of the article is not limited to pages (including tables and images with appropriate numbering). Interval 1.5. Program-Sylfaen. Font size 12, the article must be accompanied by an abstract in Georgian of no more than 300 words.
- The article should use International System of Units (SI), as well as those units that are equated to this system.
- Mathematical and chemical formulas should be clearly indicated so that the difference between Capital (upper case) and Nuskhuri (Georgian script AD 800-1100) (lower case) letters, quality coefficient and co-multiplier can be easily discerned. All letter designations in the text of the article and formula are subject to decoding. Different concepts can not be represented by the same symbol.
- The literary source should be indicated at the end of the article as follows: for a book - indicating the author, title, title of publication, place of publication, year of publication and total number of pages;

  for a journal - indicating the author of the article, the name of the journal, year of publication, volume, number, beginning and end pages of the article;

  Foreign surnames, the title of the book and journal must be in the original language without abbreviation, it is not allowed to refer to unpublished work.
- When using a copyright certificate, it is necessary to refer to the bulletin of the invention (where the formula of the invention is published) indicating the number and year of publication.
- Pictures and drawings should be presented only in text in one copy in computerized form, they should not be overloaded with details and inscriptions. The position must be indicated by numbers and decoded by inscriptions under the picture;
- The article must be signed by one of the authors. It is necessary to indicate place of work, position, scientific degree, and telephone number.
- The publishing fee for foreign authors not residing in Georgia makes up 100 euros. It's free for authors residing in Georgia.

CONTENTS

UDC 543.42

STUDY OF TOXIC IMPURITIES IN WINES PRODUCED BY SMALL FAMILY WINERIES

N. Amashukeli, A. Gvanceladze, N. Rachvelishvili

Department of Chemical and Biological Technologies, Technical University of Georgia, Georgia, 0175, Tbilisi, Kostava 69

E-mail: natamashukeli@gmail.com

Resume: Purpose: The culture of wine production and consumption in Georgia has changed dramatically in recent years. Many small, family-type enterprises appeared. This process was also supported by state programs, such as "Produce in Georgia", within the framework of which many small enterprises were funded. The products of small wineries are increasing day by day in wine shops. quality control and certification, although toxicological testing of wines produced by small wineries is not universal. Heavy metals, which may be contained in wines, have a long-term harmful effect on human health. The research aims to study the wines produced by small family-type wineries on the content of heavy metals using the chromatographic method, to develop recommendations for parties responsible for wine quality. Wine is very important for our country. Georgia has an ancient wine culture. From ancient times, Georgians observed the beneficial or harmful effects of wine on human health. Wine contains magnesium, copper, zinc, iron, potassium elements necessary for the body. Due to various reasons, wine may contain harmful, toxic substances, therefore it is important for human health to study the content of wine in order to protect the limit of toxic impurities.

Method: Chromatography was chosen as the research method. Chromatography is used in wine production to determine metals in finished products, semi-products of their synthesis, and raw materials. Metals belong to the number of toxic impurities, so it is very important to know the metal content, which should not exceed the permissible limit.

Results: during the conducted studies, it was established that chromatography determines the content of metals in wine with high accuracy.

Conclusion: the obtained results show that the amount of metals contained in the wines of factory production and family wineries presented on the Georgian market does not exceed the permissible norm.

Based on the obtained data, we can conclude that the wines of family cellars are not inferior in quality to the wines of factory production.

Key words: wine from small cellars, metal replacement, chromatography.

1. INTRODUCTION

The culture of wine production and consumption in Georgia has undergone significant changes in recent years, driven by the emergence of numerous small, family-type wineries. This transformation has been supported by state initiatives,

such as the "Produce in Georgia" program, which has provided funding to many small enterprises. Consequently, the presence of products from these small wineries in wine shops is increasing steadily. Despite this growth, quality control and certification remain critical, particularly concerning the toxicological testing of wines. Heavy metals in wine can have long-term detrimental effects on human health. This research aims to analyze the content of heavy metals in wines produced by small family-type wineries using chromatographic methods and to develop recommendations for entities responsible for wine quality. Understanding the metal content in wine is crucial for ensuring that toxic impurities do not exceed permissible limits, thus safeguarding public health.

2. MAIN PART

Literature review

There are many physico-chemical methods of toxic impurities research, for example 1. optical methods, namely: photocolorimetry and spectral analysis. 2. Electrical methods, for example: potentiometry, conductometry and others. 3. Chromatographic analysis methods and others

Chromatographic research method was chosen because it is a cheap, fast method that determines the content with a small error.

Air chromatography for both gasses, liquids and solids An effective method for the separation and analysis of complex mixtures Thanks to the simplicity and high efficiency of the analysis It is one of the most common methods.

Chromatography was first developed in 1903. Russian scientist - Biochemist M. Attrition divided the vegetation separated from the leaves of the plants A complex mixture of pigments, passing the solution of this mixture through a vertical glass in a column filled with calcium carbonate powder. All The components were arranged in the column in the form of colored zones, so the term "chromatography" means "color recording". directly, air chromato- The graphical method was developed in 1952 by the English scientist Martin and by James.

Starting from 1955, the industry of different countries started releasing tools for chromatography (chromatographs) and air chromatography is firmly included in the practice of analytical works.

The speed of development of the method is explained by the following reason:

Relative simplicity of hardware design and process possibility of automation; Wide range of application, 400-500^{0}C- the ability to analyze boiling substances up to; method high sensitivity, ability to analyze traces of impurities up to 10-7%; Speed of analysis.

Application of chromatography in industry became a qualitatively new stage of substances, their synthesis and intermediate in determining the composition of products. The chromatographic method of analysis is based on a sorbent layer During movement of a mixture of substances, sorption of these substances Due to the different ability to separate the test mixture into components. This time The components of the mixture are moved under the influence of the flow of the mobile phase in the sorbent layer (stationary phase) at different speeds. The mobile phase represents gas or liquid, stationary phase - liquid or solid body.

Depending on the aggregate state of mobile and stationary phases Four main types of chromatography can be distinguished Chromatography classification according to the aggregate state of stationary and mobile phases:

Liquid-adsorptive, gas-adsorptive, liquid-liquid, gas-liquid.

The main part: two types of factory production and two types of family small Mern wine were selected, which were presented on the market, a chromatographic study was conducted on metals: copper, iron, zinc, lead. In gas-liquid chromatography, substances are separated by separation As a result of the distribution (dissolution) of substances in the liquid stationary phase and mobile between the gas phase. A necessary condition for division is that the components are different Solubility in liquid stationary phase. Separation of components is carried out analytically in instruments (chromatographs). Liquid stationary phase in air chromatographs applied in the form of a powder on the surface of a solid carrier,

which is placed in chromatographic columns. of the research mixture containing different components

A certain volume is introduced into the mobile phase (gas) flow with a dosator. air The sample introduced by the carrier stream is transferred to the chromatographic column, which is placed in a thermostat, at a certain temperature for maintenance. As a result of the interaction with the stationary phase in the column, the components of the mixture slow down their movement and acquire different speeds. The difference in the movement speeds of the components in the column allows the formation of zones of binary mixtures (component + mobile phase), which are divided by the zone of the pure mobile phase.

As the components move further through the column, the clear mobile phase zone between them increases until the components elute from the column with the flow of the carrier gas or mobile phase. After leaving the column, the components in the same order will enter the detector - a device that converts the change in the composition of the mobile phase into an outgoing electrical signal. This signal is registered in the form of a self-recording graph, which is called a chromatogram. The horizontal axis is the time axis, the vertical axis is the concentration of the substance in the air-carrier flow. Usually, it is expressed in millivolts of the self-recording scale.

A chromatogram consists of a number of peaks located on the main line, each peak corresponding to one component in the case of complete separation, therefore, the number of peaks is usually equal to the number of components in the mixture.

Two main tasks can be solved by the air-chromatographic method: qualitative analysis of the separated substance and determination of the amount of this substance.

The main characteristic of the analyte is the retention time, i.e. The time from the moment of sample introduction to the appearance of the peak maximum. At a given temperature and a given speed, on a certain stationary phase, this value is constant and characterizes the interaction of the component with the stationary phase.

The holding time multiplied by the volume velocity of the air carrier is called the holding volume. Retention times and retained volume

values can be used to identify peaks on a chromatogram.

The basis of all quantitative determinations in air chromatography is the proportionality of the area under the peak and the content of its corresponding components in the mixture. Chromatographs Tsvet 800, Gals-311, Crystal-xoox and others are used in wine production. We used Tsvet 800.

Chromatograph consists of the following nodes: a chromatographic column, where the mixture is separated. A detector, a device that characterizes the composition of the gas stream. A recording device and an auxiliary device for maintaining a certain pressure, temperature and flow rate of the air-carrier. All the main nodes of the chromatograph are interconnected, so the instrument can work well

Under the conditions of correct operation of each node. It is usually used as an air carrier (mobile phase). inert gasses (helium, nitrogen) or hydrogen. We used helium.

The gas carrier enters the air chromatographic system from the gas cylinder through the flow regulator, where it is under a pressure of up to 15 MPa.

The flow rate of the air carrier was regulated by special valves, which ensure the constancy of speed during the analysis process. air flow Velocity measurement produces air gauges, rheometers and through rotameters. A typical volumetric flow rate is 30-60 cm3/min.

10 ml of sample was introduced into the column. The temperature of the evaporator should be high enough to ensure rapid evaporation of the substance and to avoid washout of the sample, which impairs the separation of components. To achieve rapid evaporation, we kept the evaporator temperature 50-1000C higher than the column temperature. Some substances cannot withstand the high temperature of the evaporator and at this time undergo decomposition or isomerization, followed by the appearance of false peaks on the chromatogram. The selection of stationary liquid phase is especially important in the development of the air chromatography method, since it determines the possibility of separation of analytes. The phase selection depends on the composition of the mixture. In order to achieve separation, the liquid phase must be similar in nature to the components of the mixture. For example, hydrocarbons are better partitioned to the hydrocarbon liquid phase and eluted from it in an order corresponding to increasing boiling temperatures. For the separation of compounds containing different functional groups, it is better to use phases that also contain some functional groups.

A solid carrier is usually necessary for a porous liquid phase to absorb the quantity. During this time, the surface must remain dry with micars and move freely with the air carrier

in the column. No carrier

It should be highly brittle so that it does not crumble when filling the column.

of solid carriers mostly used in air chromatography The raw material is diatomite (diatomite or kieselgur land). Diatomite Consists of diatomaceous microscopic unicellular algae from armors, which are mainly represented by chemical composition Silicon oxide is a minor oxide of various metals with impurities.

There are different brands of solid carriers that differ from each other in the way of preparation and quality of cleaning.

To lower the adsorption properties of carriers (deactivation), they are washed with mineral acids and the surface is treated with chlorosilanes. We used solid carrier fractions with a particle size of 0.20-0.25 mm.

The column can be made straight, curved (U-shaped column) or Spiral tube, copper, glass or stainless steel. Columns made of stainless steel are most often used. which The longer the column length, the better the division. conventional analytical columns Length varies from 1 to 3 meters, inner diameter from 2 to 4 mm. The chromatographic column is filled with a column consisting of a stationary from a solid carrier coated with a liquid phase. number of piles (weight), which is spent to fill a column of 1 m length and 3 mm inner diameter It is 2-2.5 g. To check the separating ability of the prepared column, it is measured efficiency. Column efficiency n is characterized by the number of theoretical plates (t,p) and calculate with the formula:

$$n = 5{,}545\left(\frac{Dx}{a_{\frac{1}{2}}}\right)^2$$

where: dx is the distance from the air peak maximum to the substance peak to the maximum; a1/2 – the width of the substance peak at half its height.

Column efficiency report:

The efficiency of the prepared columns is 800-1000 t.h. column length 1 meter. Through the thermostat, the temperature of the column is maintained fairly high, so that the analysis time is small, but at the same time, quite low, to ensure the required separation. boiling temperature A mixture of components with very different sizes (for example, essential oils) during chromatography, high-boiling components come out from the column very slowly. Allowing column temperature to rise during analysis Allows us to speed up the passage of components in the column. In such a case, division They are first held at a lower temperature, and at low boiling point As the components come out, the temperature gradually increases. Such a programmed increase in temperature allows not only To reduce the analysis time, but also to improve the separation of components.

The detector registers the presence of each component and allows its quantity to be measured in the air-carrier stream, which exits the chromatographic column. detector preferred Features include high sensitivity to analyte compounds, Universality and low sensitivity to flow rate and to temperature changes.

Detection is based on a number of properties of the substance. Currently Most of the detectors used are analytical based substance vapor and mobile phase (helium or hydrogen) on the difference in thermal conductivity, or during ionization of the analyte different electrical conductivity.

Quantitative analysis is performed on the constructed chromatograms through processing. It is assumed that the area of each peak on the chromatogram is proportional to the concentration of the component.

Peak area can be determined by various means. peak To account for the area S, it will be seen as a triangle whose area is easily determined by multiplying the peak height h by half the width a1/2 S = h a1/2

This method is the fastest and easiest. The height of the peaks which Corresponds to the main components of the analysis mixture, should be composed At least 2/3 of the self-recording tape, and the width should not be half the height be less than 5 mm.

We used automated processing of chromatograms. For this purpose, a special integrating device, type *И*-05 digital integrator, was used. Higher accuracy of quantitative results is achieved by the calibrator

Using the coefficients, since the area of the peaks of the components It is not directly proportional to the percentage content, thus it is Depending on the structure of the component, and sometimes significantly varies in size. The mass share of each component C1 (in %) is calculated by the formula:

$$C=\frac{sk100}{\sum_1^n sk}$$

where: S – is the peak area of the determining component; K – to be determined relative calibrating coefficient of the component; ∑SK – sum, peak area multiplied by the corresponding calibration coefficient.

Calibration coefficients are defined by the same chromatography In the conditions in which the analysis product, on specially prepared mixtures.

In practice, relative calibration coefficients Ki, recalculated to the standard compound (usually this analyte is the substance in the mixture).

$$K_i=\frac{m_i s_{st}}{m_{st} s_i}$$

where: mi - the mass of the research component, mst - the mass of the standard compound; Sst – peak area of the standard compound; Si – detectable peak area.

A calibration factor of one relative to the standard compound They are accepted as equals. Analysis of a mixture of structurally similar components Calibration coefficients are also taken as equal to one.

The internal normalization method is the simplest and most convenient, Because it does not require accurate dosing of the sample and repeated determination while observing the same conditions of the analysis. On the input of an internal standard, a precisely known quantity. The internal standard method is usually used to account for individual components in a multicomponent mixture, or when not all components of the mixture elute from the column (ie, the mixture contains a heavy non-eluting residue). The mass share of each component of the analytical product C1 (in %) is calculated by the method of the internal standard with the formula Type equation here:

$$K_i=\frac{m_i s_{st}}{m_{st} s_i}$$

where: mst – mass of internal standard; Si – peak area of the research component; Ki – relative calibration coefficient; mi – weighted mass of substance; Sst – internal standard peak area.

The air chromatographic method allows us to conduct research Identification of separable components of mixtures, i.e. of chromatogram peaks Attribution to this or that component. As mentioned earlier, The basis for identification is retention time or volume.

For identification, use the relative retention time or with relative retained volume values that are smaller dependent on air-carrier speed, pressure, sample volume. In this case, the retention parameters of the components display their relative

to one of the studied substances. The relative retention time tR is defined by the formula:

$$tR = t/tst,$$

where: t - retention time of the research ubstance; tst – the same value Substance - for standard.

The relative retention time of the substance-standard is equal to one. When the task is reduced to a mixture of any certain compound Upon confirmation of its presence, it is added to the sample and subjected to chromatography division into two phases of different polarity. If the assumption in the mixture of this compound presence is correct, then the height of the corresponding peak on the chromatogram increases, And if the assumption is wrong, a new peak appears on the chromatogram.

During the analysis of a mixture of unknown composition, the components in the column After passing through, they are collected in holders and then identified by different methods of chemical and physico-chemical analysis (for example, by spectral analysis methods). This variation of the chromatographic method is called preparative gas-liquid chromatography.

Concentrations of metals in red and white wines

components	Red wine 1	Red wine 2	White wine 1	White wine 2
Al mg/l	0.195-1.38	0.34-1.5	0.395-2.556	0.328-1.9
Ba mg/l	0.05-0.34	0.131-0.320	0.042-0.18	0.053-022
Ca mg/l	0.04-0.089	0.057-0.086	0.036-0.054	0.018-0.093
Co mg/l	0.004-0.013	0.01-0.017	0.009-0.023	0.003-0.012
Cr mg/l	0.008-0.023	0.015-0.032	0.008-0.015	0.007-0.021
Cu mg/l	0.034-0.98	0.03-0.122	0.059	0.045
Fe mg/l	1.268-2.343	1.4-2.5	0.6-1.3	0.42-2.1
K mg/l	0.543	0,544	0.514	0.327
Li mg/l	0.007	0.015	0.01	0.014
Mg mg/l	0.056	0.06	0.038	0.031
Mn mg/l	0.857	0.5	0.58	0.454
Pb mg/l	0.0007	0.0008	0.0002	0.0009
Sr mg/l	0.488	0.96	0.55	0184
Zn mg/l	0.026	0.12	0.08	0.07
Na mg/l	0.8	0.76	0.69	0.81

The specialty of preparative chromatography is the size of the column Relative magnification of input sample sizes. For example, a sample that Divided into a column with a diameter of 10 mm, about 10 times more than the maximum Admissible sample for a column with a diameter of 3 mm. Doubling the column length Roughly doubles the maximum allowable sample size, but it's there There are many exceptions and sample sizes are approximate. Usually, the sample injected into the preparative chromatography is measured in milliliters.

wine 1-[Cu-0,1];[Fe-0,51];
[Zn-0,26]-[Pb-0,0008] mg/l
wine 2-[Cu-0,09];
[Fe-0,4];[Zn-1,2] –[Pb-0,001] mg/l
wine 3-[Cu-0,2];[Fe-0,35];
[Zn-0,7]-[Pb- 0,0009] mg/l
wine 4-[Cu-0,1];[Fe-0,49];
[Zn-0,9][Pb-0,0007] mg/l

The data of all four wines differ slightly from each other and fall within the acceptable limits.

Summary: the obtained results show that the amount of metals contained in the wines of factory production and family wineries presented on the Georgian market does not exceed the permissible norm.

Based on the obtained data, we can conclude that the wines of family cellars are not inferior in quality to the wines of factory production.

3. CONCLUSION

The chromatographic analysis conducted in this study reveals that the metal content in wines produced by both factory and family-type wineries in Georgia does not exceed the permissible limits. These findings suggest that the wines from small family cellars are comparable in quality to those produced by larger factory operations. This parity in quality is reassuring for consumers and highlights the effectiveness of current production practices in maintaining safety standards. Given the cultural and economic significance of wine in Georgia, these results support the continued growth and development of small wineries, ensuring that they can compete effectively while maintaining high standards of quality and safety.

REFERENCES

1. Anderson, J.L., & Berthod, A. (2013). Perspectives in Modern Chemical Chromatography. Journal of Chromatography A, 1281, 1-6. https://doi.org/10.1016/j.chroma.2013.01.026
2. Dziomba, S., & Bocian, S. (2019). Advances in Gas Chromatography Techniques and Applications. Journal of Separation Science, 42(7), 1268-1279. https://doi.org/10.1002/jssc.201801027
3. Fanali, S., Haddad, P. R., Poole, C. F., Riekkola, M. L., & Schoenmakers, P. (Eds.). (2013). Liquid Chromatography: Applications (2nd ed.). Elsevier.
4. Fekete, S., Beck, A., Veuthey, J.L., & Guillarme, D. (2015). Theory and Practice of Size Exclusion Chromatography for the Analysis of Protein Therapeutics. Journal of Pharmaceutical and Biomedical Analysis, 113, 137-147. https://doi.org/10.1016/j.jpba.2015.05.012
5. Gehrke, C.W., & Leimer, K.W. (1971). Quantitative Gas Chromatography for Chemists and

Biochemists. Analytical Chemistry, 43(10), 1406-1407. https://doi.org/10.1021/ac60305a035

6. Gross, L. (2011). High-Performance Liquid Chromatography: Advances and Applications. Analytical and Bioanalytical Chemistry, 400(8), 2285-2297. https://doi.org/10.1007/s00216-011-4954-5
7. Heemstra, J. M., Liu, D. R., & Lin, W. (2015). Modern Trends in Affinity Chromatography. Accounts of Chemical Research, 48(12), 2859-2867. https://doi.org/10.1021/acs.accounts.5b00310
8. Hennion, M. C. (1999). Solid-Phase Extraction: Method Development, Sorbents, and Coupling with Liquid Chromatography. Journal of Chromatography A, 856(1-2), 3-54. https://doi.org/10.1016/S0021-9673(99)00832-8
9. Iwatsuki, M., & Suzuki, K. (2002). Advances in Ion Chromatography for Environmental Applications. Journal of Chromatography A, 956(1-2), 3-10. https://doi.org/10.1016/S0021-9673(02)00315-1
10. Jandera, P. (2008). Stationary and Mobile Phases in Hydrophilic Interaction Chromatography: A Review. Analytica Chimica Acta, 624(1), 1-25. https://doi.org/10.1016/j.aca.2008.05.015
11. Jinno, K. (2005). Miniaturized Chromatographic Techniques. Journal of Chromatography A, 1064(1), 1-12. https://doi.org/10.1016/j.chroma.2004.12.027
12. Kavaliunas, D., & Haddad, P. R. (1998). Ion Chromatography: A Review of Recent Developments and Applications in Environmental Analysis. Analytica Chimica Acta, 370(1), 123-141. https://doi.org/10.1016/S0003-2670(98)00289-5
13. Khalaf, R.G., & Bartle, K.D. (2013). Supercritical Fluid Chromatography in Pharmaceutical Analysis. Journal of Chromatography A, 1318, 102-113. https://doi.org/10.1016/j.chroma.2013.10.007
14. Khaw, B., & Svec, F. (2010). Advances in Monolithic Column Technology for High-Performance Liquid Chromatography. Journal of Separation Science, 33(6-7), 813-822. https://doi.org/10.1002/jssc.200900757
15. Kuhn, H., & Poole, C. F. (2003). Contemporary Practice of Chromatography. Journal of Chromatography A, 1000(1-2), 1-28. https://doi.org/10.1016/S0021-9673(03)00494-4
16. MacNair, J. E., Patel, K. D., & Jorgenson, J. W. (1999). Ultra-High-Pressure Reversed-Phase Liquid Chromatography in Packed Capillary Columns. Analytical Chemistry, 71(3), 700-708. https://doi.org/10.1021/ac980796p
17. Marengo, E., Robotti, E., & Bobba, M. (2012). Multidimensional Chromatography for Metabolomics: Methods and Applications. Journal of Chromatography A, 1259, 191-210. https://doi.org/10.1016/j.chroma.2012.03.018
18. Majors, R.E. (2011). Trends in Sample Preparation for Chromatography. LC GC North America, 29(11), 1164-1173.
19. Majors, R. E., & Hopper, T. (2005). New Trends in High-Performance Liquid Chromatography for Environmental Analysis. TrAC Trends in Analytical Chemistry, 24(7), 590-600.

https://doi.org/10.1016/j.trac.2005.04.003
20. Molnár, I., & Rieger, H. J. (2012). Advanced Chromatographic Techniques in Pharmaceutical and Biomedical Analysis. Journal of Pharmaceutical and Biomedical Analysis, 69, 1-10. https://doi.org/10.1016/j.jpba.2012.01.003
21. Mondello, L., & Dugo, P. (2002). Comprehensive Chromatography in the Analysis of Food and Natural Products. Journal of Chromatography A, 973(1-2), 1-10. https://doi.org/10.1016/S0021-9673(02)01258-0
22. Sandra, P., & David, F. (2004). Comprehensive Two-Dimensional Gas Chromatography: A Powerful and Versatile Tool for the Analysis of Complex Samples. Journal of Chromatography A, 1000(1-2), 133-166. https://doi.org/10.1016/S0021-9673(03)00668-2
23. Snyder, L. R., Kirkland, J. J., & Dolan, J. W. (2010). Introduction to Modern Liquid Chromatography (3rd ed.). John Wiley & Sons.
24. Stoll, D.R., & Carr, P.W. (2017). Two-Dimensional Liquid Chromatography: A State of the Art Tutorial. Analytical Chemistry, 89(1), 519-531. https://doi.org/10.1021/acs.analchem.6b03506
25. Xia, Y. Q., Liang, X., Chen, G. L., & McNally, M. E. (2008). Hydrophilic Interaction Chromatography and Its Application in Drug Development. Journal of Separation Science, 31(6-7), 895-909. https://doi.org/10.1002/jssc.200700510

უაკ **543.42**

მცირე ოჯახური მარნების წარმოებულ ღვინოებში ტოკსიკური მინარევების კვლევა

ნ. ამაშუკელი, ა. გვანცელაძე, ნ. რაჭველიშვილი

ქიმიური და ბიოლოგიური ტექნოლოგიების დეპარტამენტი, საქართველოს ტექნიკური უნივერსიტეტი, საქართველო, 0175, თბილისი,კოსტავას 69

E-MAIL: natamashukeli@gmail.com

რეზიუმე: მიზანი: ღვინის წარმოების და მოხმარების კულტურა საქართველოში, ბოლო წლებში მკვეთრად შეიცვალა. გაჩნდა უამრავი მცირე,ოჯახური ტიპის საწარმო. ამ პროცესს ხელი შეუწყო სახელმწიფო პროგრამებმაც, როგორიცაა მაგალითად „აწარმოე საქართველოში“, რომლის ფარგლებშიც მრავალი მცირე საწარმო დაფინანსდა.ღვინის მაღაზიებშიც დღითიდღე იზრდება მცირე მეღვინეობების პროდუქცია.სსიპ ღვინის ეროვნული სააგენტოს საქმიანობა, რომელიც შექმნილია „ვაზისა და ღვინის შესახებ“ საქართველოს კანონის საფუძველზე, მოიცავს ღვინის წარმოების ხარისხის კონტროლსა და სერტიფიცირებას, თუმცა მცირე მარნების წარმოებული

ღვინოების ტოკსიკოლოგიური შემოწმება არ არის საყოველთაო. მძიმე მეტალები, რომლებსაც შესაძლოა შეიცავდეს ღვინოები, ადამიანის ჯანმრთელობაზე ხანგრძლივი დამაზიანებელი გავლენა აქვს. კვლევა მიზნად ისახავს შეისწავლოს მცირე საოჯახო ტიპის მარნების წარმოებული ღვინოები მძიმე მეტალების შემცველობაზე ქრომატოგრაფიული მეთოდით, შეიმუშაოს რეკომენდაციები ღვინის ხარისხზე პასუხისმგებელი მხარეებისთვის. ღვინო ძალიან მნიშვნელოვანია ჩვენი ქვეყნისთვის.საქართველოს უძველესი ღვინის კულტურა აქვს. ძველი დროიდან ქართველი აკვირდებოდა ღვინის სასარგებლო თუ მავნე ზეგავლენას ადამიანის ჯანმრთელობაზე. ღვინო შეიცავს ორგანიზმისთვის აუცილებელ ელემენტებს მაგნიუმს, სპილენძს, თუთიას, რკინას, კალიუმს. სხვადასხვა მიზეზის გამო ღვინო შესაძლოა შეიცავდეს მავნე ,ტოკსიკურ ნივთიერებასაც, ამიტომ ადამიანის ჯანმრთელობისთვის მნიშვნელოვანია ღვინის შემცველობის კვლევა,რათა დაცული იყოს ტოკსიკური მინარევების ზღვრული შემცველობა.

მეთოდი: კვლევის მეთოდად შეირჩა ქრომატოგრაფია. ღვინის წარმოებაში ქრომატოგრაფიას იყენებენ ლითონების განსაზღვრისთის მზა ნაწარმში, მათი სინთეზის ნახევარპროდუქტებსა და გამოსავალ ნედლეულში. ლითონები მიეკუთვნება ტოქსიკური მინარევების რიცხვს, ამიტომ მეტად მნიშვნელოვანია ლითონის შემცველობის ცოდნა, რომელიც არ უნდა აღემატებოდეს დასაშვებ ზღვარს.

შედეგები: განხორციელებული კვლევებისას დადგინდა რომ ქრომატოგრაფია მაღალი საზუსტით ადგენს მეტალების შემცველობას ღვინოში.

დასკვნა: მიღებული შედეგებით დგინდება, რომ ქართულ ბაზარზე წარმოდგენილი ქარხნული წარმოების და საოჯახო მარნების ღვინოების შემადგენლობაში შემავალი მეტალების რაოდენობა არ სცილდება დასაშვებ ნორმას.

მიღებული მონაცემებით შეგვიძლია დავასკვნათ, რომ საოჯახო მარნების ღვინოები ხარისხით არ ჩამოუვარდება ქარხნული წარმოების ღვინოებს.

საკვანძო სიტყვები: მცირე მარნების ღვინო, მეტალების შეცველობა, ქრომატოგრაფია.

UDC 666.367

PRODUCTION AND STRUCTURAL STUDY OF LOW-TEMPERATURE PORCELAIN-LIKE DECORATIVE CERAMICS

***G. Gaprindashvili, *Z. Kovziridze, *L. Targamadze, *T. Loladze, *N. Nizharadze, *V. Kinkladze, *M. Kapanadze, **E. Uchaneishvili, **M. Chakhunashvili. **A. Usupashvili, **N. Enageli, **N. Kvelaidze, **L. Kakachia**

*Georgian Technical University. Faculty of Chemical technology and Metallurgy, Institute of Bio-nanoceramics and Nanocomposite Technology, Bio-nanoceramic and Nanocomposite Materials Science Center, Georgia, 0175, Tbilisi, 69 M. Kostava St.

** Public school #178, Tbilisi

E-mail: kowsiri@gtu.ge

Resume: Production and studying low-temperature ceramic products obtained by porcelain production technology. **Method:** Casting aqueous suspension (shlicker) in plaster moulds was selected for manufacturing the products. The chemical composition (wt. %) of fired ceramic materials, the nature of changing and redistribution of pore sizes in the structure of fired ceramics at different temperatures and their electron microscopic images were studied; a linear analysis of ceramic material closed porosity was carried out; change of water absorption of ceramic materials depending on temperature and operational properties of materials were also researched. **Results:** With the increase in firing temperature of ceramic materials up to 1080-1120^{0}C, the viscosity of the material is decreased and the action of surface forces on the phase boundaries is increased. As the crystal grains draw closer together, the material hardens and its water absorption decreases to zero, depending on the porosity. The material acquires high operational properties. **Conclusion:** Based on the experimental results, ceramic products with high operational properties can be obtained by porcelain production technology.

Key words: aqueous suspension - schlicker, moulding method, plaster moulds, water absorption of materials, operational properties.

1. INTRODUCTION

The technological part of the experiment was carried out with the involvement of five eleventh-grade students of Tbilisi Kakutsa Cholokashvili Public School #178. They took part in structural research of materials.

For manufacturing ceramic products, the method of casting from aqueous suspension (schlicker) in plaster moulds was used. The schlicker was prepared by the students. The students formed different shape products by casting method. Schlicker is a colloid-dispersion system in which the mineral particles that make up the ceramic mass are

in a weighted state. The casting schlicker must meet the following requirements:

1. Flowability of the schlicker has to ensure its smooth transfer through pipelines and easy filling of plaster moulds.

2. It must have as little water content as possible.

3. It is essential to maintain the stability of the shlicker, ensuring that none of its constituent parts separate or precipitate from the mass

The moulding of products is based on the ability of plaster moulds to absorb water from the liquid mass poured into them. While the plastic mass layer on the mould surface transfers part of its moisture to the porous mould and the surrounding environment, it gradually thickens. After measuring the thickness of the product, the students poured the shlicker out of the mould, turning the mould upside down to remove the excess shlicker. After about an hour, the form was placed upright again. The product is shrinking in volume and is separated from the mould. Depending on the product wall thickness, the following methods of forming are used: "casting" – for casting thin-walled products and "pouring" for manufacturing thick-walled or whole products.

The stability, flowability and water content of shlickers are determined by two factors: the adsorption properties of the system and the water-mineral particle relationship.

The constituent particles of schlicker mass are crystalline bodies. Crystal surfaces are electroactive. They can attract and then adsorb ions from the liquid phase.

Natural waters, surrounding clay particles, frequently contain various soluble salt ions. Exchange adsorption occurs, altering the composition of the clay particle shells. Shlicker can be liquefied by adding electrolytes. As a result, its concentration in the solution is increased. This reduces the dissociation of absorbed sodium, increasing water thickness. As a result, the shlicker is liquefied. After the addition of electrolytes, the dimensions of the water membranes reach critical values. At this time the water membranes can no longer resist the mutual attraction of the particles, and the particles begin to stick together. Shlicker is coagulated. At this time, free water appears between the glued particles, and as a result, the amount of free water is reduced and the viscosity of the shlicker is increased.

During moulding by the "casting" method, after the formation of a dense layer (2) on the inner surface of the mould (1), the shlicker is poured out. The remaining hollow product continues to transfer moisture directly to the atmosphere and the capillaries of the mould, decreasing in size, are gradually separated from the mould. The hollows (3) and protrudes on the second part of the mould ensure the correct matching of the mould parts.

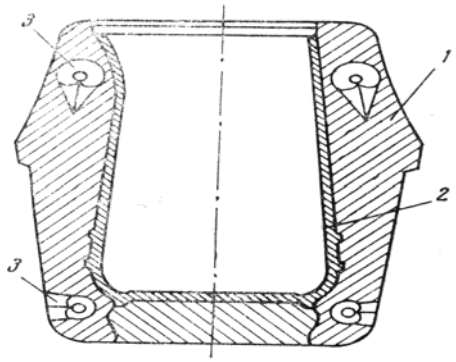

Fig. 1. A mould for making a product by the "casting" method

When using the "pouring" method, the shlicker is poured into the cavity between the two (1) and (2) plaster moulds, corresponding to the shape of the product (Fig. 2). The casting's shape and dimensions exactly match those of the cavity. The dense layer forms twice as fast compared to the casting method, as the mass loses moisture from both sides. Between two layers of hardened mass near the surface of plaster moulds liquid mass remains until the end of the forming process. Its deficit must be filled (4) through channels (5). Various massive products can be poured using the "pouring" method.

The moisture content of shlicker is 28-35% depending on the raw materials used, their type and percentage composition. The grain size of the solid phase in the shlicker should be less than 60 μm and the granulometric fraction must be 10-50 μm. Their content is on average 40-65 wt. %. The 5-1 μm fraction is approximately 5-10 wt.%, and the fraction less than 5 μm should be 32-70% on average.

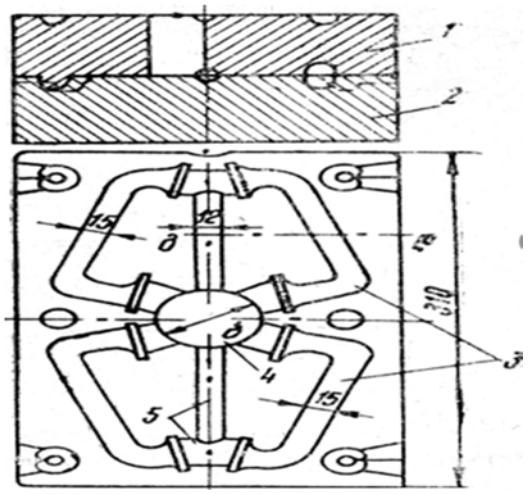

Fig. 2. The mould for forming handles using the "pouring" method.

Thus, the degree of shlicker dispersion is mainly determined by these three fractions, because three fractions are optimal for the formation of a dense arrangement system.

2. MAIN PART

The schlicker was prepared in two stages from the components presented in Tables 1, and 2. Ukrainian fire-proof clay from the Vesiolovoe deposit and perlite from the Aragats deposit in Armenia were used. Glass and earthenware shards were used as dopants. Liquid glass and water were also added.

Fireclay, perlite, glass and earthenware shards were crushed and charged into the mill. During the first charging, grinding was carried out for 8 hours.

During the second charging, fire-proof clay, water and soda are added (Table 2). Grinding lasts for 4 hours.

Ready schlicker was passed through a 05 sieve and poured into premade forms. The schlicker was held in the mould until the desired thickness was obtained. As soon as a layer of the desired thickness of ≅2.5 mm was formed in the mould, the remaining schlicker was poured out. The mould was left upside down for an hour until the remaining drops drained. After 2-4 hours, we opened the moulds and took out the samples. The formed sample was air-dried for 24 hours, then dried in a thermostat at 80°C and sintered in the furnace at 1000°C with a mode of 5°C/min, and was held at the final temperature in a muffle furnace with nichrome heaters for 40 minutes. They were cooled down in a free mode. After this, sintered products were obtained (Fig. 3).

Table 1

The first charging

N	Material Name	Substance Content in grams
1.	Fire-proof clay	180
2.	Perlite	660
3.	Earthenware shards	48
4.	Glass Cullet	12
5.	Liquid Glass	3
6.	Water	600

Table 2

The Second charging

N	Material Name	Substance Content in grams
1	Fire-proof clay	300
2	Water	200
3	Soda	1

Fig. 3. Low-temperature ceramic products made by students

Sintering with the liquid phase is typical for household decorative ceramic materials, e.g. clay-containing materials, particularly for porcelain ceramics. Liquid phase sintering depends on: 1. Surface tension at the phase boundary; 2. Viscosity of the liquid phase; 3. Dispersion of crystal particles.

The influence of such factors on settling, which is defined as the approximation of the centres of two particles, is calculated by the formula:

$$\Delta l = \frac{3\gamma L0}{4Er} xt \quad (1)$$

where γ – Surface Tension;

L_0 – Distance Among Grains Before Sintering;

E – Viscosity of the Liquid Phase;

r – Particle Radius;

t – Temperature.

Sintering With Liquid Phase

Sintering with liquid phase has the biggest technical application, it plays the role of a binder during crystallisation, and it cements the product as a whole. Such Technologies, involving the liquid phase, are widely used in ceramic production.

The kinetics of the sintering processes with the coexistence of the liquid phase depends on the porosity of the pressed material, the amount of the liquid phase, the linear dimensions of grains, the degree of wetting the solid phase by the liquid phase, the mutual solubility of the phases, and others. A complete description of the processes involving the liquid phase is challenging, but some aspects are discussed in the given article.

Let's consider the case when the liquid phase is formed based on an easily soluble component with the assumption that the hard-to-melt component partially melts and dissolves in the molten solution [1-4].

The porous structure of ceramic material is a combination of solid matter (crystalline and vitreous) and voids. It is formed during heat treatment due to growing nucleated bubbles and is obtained while sintering the initial charge. Let's consider this phenomenon in the case of masses containing perlite. Perlite is a fluxing and gas-generating material. When released, the gas generator reduces perlite viscosity to 10^9-10^6 poise [5]. Theoretically, some nucleated bubbles should grow in this temperature range. Later, when a new crystalline phase is separated and the material is sintered its pores start to shrink. The nature of the change and distribution of the pore size in the ceramic structure depending on the temperature is visible in Fig. 4 and 5. In composition #5, only the fire-resistant white-burning Ukrainian Vesyoloe geopolymer and Aragats perlite are taken in a ratio of 55:45. In composition #2, for the intensification of processes, the same geopolymer, Aragats perlite and window glass cullet are taken in a ratio of 50:40:10 (Table 3).

At the temperature of 1000°C, both materials are characterised by open porosity and have an incorrect geometrical shape. The surface is covered with a frequent, dense pore mesh, with a diameter of 4-18 μm. Large pore inclusions are rare. At 1050°C closed porosity is observed in #2 ceramic, and water absorption is <0.5%.

Table 3

Material and chemical compositions of masses (wt.%)

Mass Index	Charge composition					Chemical composition, (wt.%)									
	Aragats Perlite (Armenia)	Clay From Vesyoloe Ukraine	Askana Clay	Earthenware shards sintered at 1080°C	Glass Cullet	SiO_2	TiO_2	Al_2O_3	Fe_2O_3	CaO	MgO	Na_2O	K_2O	SO_3	Sintering Temperature, T°C
P_1^*	50	35	-	-	15	68.92	0.66	19.27	0.70	1.95	1.10	4.10	3.30	-	1050
P_2	50	40	-	-	10	68.20	0.73	21.00	0.74	1.56	0.95	3.46	4.05	-	1050
P_3	38	40	5	7	10	63.20	0.69	20.75	0.87	2.73	1.35	3.94	2.86	0.18	1050
P_4	40	50	-	2	8	66.14	0.87	23.54	0.80	1.59	1.04	3.10	3.02	-	1080
P_5	55	45	-	-	-	67.89	0.82	23.17	0.84	0.90	0.65	2.30	3.45	-	1100
P_6	55	38	-	7	-	68.62	0.78	22.40	0.79	0.87	0.62	2.39	3.54	-	1100
Tile Mass	49	28	5	6	12	72.43	0.58	17.09	0.93	1.49	0.93	3.24	3.62	-	1050
MPC						68.50	0.27	26.69	0.44	0.47	0.27	0.89	2.47	-	1350

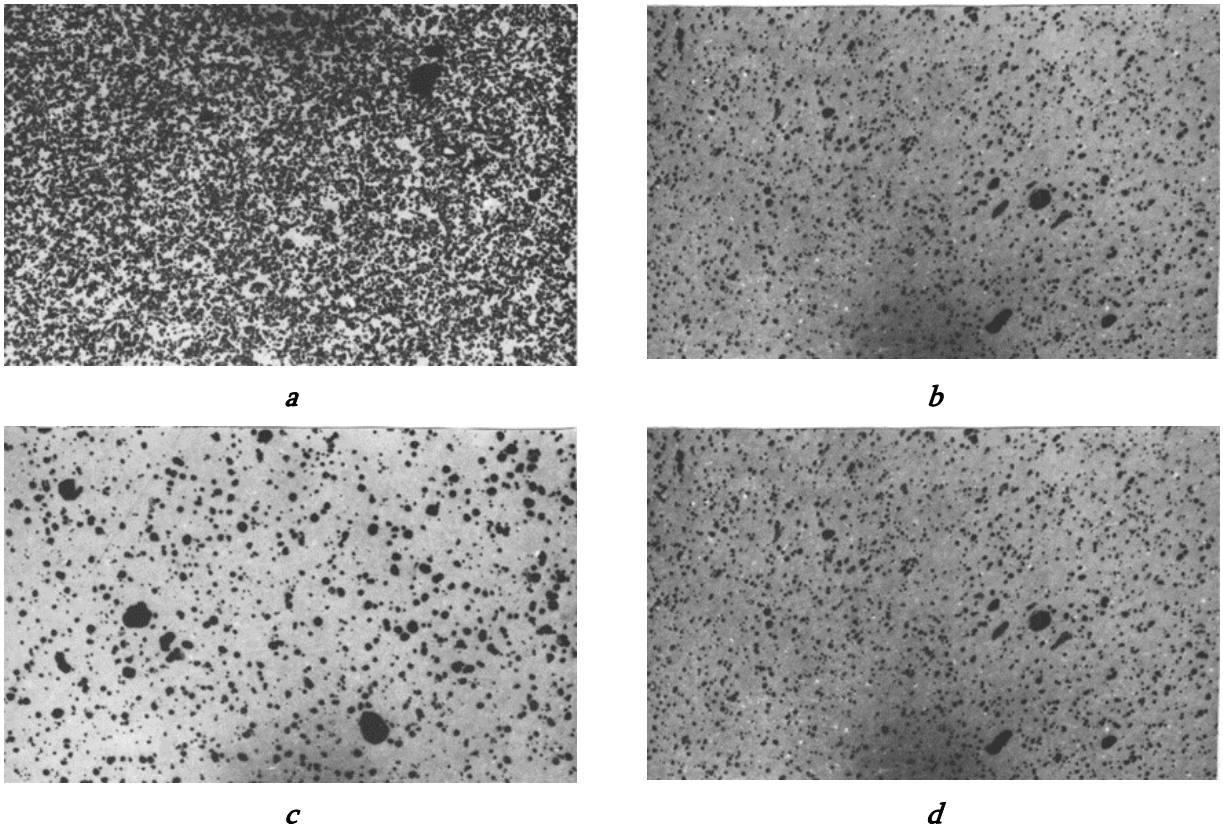

Fig. 4. Character of change and redistribution of pore size in #5 ceramic structure: a) 1000°C; b) 1100°C; c) 1150°C; d) 1220°C.

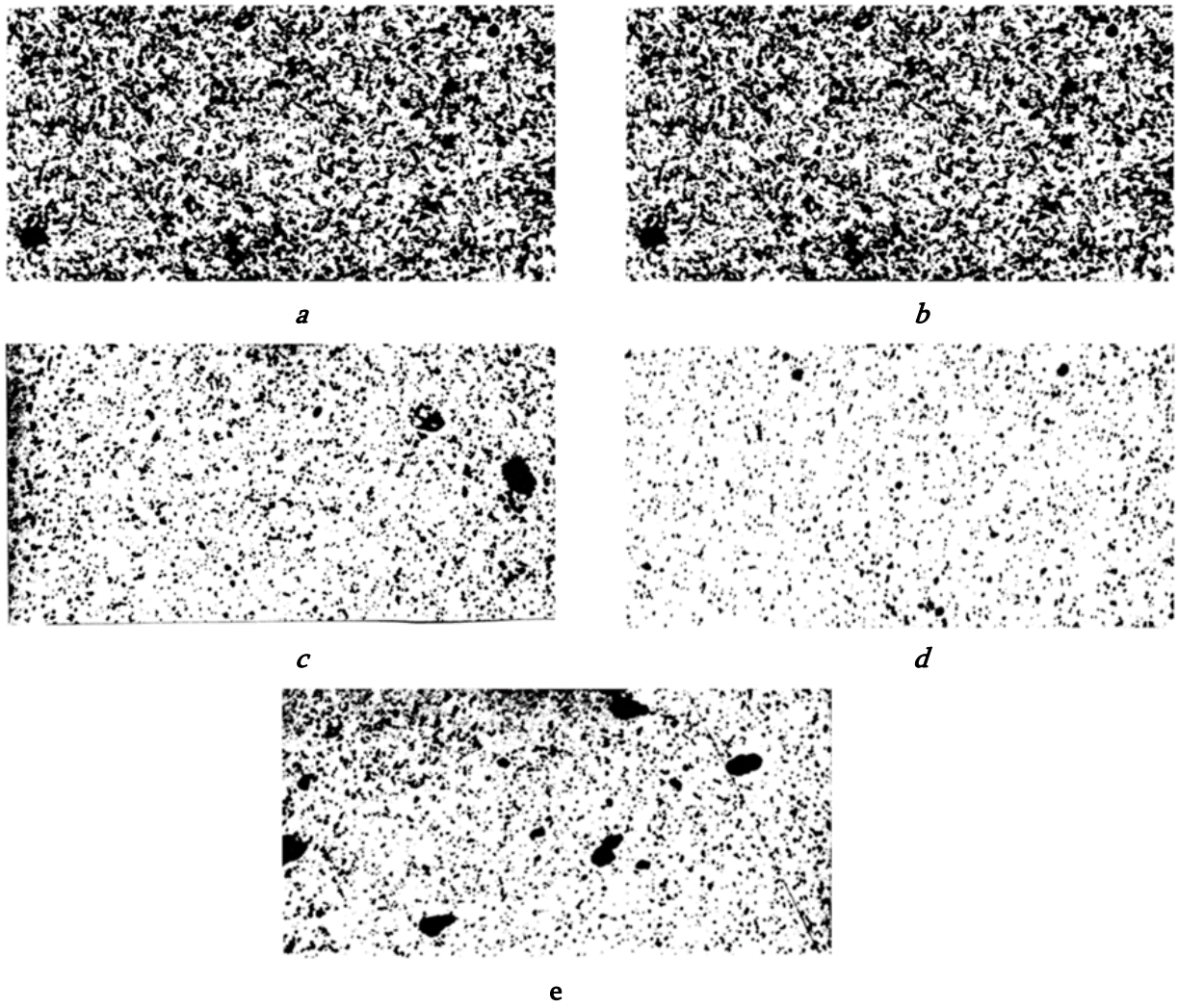

Fig. 5. Character of change and redistribution of pore size in ceramic structure #2: a) 1000°C; b) 1050°C; c) 1100°C; d) 1150°C; e) 1220°C

Ceramic #2 is sintered at 1050-1100°C, and #5 - at 1100-1150°C. At these temperature conditions, both materials have their best operating properties. The pores are rounded, with an average size of 5-7 μm, and the average distance between them in the matrix is 60-90 μm (Table 4).

Table 4

Matrix Properties of Ceramic Materials

Temperature T°C Indicator	1050	1080	1100	1150	1280	1220
P2						
Average Pore Size, d μM	-	5.4	5.1	7.8	7.8	8.0
Average Distance Between Pores, l μM	-	-	79.8	92.2	89.4	85.0
Pore General Content, V,%	-	-	7.0	6.8	8.0	10.4
P-5						
Average Pore Size, d μM	4.0	4.1	5.2	5.7	6.2	6.7
Average Distance Between Pores, l μM	19.2	19.8	28.6	63.8	98.0	85.0
Pore General Content, V,%	16.4	15.2	9.4	8.2	5.9	6.4

At a temperature of 1200°C in #2, the pressure developed in the pores initiates the bloating process. Pores lose their rounded-spherical shape, coagulate, merge and increase in size. The process is shown in Fig. 4, where ceramic #5 at 1220°C is "overfired". Figures 6 and 7 illustrate the outcomes of the linear analysis of closed porosity for materials #2 and #5. Porosity frequency and total frequency curves are plotted for #5, heat treated at 1100-1150°C and #2 at 1050-1150°C, i.e. from the initial to the final stage of sintering. According to the pore distribution in the matrix, at the initial stage of sintering ceramic material #5 contains 80% pores less than 6 μm in size, and the summary curve shows that the content of pores less than 12 μm is 98%. At 1150°C, the material contains 62% pores less than 4 μm, and the summary curve shows 93% pores less than 14 μm in size in the matrix. The matrix pore distribution curves in material #2 are relatively even.

At 1050°C, the ceramic contains 78% of pores smaller than 2 μm, and the cumulative curve indicates that 97% of pores are smaller than 11 μm. At this temperature, material #2 is ready for application. At 1100°C, the matrix pore distr-ibution curve shows 45% smaller than 1 μm and 58% smaller than 6 μm pores, and the summary curve shows 96.5% smaller than 11 μm pore content in the matrix. When the temperature is raised to 1150°C, the distribution curve reveals 56% of pores with a size of less than 6 μm, and on the summary curve - 97% with a size of less than 11 μm. Based on the linear analysis, it can be concluded that only 3-8% of the pores in the ceramics are larger than the optimal size relative to the total porosity. These ceramics are fully sintered in the 1080-1150°C temperature range and exhibit their best operational properties.

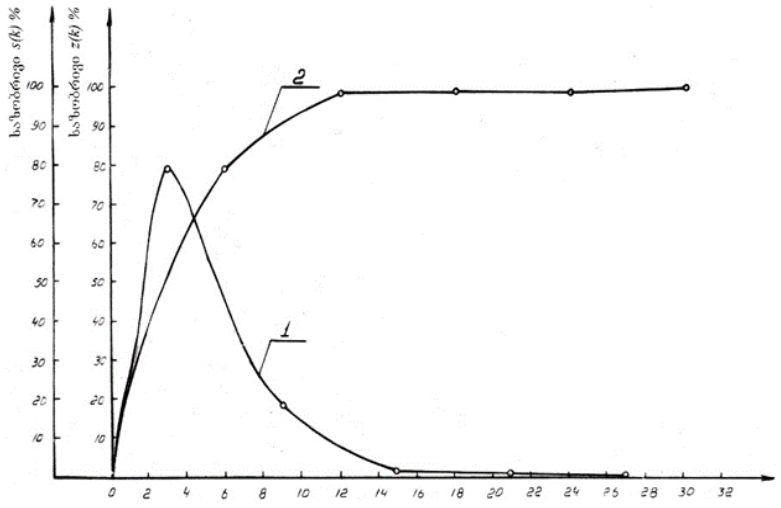

a

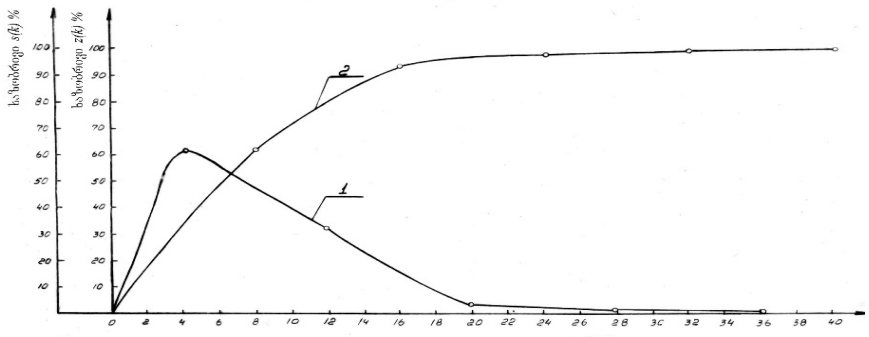

b

Fig. 6. Linear closed porosity analysis of ceramic material #5.
Sintered: a) 1100°C; b) 1150°C. 1. Frequency of pores;
2. Total frequency of porosity

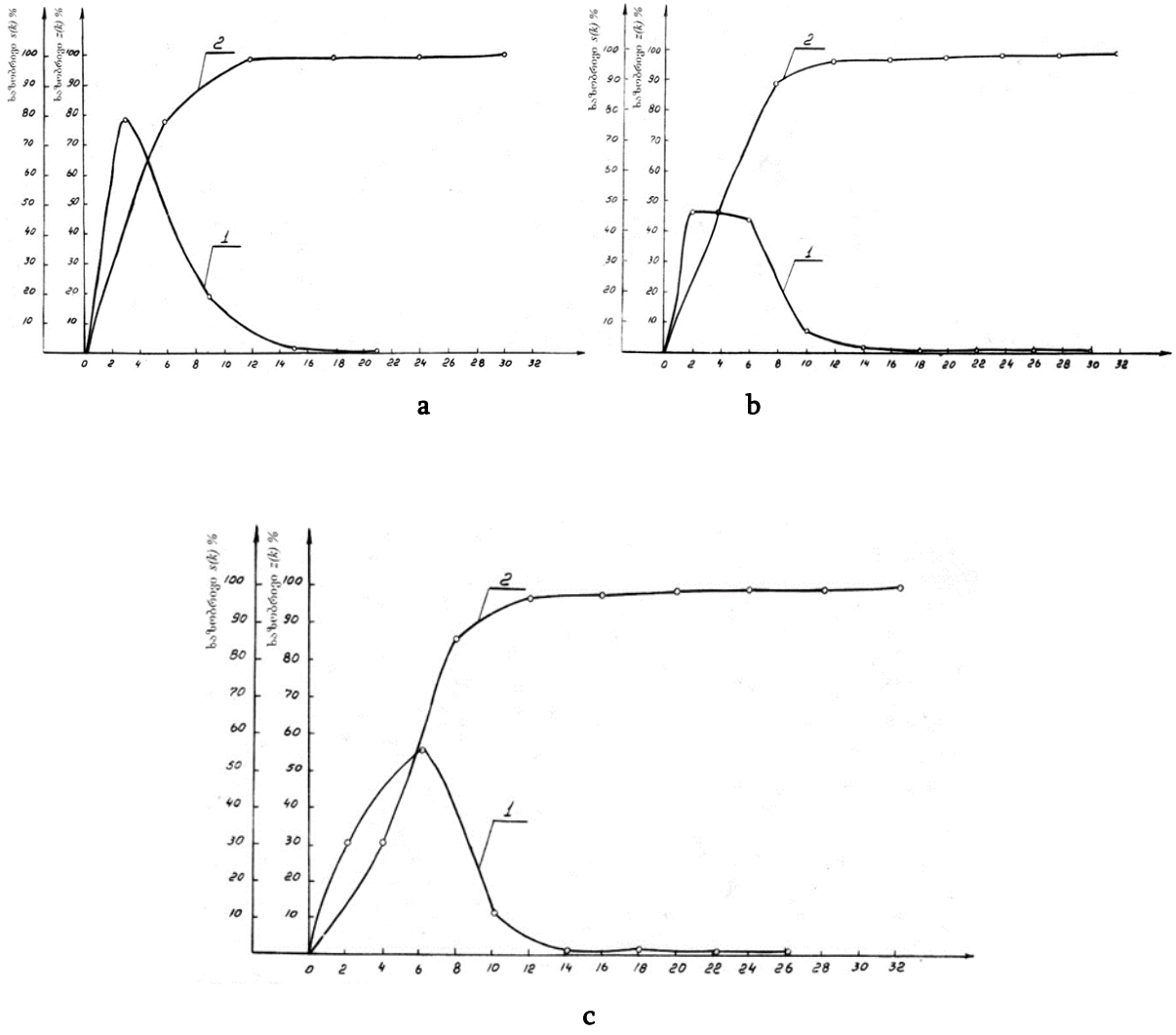

Fig. 7. Linear closed porosity analysis of ceramic material #2. Sintered: a) 1050°C; b) 1100°C; c) 1150°C. 1. Frequency of pores; 2. Total frequency of porosity.

Based on the above and the general complex studies of the materials in practice, it is necessary to consider the total percentage of closed porosity, which in synthesized ceramics varies mainly within 2-9% and the size of individual pores. During heat treatment, the apparent density variation of the ceramic is a function of mass and volume. Using these relationships, volumetric changes at sintering as a function of porosity and material volume change can be plotted [6]. For the last stage of firing glass phase containing ceramics, when weight loss and major phase transformations are over and no changes in mass and true density occur, these formulas are valid:

$$A_{vol.} = (\rho_1/\rho_2 - 1)x100\% \quad (2)$$

$$A_{vol.} = \Pi_2-\Pi_1/100-\Pi_2 \text{ x } 100\% \quad (3)$$

Subscripts 1 and 2 mean that the given value refers to the semi-finished product and the fired material, $A_{vol.}$ - is the change of the material during

firing, in%. In practice, it is more convenient to depict shrinkage not by volume, but by linear characteristics:

$$A_{\text{lin.}} = [\sqrt{1 + A_{\text{vol.}}/100 - 1}]x100\% \quad (4)$$

Hence, the variation in the density of semi-finished products during moulding and throughout all stages of subsequent heat treatment must be considered in the technological process. This phenomenon can significantly affect the porosity, pore size and distribution in the ceramic matrix, which further determines the properties of the finished product. Summarizing the above, and based on lots of experimental materials, which were analyzed while studying the synthesis of ceramic products, we tried to theoretically generalize the possible processes that occur in the material with a significant amount of vitreous phase content [7-10]. When comparing the description of the shrinkage kinetics with the provided experimental data, we can consider the case where the liquid phase is revealed by melting easily meltable components, assuming that the refractory component is partially soluble in the molten mass. To form a liquid phase, it is energetically appropriate for two particles to be separated by the liquid phase when these particles are in direct contact. The process requires the following conditions:

$$2\alpha_{\text{my.}}\text{Tx}.\, x\cos f < \alpha_2 \quad (5)$$

$$2a\text{solid. liquid.}\, x\cos f < a_2 \quad (6)$$

The condition is fulfilled at any value of the angle f = f_0+2θ, if / α_{solid} liquid<α_2/2, where α_{solid} liquid is the surface energy at the boundary of solid and liquid phases, α_2 is surface energy at the boundary of two grains, f_0 is the angle between the tangents at the point of contact of the two-grain surfaces, θ is the wetting angle [11].

During the thermal treatment, the liquid phase resulting from the melting of perlite, along with the glass cullet, fills the intergranular voids. The presence of an intergranular liquid cuff under certain conditions generates forces, that lead the grains to be attracted to each other, which causes the material to harden and thus affects the sintering kinetics. The movement is accompanied by the reduction of the free surface of the liquid phase, carried out under the influence of pressure, caused by surface curvature. It seems that we are dealing with a volume diffusion mechanism, when the sink of excess vacancies, which are formed near the surface of the concave throat, is the convex surface of the grains. In this case, increasing contact area should be accompanied by the approximation of the grain centers. As is known, volume diffusions are characterized by large activation energy, stipulating volume diffusion mainly while approaching "Tammann temperatures" (0.52 Tm, where Tm is the melting temperature in °C). The Tammann temperature corresponds to the beginning of the movement of atoms or ions in the lattice and is, therefore, very important. Tamman temperature range for the main mineral kaolinite of the used geopolymer - a fireclay from Vesyoloe coincides with the first exopeak temperature - 925-940°C when the strong destruction of its structural package occurs. For the kaolinite chemistry the distribution of bonds in tetrahedrons $[SiO_4]^{4-}$ and octahedrons $[AlO_6]^{-6}$ can be essential. The sp^3 configuration provides stability to the electronic configuration relative to the silicon atom in silicates [12]. The occurrence of these connections in tetrahedra and octahedra is not uniform, particularly, **p** connections are much

stronger than **s** connections, leading to a relatively prolonged morphological correspondence between the structure of the silicate crystal and the liquid phase. In this temperature interval, gaseous substances (2-5 wt.%), separated from perlite, contribute to the breaking bonds, loosening of the material structure, and relatively intense diffusion processes [12, 13]. As a result, **p** bonds in tetrahedrons and octahedrons are broken, the structural sequence Si-O-Al is violated, Al and Si ions are freed and a prerequisite is created for their diffusion in the solution. The viscosity is significantly reduced due to the breakdown of the structure. In the raw material mixture, minerals are decomposed, and water vapour and other gaseous products are emitted. At the same stage, the internal molecular changes in kaolinite, the main mineral of the geopolymer, are ongoing. The dissociation of hydrogen bonds H_2O and OH^- and the process of releasing water from the perlite somewhat hinder the crystal nucleation from Al_2O_3 and SiO_2 particles. Over this temperature range, there is intensive interaction between the geopolymer substance and perlite, which is greatly facilitated by the presence of a glass cullet. Being an easy-melting component of the mixture, it accelerates the liquid phase formation and forms silica-perlite glass with perlite, excess amorphous silicon dioxide and decomposition products of kaolinite geopolymer. In the liquid phase of perlite and glass, there is an energetic interaction between two main refractory oxides. As a result, a new crystalline formation - mullites is formed by crystallization from the solution, contributing to the creation of the carcass and the reinforcement of the vitreous phase [14-18]. The formation of mullite can hardly be observed in the research materials that focus on temperatures up to 1000°C. Only over this temperature, when the free particles of SiO_2 and Al_2O_3, due to the absence of chemical bonds immediately after the decomposition of kaolinite, are in a relatively high chemically active state and the chemical reaction of mullite formation proceeds at a higher rate, contributing to the formation of crystals, mullite can be observed. The process can be observed in the $П_2$ sample at the temperature of 1020-1030°C.

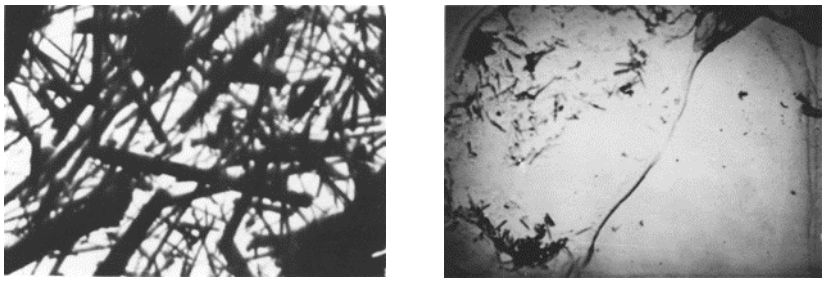

a **b**

Fig. 8. Electron-microscopic images of #2 ceramic material fired at 1050°C. a - network of large needle-like crystals of mullite; b - fine needle-like crystals of mullite. x 5400

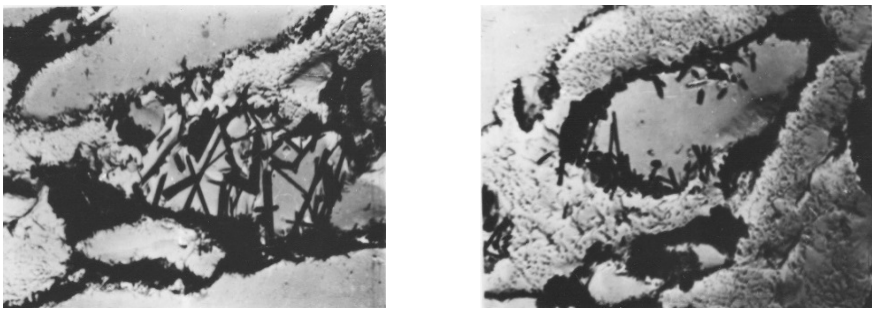

a

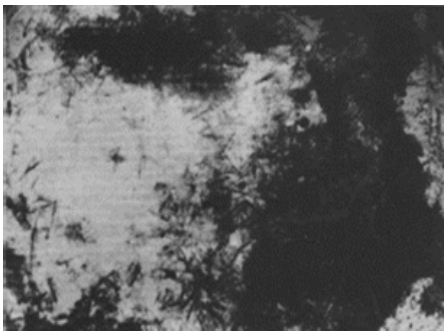

b

Fig. 9. Electron-microscopic images of ceramic material #5. Baked at 1100°C. a – large needle-like crystals of mullite; b - fine needle-like and scaly crystals of mullite. x 540.

Such a small amount of the crystalline phase in the nucleation state will not be able to contribute to the formation of a solid carcass of earthenware with high physical and technical properties. The presence of a large amount of liquid phase can significantly affect the sintering kinetics of the material. In this case, even if the raw material mixture has low porosity, closed pores are easily formed, especially in the liquid layer between the particles. Gas pressure in such pores partially inhibits shrinkage. This feature was revealed while determining the water absorption of the samples (Fig. 10).

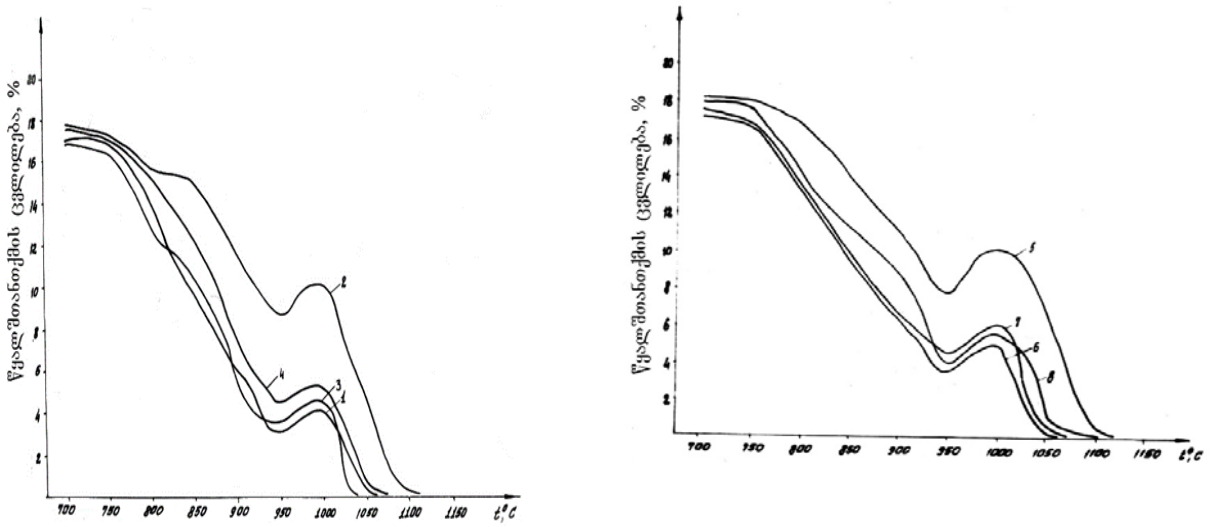

Fig. 10. Change of water absorption of ceramic materials depending on temperature. 1–#1; 2–#5; 3–#7; 4–#8; 5–#6; 6–#2; 7–#3; 8–#4

The formed solid phase inhibits the release of volatile components from the perlite due to their entrapment by the liquid layer between the particles. As the temperature increases, so does the pressure in the closed pores. The pores begin to expand and tend to separate from the material. The degassing process of perlite starts from 860°C, when gaseous substances are emitted from perlite, and continues up to higher temperatures of 90-120°C and coincides with the first exopeak of kaolinite. The process is changed from shrinking to 'growing', as was observed on the samples. This event is significantly contrary to the regularity of shrinkage. However, it is considered that the processes that occur at the given temperature interval have a decisive influence on ceramic material sintering, because water, as a gas-generating and melting agent, exhibits a mineralising effect as it is released during the thermal treatment. It loosens the structure of the ceramic material and strength of the crystal carcass resulting in the decrease of the molten silicate viscosity, which should facilitate the full and intensive course of diffusion processes [15 - 20]. With the temperature increase up to 1080-1120°C, the viscosity of the molten mass is decreased and the action of surface forces on the phase boundaries becomes stronger. The crystal grains approach each other, the mass is hardened and the water absorption is decreased to zero depending on the porosity. The material achieves high performance characteristics as confirmed by the analysis of operational properties [13] (Table 5).

Table 5

Material Properties

№	Properties	Material Index						
		P_1	P_2	P_3	P_4	P_5	P_6	Mass of tiles
1	Firing Temperature, T°C	1050	1050	1050	1080	1100	1120	1050
2	Total shrinkage, α, %, 750°C	4.8	4.7	4.7	6.3	4.7	6.3	4.8
3	Shrinkage After Firing at the Final Temperature	14.1	14.6	14.4	15.0	14.5	15.0	13.2
4	Water Absorption, Ẃ, - at 750°C - at the Final Temperature	17.2 0.1	17.1 0.8	17.6 0.6	17.5 0.09	17.6 1.2	17.1 0.43	17.6 0.1
5	Bending Mechanics, $\sigma_{bend.}$, N/m² - at 750°C - at the Final Temperature	9-10 70-71	9-10 82-83	8-9 72-73	13-14 77-78	9-10 78-77	10-11 80-81	8-9 62-63
6	Compression Mechanics, $\sigma_{compr.}$, N/m2 - at 1100°C - at 1150°C - at 1200°C	- - -	54.9 32.2 -	- - -	- - -	21.2 38.0 37.9	- - -	- - -

When considering sintering kinetics, it is important to know whether solid particles are partially or fully soluble in the intergranular, liquid layer. This phenomenon is confirmed by structural studies, where fused grains of quartz and perlite are observed. The small perlite particles are completely melted and mixed with the basic mass (Fig. 8-9). In this case, the force of interaction between grains is due to:

1. Curvature of the liquid surface

$$F1 = ae(1/r1 - 1/r)S \quad (7)$$

2. The free surface of the liquid constituent tending to decrease and not depending on its curvature

$$F2 = La\text{eo}\Psi(V,\theta) \quad (8)$$

Where L is the length of the wetting perimeter, Ψ (V, θ) is a function that depends on the wetting boundary angle θ, the volume (V) of liquid bounded by the grains, and the grain geometry. For spherical grains the radius R will be:

$$S = \pi R^2 \sin 2f \quad (9)$$

$$\Psi(V,\theta) = \sin x \sin(f+\theta) \quad (10)$$

$$\frac{F}{r} = F^1 + F^2 = a_{eo}[\pi R^2 \sin^2 f(\ _1 + 1/r) + 2\pi r \sin fx sin(f+\theta) \quad (11)$$

Where:

$$r1 = R\sin f - [R(1-\cos f)\lambda/2]1 - \sin(\theta + f)\cos(\theta + f) \quad (12)$$

$$R = 2R(1-\cos f) + \lambda/2/2\cos(f+\theta) \quad (13)$$

λ is the gap between the grains.

The formula is valid when the distortion of the liquid meniscus by the force of gravity can be neglected.

Above the optimum temperatures, the wetting angle reaches its critical value

$$\Theta = \pi - f/2 \quad (14)$$

The force that attracts the grains will be neutralised, and in the presence of a large amount of liquid phase, a repulsive force develops between the grains. [21,22]. In this regard, there is a prerequisite for the deformation of the material and the deterioration of its technical properties, as observed in laboratory and production conditions based on the product's overfiring temperatures. Based on the above considerations, a mathematical calculation of the material consolidation process for cases where liquid-phase sintering occurs is presented. Considering that over 1050°C in materials with such composition intensive sintering processes begin due to the formation of a large amount of liquid phase, we recommend stopping firing materials at an early stage of sintering, i.e. at 1050-1080°C due to the long time interval of melting perlite.

Due to the high viscosity of the glaze, the ceramic product does not deform during the firing stage, which has consistently been confirmed.

3. CONCLUSION

The presence of a certain number of mullite crystals in the material in a finely dispersed state, reinforcing the vitreous phase, should contribute to increasing the mechanical characteristics of the product. Optimum sizes of quartz grains, with a little melt around them, favouring the development of tangential stresses, high content of silicon in perlite (≅74 wt.%) and the coexistence of aluminium oxide in the acid vitreous phase should promote the development of Si-0-Al bonds, which, in our opinion, determines the high operational properties of the material.

REFERENCES

1. Geguzin Y.E. – FMM. 1956. vol.2. With. p. 406.
2. Pines B.Ya., Sukhanin N.I. – JTF. 1956. v.26. p.2100.
3. Eremenko V.I., Solomko V.P. – Works of the Institute of Ferrous Metallurgy, Academy of Sciences of the Ukrainian SSR. 1954. No. 8. p.80.
4. Pines B.Ya., Sirenko A.F. – JTF. 1959. v.29. p.653.
5. Zhukov A.V. – Materials and products based on expanded perlite. Publishing house of literature on construction. M. 1972. p. 14-28.

6. Budnikov P.P., Poluboyarinov D.N. – Chemical technology of ceramics and refractories. Literary publishing house on construction. M. 1972. p. 117.
7. Yavits P.N. – On the study of the viscosity and fusibility of some volcanically hydrous glasses. Proceedings of ROSNIIMS 25. 1962. pp. 54-63.
8.Ross G.S., Smith R.H. – Water and other volatiles in volcanic glases. Amer. Mineralogist. V. 40. #11-82. 1955. p.1071-1083.
9. Polinkovskaya A.I., Sergeev N.I., Chernova O.A. – Expanded perlite - lightweight concrete filler. Publishing house of literature on construction, M. 1971, pp. 22-30.
10.Belyankin D.S. – About water in magmas and igneous rocks. Geological Herald. v.6. 1-3.1928. With. pp.19-27.
11. Budnikov P.P., Gevorkyan Kh.O. – On the role of feldspar in the formation of porcelain structure. "Glass and Ceramics". 1952. 3. pp. 19-20.
12. A.I. Augustinic - Ceramics. Leningrad. Stroiizdat. 1957. 8. p. 4-24.
13. G.G. Gaprindashvili, F.Ya. Kharitonov, Z.D. Kovziridze – On the processes occurring during heat treatment of low-temperature ceramics. Georgian Technical University. Tbilisi. 1998.
14. M.P. Volarovich, A.L. Leontieva – Study of the viscosity of obsidians in connection with the question of the genesis of pumice. DAN vol. XVII/ #8 1937/ p.419-421.
15. Lifshits I.M., Slezov V.V. – JETF. 1958. v.35. p.1401.
16.Wagner C. – Z. Electrochemie/ 1961. Bd.65. p. 581.
17. Masuda Y., Watanabe R. – In: Sintering Processes: Material Science Research/Ed. Kuzsynski G.C. – N.Y.; L.: Plenum Press. 1980. V. 13.p.3.
18. Giseron G. Lacombe P. – Rev. Met., 1955. v.52. p.77
19. – Powd. Met. Intern. 1979. v.11. p.1.
20. Ross G.S., Smith R.H. – Water and other volatiles in volcanic glasses. Amer. Mineralogist. V. 40. #11-82. 1955. P. 1071-1083.
21. Polinkovskaya A.I., Sergeev N.I., Chernova O.A. – Expanded perlite is a lightweight concrete filler. Publishing house of literature on construction, M. 1971, pp. 22-30.
22. Belyankin D.S. – About water in magmas and igneous rocks. Geological Herald. v.6. 1-3.1928. p. 19-27.

უაკ 666.367

დაბალტემპერატურული ფაიფურისმაგვარი დეკორატიული კერამიკის მიღება და სტრუქტურული კვლევა

*გ. გაფრინდაშვილი, *ზ. კოვზირიძე, ლ. თარგამაძე, *თ. ლოლაძე, *ნ. ნიჟარაძე, *ვ. ქინქლაძე, *მ. კაპანაძე, **ე. უჩანეიშვილი, **მ. ჩახუნაშვილი, **ა. უსუფაშვილი, **ნ. ენაგელი, **ნ. ყველაიძე, **ლ. კაკაჩია

*საქართველოს ტექნიკური უნივერსიტეტი. ქიმიური ტექნოლოგიისა და მეტალურგიის ფაკულტეტი, ბიონანოკერამიკისა და ნანოკომპოზიტების ტექნოლოგიის ინსტიტუტი, ბიონანოკერამიკისა და ნანოკომპოზიტების მასალათმცოდნეობის ცენტრი. საქართველო, 0175, თბილისი,, კოსტავას 69.

**თბილისის 178-ე საჯარო სკოლა

E-MAIL: kowsiri@gtu.ge

რეზიუმე: მიზანი: ფაიფურის წარმოების ტექნოლოგიით დაბალტემპერატურული კერამიკული ნაკეთობების მიღება და შესწავლა. **მეთოდი:** ნაკეთობების მისაღებად შერჩეულ იქნა წყლიანი სუსპენზიის - შლიკერის ჩამოსხმის მეთოდი თაბაშირის ყალიბებში. შესწავლილ იქნა გამომწვარი კერამიკული მასალების ქიმიური შედგენილობები (მას. %), კერამიკული მასალის დახურული ფორიანობის ხაზობრივი ანალიზი. ფორების სიდიდის ცვლილების და გადანაწილების ხასიათი სხვადასხვა ტემპერატურაზე გამომწვარი კერამიკის სტრუქტურაში და მათი ელექტრონულ-მიკროსკოპიული სურათები.კერამიკულ მასალათა წყალშთანთქმის ცვლილება ტემპერატურისაგან დამოკიდებულებით. მასალათა საექსპლოატაციო თვისებები. **შედეგები:** კერამიკული მასალების გამოწვის ტემპერატურის მომატებით 1080-1120^{0}C-მდე, მასალის სიბლანტე მცირდება, ძლიერდება ზედაპირული ძალების ქმედება ფაზების საზღვრებზე. კრისტალური მარცვლები უახლოვდებიან ერთმანეთს, მასა განიცდის გამკვრივებას და წყალშთანთქმა ფორიანობის მიხედვით მცირდება ნულამდე. მასალა იძენს მაღალ საექსპლოატაციო თვისებებს. **დასკვნა:** ექსპერიმენტების შედეგებიდან ჩანს, რომ მაღალი საექსპლოატაციო თვისებებით კერამიკული ნაკეთობების მიღება შესაძლებელია ფაიფურის წარმოების ტექნოლოგიით.

საკვანძო სიტყვები: წყლიანი სუსპენზია - შლიკერი, ჩამოსხმის მეთოდი, თაბაშირის ყალიბები, მასალათა წყალშთანთქმა, საექსპლოატაციო თვისებები.

UDC 615.2

ROLE OF NANOCOMPOZITES IN PHARMACY

R. Gigauri[1], N. Lekishvili[2], E. Tomasian[3], L. Khvichia[1]

[1]Ivane Javakhishvili Tbilisi State University R. Agladze Institute of Inorganic Chemistry and Electrochemistry, 11, Mindeli St., 0186, Tbilisi, Georgia

[2]Ivane Javakhishvili Tbilisi State University, 1, Chavchavadze Ave., 0179, Tbilisi, Georgia

[3]Kuban State Medical University (Russian Federation)

E-mail: gigaurirusudan@gmail.com

Resume: **Purpose.** The preparation and production of nanocomposite anthelmintics is one of the research and development lines of our institution. Anthelmintic drugs are divided into several groups. Among them, the benzimidazole derivatives are the most popular and widely used. Albendazole is one of the benzimidazole derivatives.

Method: Albendazole and zinc phosphate provide a basis for a nanocomposite anthelmintic synthesized by us, which has an obvious advantage over the available and currently used albendazole-containing anthelmintic drugs in terms of sustainability and minimum side effects. The X-ray fluorescence (XRF) spectroscopy was used to study the structure of the composite; the nanosizes of the composite in nanometers were determined by means of the scanning electron microscope (SEM). Under way are intensive studies to evaluate the anthelmintic physiological activity of our composite on the behavior of mice Line-1 using the standard elevated plus maze (EPM).

Results: Albendazole taken alone and the composite synthesized by us were compared. As a result of observation, the composite was found to have minimum side effects and be devoid of the unbearable weakness and diarrhea, characteristics features of the albendazole-containing anthelmintics. It is also important to check and ensure the drug stability and quality of action, which is so demanded by farmers and zoo veterinarians. Trials in this direction continue.

Conclusion: We have derived a nanocomposite anthelmintic with novel activity from the existing drug (albendazole). Albendazole taken alone has recently been found to act as an angiogenesis inhibitor, implying its use in anti-cancer therapy. It is a drug with anti-carcinogenic properties. Our nanocomposite with its properties and high efficiency will be environmentally safe and cost-effective for manufacturers. Its production will become competitive, both for Central Asian countries and Europe, because scientists have taken into account the request of veterinarians to develop such an anthelmintic drug, which will not be resistant to animals, will have minimum contraindications and maximum activity. We are also waiting for feedback from the manufacturers. Pilot testing on sheep and other large animals is their prerogative. Our prerogative was and still is to develop the most potent and safe anthelmintic

drug by using the up-to-date laboratory equipment and facilities that enabled us to carry out and practically implement quality scientific research.

Key words: nanocomposite, anthelmintic, albendazole, pharmacological group, moniosiosis.

1. INTRODUCTION

Scientists around the world are trying to develop and create effective anthelmintic drugs that will play a positive role, both for human and animal health. As you know, anthelmintics are a group of antiparasitic drugs. They disable or kill the parasites in the body and expel them from the body without causing even the slightest harm thereto. Central Asian countries still use anthelmintics, pentavalent arsenic compounds, such as tin (II) hydrogen arsenate, zinc (II) hydrogen arsenate and others. Despite the fact that these hydrogen arsenates are characterized by persistence, that is, the animal is not resistant to the drug, European countries still demand to replace them with albendazole or other drugs that are resistant to animals. Manufacturers are forced to increase the concentration of albendazole in these drugs or brand them otherwise. With such approaches, mistrust on the part of consumers increases even more. Our goal is to develop and produce such nanocomposite anthelmintics which will be characterized primarily by stability, fewer contraindications, environmentally friendly. Novel activity of the available drug shall be credited as the discovery of a new anthelmintic medication.

2. MAIN PART

The object of our research is an anthelmintic nanocomposite material consisting of albendazole and zinc phosphate with the following molecular formula:

$$C_{12}H_{15}N_3O_2S \cdot Zn_3(PO_4)_2.$$

These two ingredients create a composite material that is completely different from the existing albendazole group drugs. A visual image of the synthesized composite material is given below.

Fig 1. Nanocomposite anthelmintic

The X-ray structural analysis of the synthesized nanocomposite was made to clearly demonstrate an insignificant role of zinc phosphate on the structural change of albendazole, which is shown graphically below.

The XRF spectroscopy fixed an inorganic part in the nanocomposite in metallic form (Zinc), shown graphically below.

Further studies were carried out using transmission electron microscopy. A composite suspension was prepared and a dried sample was spread and measured on a special (5 A and 15000 mm) sieve. Based on the calculation, the nanosize of our composite anthelmintic makes 333 μm. See a visual picture below.

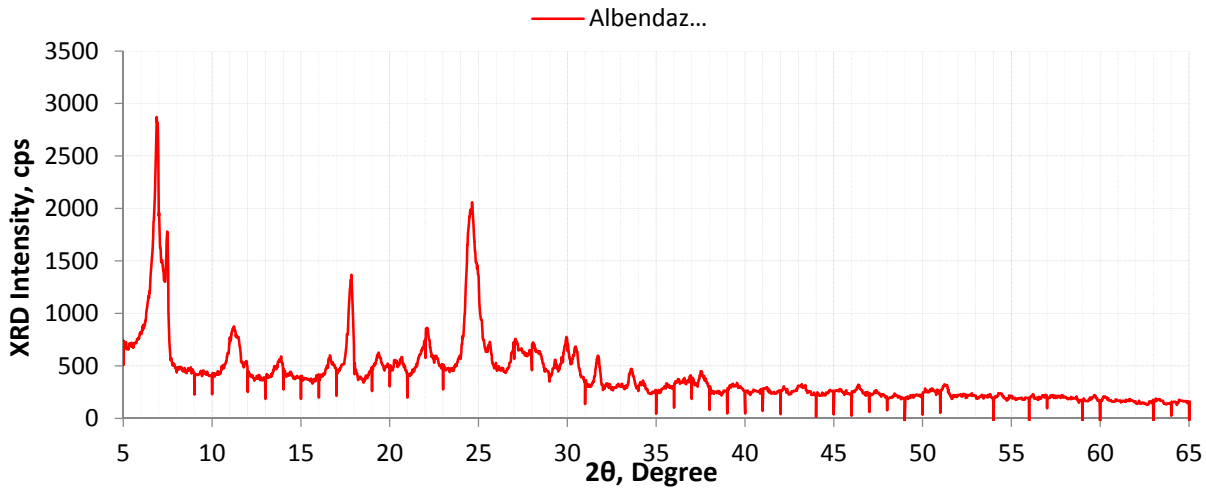

Chart 1. X-ray structure

of the nanocomposite

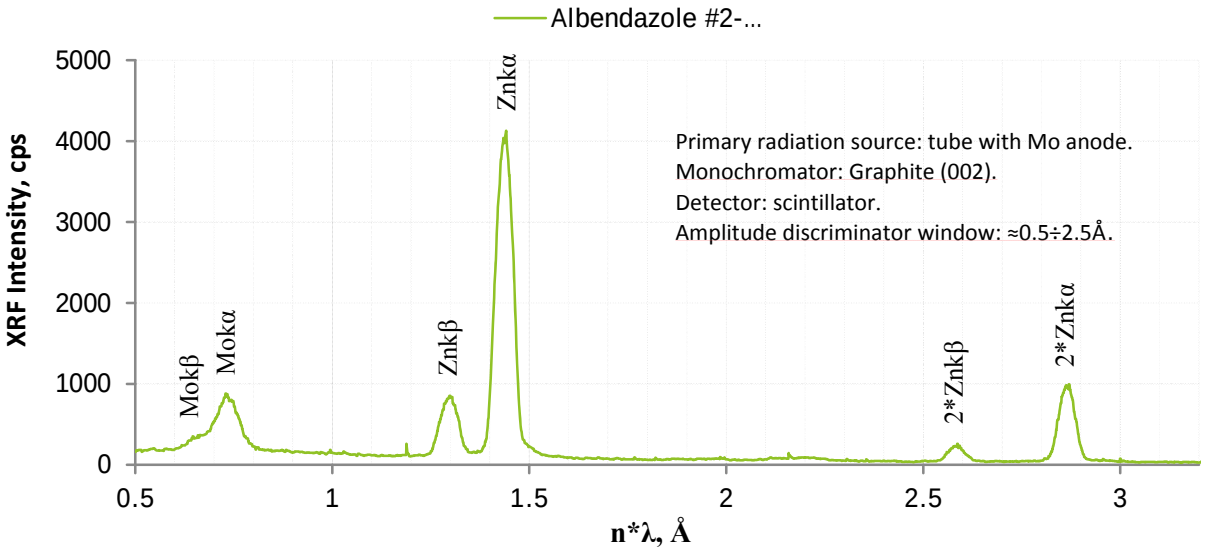

Chart 2. XRF spectroscopy

of the nanocomposite anthelmintic

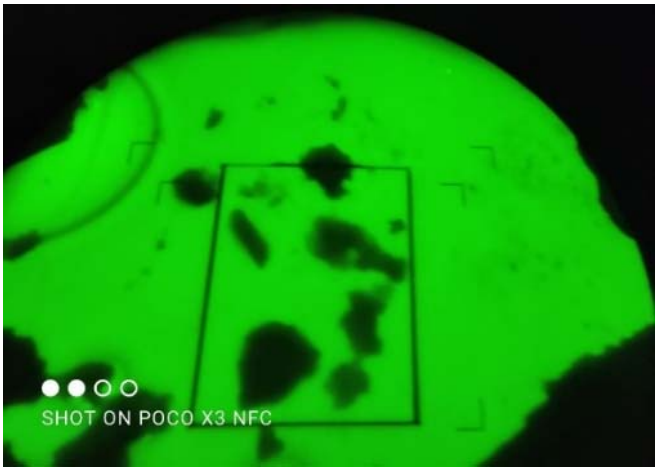

Fig 2. Transmission electron microscopy of the nanocomposite

Based on the obtained results, it was found that that the beam was transmitted only to the surface of the composite and not to the entire depth. This condition may also help to increase the resistance coefficient of the composite anthelmintic. This will already imply our great success, because resistance to the drug will decrease. Under way are studies to evaluate the anthelmintic physiological activity of our composite on the behavior of mice Line-1 using the standard elevated plus maze (EPM). The results of the comparative study of the existing albendazole drug and our composite will be summarized. As a result of the comparison, novelty and favorable results will be revealed, both in terms of sustainability and in the direction of contraindications.

RESULTS AND DISCUSSIONS

The relevance of the nanocomposite anthelmintic presented by us lies in the fact that the drug is characterized by a synergistic action, belongs to the anti-anoplacephalitis remedy, which acts as a catalyst in the process of cell oxidation. In the case of lactose, oxidase and other cases, the composite stops bleeding, oxidizes enzymes, enhances the formation of erythrocytes and leukocytes, maintains the immune system, promotes the growth and development of animals, reduces the risks of any waste retention in the body, and completely frees the body from helminths without irritating it. If we consider the results of the X-ray structural study of the nanocomposite obtained by us, we can see that the inorganic part included in the composition does not participate in the change of the structure of albendazole, which makes us think that it will have a positive effect on the final results. The purpose of adding an inorganic ingredient should be to strengthen resistance, as well as to reduce contraindications (weakness, diarrhea). Based on the results of X-ray fluorescence studies, the inorganic part in the composite appeared in metallic form (zinc). As for the results shown on the transmission electron microscopy, nano-sizes

of rather large crystals (333 nm) were determined. Given that the beam was reflected only on the surface of the sample, we may allegedly opine that this will positively influence the stability of the composite.

3. CONCLUSION

We have derived a nanocomposite anthelmintic with novel activity from the existing drug (albendazole). Albendazole taken alone has recently been found to act as an angiogenesis inhibitor, implying its use in anti-cancer therapy. It is a drug with anti-carcinogenic properties. Our nanocomposite with its properties and high efficiency will be environmentally safe and cost-effective for manufacturers. Its production will become competitive, both for Central Asian countries and Europe, because scientists have taken into account the request of veterinarians to develop such an anthelmintic drug, which will not be resistant to animals, will have minimum contraindications and maximum activity. We are also waiting for feedback from the manufacturers. Pilot testing on sheep and other large animals is their prerogative. Our prerogative was and still is to develop the most potent and safe anthelmintic drug by using the up-to-date laboratory equipment and facilities that enabled us to carry out and practically implement quality scientific research.

REFERENCES

1. Gigauri R., Khvichia L., Arabuli L. Role of anthelmintic compounds in zoological medicine. Advanced Polymer Structures. Chemistry for Engineering Applications, pp. 467-472. CANADA 2024. CRC Press. ISBN : 978-1-7749-301-7 (hlk)
2. Nukita Maruti Gaikwad, et al. Abendazole repurposing on VEGFR-2 for possible anticancer application: In-silico analysis. PMC10431642. PMDI:37585409. 1642. DOI 10.137/journal.pone.0287198.
3. Gogichadze G. Albumins – basic globular proteins, ISBN: 978-9941-10-427-5mfn 146200.
4. Gigauri R., Gigauri N., Kemularia T. Beneficial methods of synthesis of tin (II) hydrogen arsenates, 141/75 /01.2018.
5. Khattab M. and Al-Karmalawy A.A. Computational repurposing of benzimidazole anthelmintic drugs as potential colchicine binding site inhibitors, Future Med. Chem., vol.13, no. 19, pp. 1623-1638, ser. 2021. DOI: 10. 4155/ fmc-2020-0273 [Google Scholar].
6. Gigauri R., Lekishvili N., Barbakadze Kh. Advanced compounds and materials based on natural and secondary resources of Georgian Region, 43.#1. Chem. Georgian Nat. Acad. of Sciences, 2017.
7. Gegenava A., Ugulava M. Methods of chemical analysis in veterinary medicine, St.15642052-002-98.
8. Doudican N., Rodriguez A., Osman I., and Orlow S. J., Mebendazole induces apoptosis via Bcl-2 inactivation in chemoresistant melanoma cells, Mol. Cancer Res., vol. 6, no. 8, pp. 1308–1315, Aug. 2008. pmid:18667591 View article on PubMed/NCBI Google Scholar
9. Ghasemi F., Black M., Vizeacoumar F., Pinto N., Ruicci K. M., Le C. C. S. H., et al. (2017). Repurposing Albendazole: new potential as a chemotherapeutic agent with preferential activity against HPV-negative head and neck squamous cell cancer. Oncotarget, 8(42), 71512.

pmid:29069723 View article on PubMed/NCBI Google Scholar

10. Movahedi F., Li L., Gu W., & Xu Z. P. (2017). Nanoformulations of albendazole as effective anticancer and antiparasite agents. Nanomedicine, 12(20), 2555–2574. pmid: 28954575 View article on PubMed/NCBI Google Scholar,

---

უაკ 615.2

ნანოკომპოზიტების როლი ფარმაციაში

რ. გიგაური[1], ნ. ლეკიშვილი[2], ე. ტომასიანი[3], ლ. ხვიჩია[1]

[1]ივანე ჯავახიშვილის თბილისის სახელმწიფო უნივერსიტეტი რ. აგლაძის არაორგანული ქიმიისა და ელექტროქიმიის ინსტიტუტი

[2]ივანე ჯავახიშვილის თბილისის სახელმწიფო უნივერსიტეტი

[3]ყუბანის სახელმწიფო სამედიცინო უნივერსიტეტი (რუსეთის ფედერაცია)

E-MAIL: gigaurirusudan@gmail.com

რეზიუმე: მიზანი: ჩვენს ერთ-ერთ სამეცნიერო მიმართულებას წარმოადგენს, ნანოკომპოზიტი ანტიჰელმინთების მიღება, წარმოება. ანტიჰელმინთური პრეპარატები რამდენიმე ჯგუფებად იყოფა. მათშორის ყველაზე მეტად გავცელებული და გამოყენებადია ბენზიმიდაზოლის ჯგუფის წარმოებულები. ერთ-ერთი წარმოებულია - ალბენდაზოლი.

მეთოდი: ჩვენს მიერ სინთეზირებული ნანოკომპოზიტი ანტიჰელმინთის ფუძეს წარმოადგენს ალბენდაზილი და ცინკის ფოსფატი, რომელიც განსხვავებულია დღემდე არსებული ალბენდაზოლის შემცველი ანტიჰელმინთური პრეპარატებისაგან : მდგრადობით, მაქსიმალური დაცულობით გვერდითი მოვლენების მიმართ. შესწავლილია კომპოზიტის რენტგენოსტრუქტურა, რენტგენოფლუორესენციური კვლევა, გამჭოლი ელექტრონული მიკროსკოპის საშუალებით დადგენილ იქნა კომპოზიტის ნანოზომები ნანომეტრებში. კვლევები ინტენსიურად მიმდინარეობს ფიზიოლოგიური აქტივობის შესწავლის მიზნით ჩვენი კომპოზიტი ანტიჰლმინთის მიმართ, რაც გამოიხატება ერთხაზიან თაგვებზე ჯვარედინი ლაბირინთის პრინციპით კვლევების განხორციელებას.

მიღებული შედეგები: შედარებულ იქნა ცალკე აღებული ალბენდაზოლი და ჩვენს მიერ სინთეზირებული კომპოზიტი. დაკვირვების შედეგად აღმოჩნდა, რომ გვერდითი მოვლენები მინიმუმამდეა დაყვანილი ჩვენს კომპოზიტში. გაუსაძლისი სისუსტე და დეარია - აღმოფხვრილია. ასევე მნიშვნელოვანია მდგრადობის შემოწმება პრეპარატის მიმართ და მოქმედების ხარისხი, რასაც ითხოვენ დღემდე ფერმერები, ზოოვეტერინარები. ცდები ამ მიმართულებით გრძელდება.

დასკვნები: ჩვენს მიერ მიღებულ იქნა, არსებული პრეპარატისგან (ალბენდაზოლი) ახალი აქტივობის ნანოკომპოზიტი - ანტიჰელმინთი. ალბენდაზოლი ცალკე აღებული ახლახანს აღმოაჩინეს, როგორც ანგიოგენეზის ინჰიბიტორის როლის შემსრულებელი, რაც კობოს საწინააღმდეგო თერაპიაში გამოყენებას გულისხმობს. იგი არის ანტიკანცეროგენული თვისებების მატარებელი პრეპარატი. ჩვენი ნანოკომპოზიტი თავისი თვისებებით და მაღალი ეფექტურობით, ეკოლოგიურად უსაფრთხო, და მომგებიანი იქნება მწარმოებლებისთვის. წარმოება კონკურენტუნარიანი გახდება, როგორც შუაზიის ქვეყნებისთვის ისე ევროპისთვის. ვინაიდან მეცნიერებმა გავითვალისწინეთ მათი მოთხოვნა, რომ შეგვემუშავებინა ისეთი ზოვეტერინალური ანტიჰელმინთური პრეპარატი, რომელიც რეზისტენტული არ იქნება ცხოველთან მიმართებაში და მოხსნის უკუჩვენებების შედეგებს. გაზრდილი იქნება მოქმედების ხარისხი . ჩვენც ველოდებით მწარმოებლებისაგან გამოხმაურებას. საპილოტე ცდა ცხვრებზე და და სხვა მსხვილფეხა ცხოველებზე მათი პრეროგატივაა. კვლევებში გამოყენებულია თანა-მედროვე აპარატურა, რამაც საშუალება მოგვცა შეგვესრულებინა მაღალი დონის სამეცნიერო კვლევები.

საკვანძო სიტყვები: ნანოკომპოზიტი, ანტიჰელმინთი, ალბენდაზოლი, ფარმაკოლოგიური ჯგუფი, მონიოზიოზი.

UDC 621.9.02

FORMULA OF MECHANICAL MODULE FOR CERAMIC MATERIALS

Z. Kovziridze

Georgian Technical University. Institute of Bionanoceramic and Nanocomposite technology. Bionanoceramic and Nanocomposite Materials Science Center Str. Kostava 75. 0175 Tbilisi. Georgia

E-mail: kowsiri@gtu.ge

Resume: Goal. A module is used to describe resistance of materials to various particular forms of mechanical strength or deformation of materials. If in its latter meaning the definition "module" is used for characterization of mechanical properties of a wide specter of materials, and in our case of ceramic materials, at the transition of materials from stable to meta-stable state, that is in the process of disintegration of materials, mechanical module should play a significant role. The research pursued to develop a formula of mechanical module, which would provide us with exhaustive answer about macro- and micro-mechanical properties, macro- and micro-structural constituents, about the role of crystal, glass and porous phases in the process of transition of materials from stable to meta-stable state.

Method. Parameters of the formula were selected on the basis of the study and generalization of micro- and macro-structural, micro- and macro-mechanical characteristics of ceramic materials.

Results. The formula covers the following macro-mechanical properties: module of shift and elasticity, mechanics: at bending with three and four point charge, at contraction and rupture. From micro-mechanical characteristics it considers: Birbaum, Brinner, Schore, all three Rockwell's parameters, properties according to Knup, Wickers and Moos's scale. From the morphological characteristics it considers: mass-volumetric and linear properties of crystalline, glass and porous phases; critical stress intensity factor. Absolutely new definition is introduced into the formula, the factor of porous phase spreading in a lattice. (National Center of Intellectual property of Georgia "Georgian Patent", Certificate of Deposition # 7136. "Formula of Mechanical Modulus of Ceramic Materials and Composites". 2017.10.11).

Conclusion. Thus the offered formula is of a cumulative character and it can be used in technology of any ceramic material and ceramic composites.

The formula doesn't consider Griffith's cracks, dislocations in crystals, nano-defects in glass, but the formula gives us thorough impression about resistance of materials to external loads, which is approximated to the values computed for strength of bonds between atoms. This is namely why the elasticity module was inserted in the formula.

Key words: mechanical module; crystalline phase; glass phase; factor of spreading of porous phase in the lattice; macro-mechanics; micro-mechanics; Kic.

1. INTRODUCTION

In the morphological study of materials, an important role belongs to the crystalline phase, which is the most reinforcing component of the structure. The distribution of the crystalline phase in the matrix and its dimensions significantly affect the mechanical properties (Fig. 1a and b). Finely dispersed sizes, less than 5 μm and their uniform distribution increase the mechanical properties of ceramics of any type, and their large sizes, for example 20-40 μM or more and uneven distribution in the mass of the material reduce not only mechanical, but also other performance properties, such as resistance to thermal and air thermal shocks, electrical and magnetic properties, durability and operation under heavy loads, for example on power lines, etc.(1-3) The glassy phase is a weak component of the matrix compared to the crystalline phase, but if crystals and pores are evenly distributed in it, then it acts as a binder and multiplexor for these phases. Of course, a small amount of the glassy phase will play a relatively positive role in this case, for example, when its volume fraction is less than 12% whilesintering with solid phases. In the case of mixed (12-30 wt.%) and liquid phasesintering (more than 30 wt.%), of course, the mechanics of materials is comparatively weak. The porous phase also has a complex effect on various properties of ceramics.

A great importance has the size of the pores, their volume fraction, shape, closed and round, penetrating or semi-penetrating. The more finely dispersed the pores in the matrix are and the more evenly distributed, the stronger, more durable and resistant the material is to thermal, air-thermal influences and mechanical influences and shocks. Pores significantly influence the complex properties of products: their correct shape, small sizes - less than 5 μM and uniform distribution increase the resistance of ceramics to external loads. When open porosity is zero in terms of water absorption, the volume fraction of closed pores in the matrix usually fluctuates between 1.5 and 9 vol%. As for microcracks invisible to the eye, they are, according to Griffiths, present in any thermally treated material (4.5). Under mechanical load conditions, e.g. during the startup of water or air turbines, the stress intensity is maximum. At this time, stress intensities appear at the crack tip, and in critical cases, cracks, especially large ones, develop (6). A crack at this time can develop at a speed of 2000 m/s and cause an instant disaster. In this case, an important role is played by the critical stress intensity factor Kic, which is associated with the critical intensity of elastic energy release or fracture toughness Gic. In the state of volumetric stresses $K^2ic=EGic\ (1-\mu^2)$, where μ is Poisson's ratio. Stress intensity factor (dik) is a value that determines the normal stress at point 6_y located at a small distance r from the crack tip and expresses local stresses near the crack.

a)

b)

Fig. 1. Morphological electron microscopic picture of the x5400 ceramic sample. (a) Glassy phase with reinforced mullite crystals. b) partially reinforced with mullite crystals. The light areas represent the glassy phase.

A body with a crack under load reaches a limiting state of equilibrium, at which the crack either begins to move or can move with a slight increase in the applied load. In this case, the stress intensity factor will be extremely critical for a given material under given load conditions. In an elastic body with a crack, if the axis is perpendicular to the direction of the crack, Dic is determined in the asymptotic approximation by the expression $K=\lim \sqrt{2\pi r}\sigma y$, Kic is a quantity characterizing the viscous decomposition of the material (6).

2. MAIN PART

Kic is an important parameter for a ceramic material, so we included this value in our formula, the mathematical representation of which is as follows:

$$M = \frac{Kvol.E.Kic.P_d}{Km.Gvol..Pvol..Pm} \quad MPa/\mu/M^2$$

Where Module dimension MPa/ μM2. Kvol isthe volume fraction of the crystalline phase in the matrix, in %; E-modulus of elasticity-MPa; Kic-critical coefficient of stress intensity; Pore redistribution coefficient in P_d material; Km is the average size of crystals in the material- μM; Gvol.-volume fraction of the glassy phase in the material, in%; Pvol.-volume fraction of the porous phase in the material-in %; Average size of Pm pores- μM. Here we will focus on a completely new value - the pore distribution coefficient in P_d material. This value was taken to be 1, and the assessment of its value is entirely up to the researcher based on the morphological picture. Depending on how the pores are distributed in the material, the coefficient value can vary from 1 to 0.8 and is defined as 1. 1st, if the pores are evenly distributed in the matrix and have approximately the same size. The pores in the fired consolidated material have a rounded shape. 2nd By 0.9 if the pore distribution is uneven, and 3rd By 0.8 if the process of pore merging has begun, i.e. the material will be subjected to heat treatment at temperatures above the temperature of its synthesis (Fig. 2 a and b).

a)

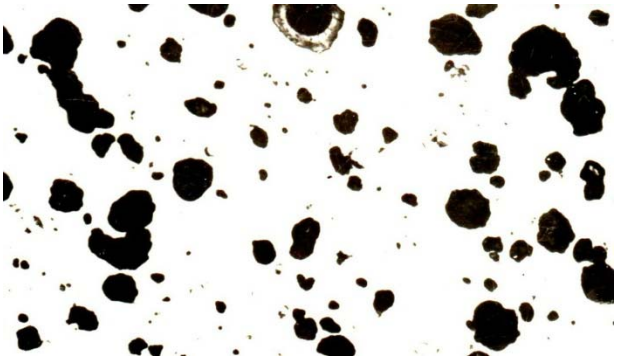

b)

Fig. 2 Morphological picture of the porous phase of Celsian electroceramics. a) Firing at 1450^{0}C, b) Firing at 1500^{0}C.

Callout: **coalescence**, growth of pores in a solid, coalescence of pores accompanied by a decrease in their total surface area while maintaining the total volume unchanged. The process of pore coalescenceis observed at the last stages of coating formation and is determined by an increase in the size of large pores due to the solubility of vacancies in small pores.

Figure 2 shows samples fired at ceramic firing temperatures of the three-component $BaO-Al_2O_3-SiO_2$ system. In both cases, the open porosity is zero in terms of water absorption.1450^{0}C is the optimal tempering temperature for this ceramic, that is, when the material is ready for industrial use. At 1500^{0}C, the ceramics is in the sintering range, water absorption is zero, and pores merge in the matrix, which is clearly visible in Figure b). Obviously, in this case the mechanical strength is reduced to 66 MPa.At 1450^{0}C the mechanical bending strength is 79 MPa. In this case, the pore redistribution coefficient is assumed to be 0.8. 79x0.8=63.2. The difference between 66 and 63.2 is an inaccuracy of -4.24%. In many other cases, the calculated coefficient of redistribution of pore material is within this inaccuracy (7-9). The remaining parameters of the formula are calculated from optical and electron microscopic images obtained as a result of structural studies.As for Kic, it is calculated using the well-known formula:

$$Kic = \frac{0.035\ HV\sqrt{a}}{F(HV/FE)^{2/5}\sqrt{b/a}}$$

Where F is the shape coefficient, which is understood as the ratio of the largest characteristic size of a particle or material to the smallest, and for ceramics it is taken on average equal to 3; HV-microhardness according to Vickers; E-modulus of elasticity-MPa; b-crack imprint length - μm; a - half of the print diagonal - μm;

In the well-known Weibull formula, which characterizes the strength or resistance of a material to various specific types of deformation and is an indicator of the quality of the stress distribution function of a brittle body (6), based on the "weak area" hypothesis. It has the following form:

$$P = 1 - \exp\{-(\sigma - \sigma_l / \sigma_o)^m$$

where, P – probability of decay; σ - breaking stress; σ_l – ultimate stress, i.e. stress which decomposition does not occur; σ_o – normalization parameter; m - is the Weibull module.

The Weibull distribution function is suitable for describing the fracture of brittle bodies in which fracture is initiated by volumetric or surface defects.

3. CONCLUSION

In the formula we developed, the process is described not only by volumetric and surface defects, but also by micro and macrostructural volumetric-surface: crystalline, glassy and porous phase composition, by their distributing in the matrix, by mass volume fraction, percentage content and their development and transformations as a result of chemical and physico-chemical processes during the process of consolidation of materials. These properties are determined experimentally. The most important factor is a completely new coefficient of redistribution of pore material, which, to our knowledge, has not been used anywhere in any formula.It is important to include in the formula the critical stress intensity factor, which includes important micro and macro-mechanical parameters. Our formula provides a

comprehensive answer to complex material properties and is applicable to all ceramic materials and ceramic composites, such as: metal-ceramics, biceramics, mine-ceramics, mine-metal-ceramics and others, which are used in many advanced fields of technology, high technology and everyday life.

REFERENCES

1. Zviad Kovziridze, Hans Walter Hennicke, Fridrich Kharitonov. Thermomechanics of Ceramics. Monograph. Fachhochschule Karlsruhe Hochschule fuer Technik. Karlsruhe. Germany. 1998
2. Hans Walter Hennicke, Friedrich Yakovlevich Kharitonov, ZviadKovziridze, son of David. Barium-containing electrical ceramics are resistant to thermal shock. Monograph Publishing House of Tbilisi University Tbilisi. Georgia. 1992.
3. Z. Kovziridze, N. Nizharadze, G. Tabatadze, J. Anelle. Ceramic and polymer composites. Monograph. Georgian Technical University. 2016.
4. Budworth D.W. Theory of pore closure during sintering. Trans. Brit. Ceram. Soc. 69. 1970 p. 29 31
5. Grifith A.A. Phil. Trans. Roy. Soc. London A.221. 1920
6. Shvedkov E.L., Kovensky I.I., Denisenko E.T., Zyrin A.V. Dictionary Handbook of New Ceramics. Naek Academy of Ukraine Institute of Materials Science Problems. Kyiv. Naukova Dumka 1991. P. 31,115-116
7. Burggraf A.I. Korngroesse. Korngroessenverteilung und Korngrenzen im Zusammenschaften 27. 1977. IV6 s.102-104
8. Dudrova E. Kubelik I. Influence of Sintering Conditions upon the porosity and the strength of compacts. Powder Met., 3. 1979 4. 1. P. 183-185.
9. W. Kollenberg. Technische Keramik. Monograph. Vulkan-Verlag Essen. Deutschland. S. 68.

უაკ 621.9.02

კერამიკულ მასალათა მექანიკური მოდულის ფორმულა

ზ. კოვზირიძე

საქართველოს ტექნიკური უნივერსიტეტი. ბიონანოკერამიკისა და ნანოკომპოზიტების ტექნოლოგიის ინსტიტუტი. ბიონანოკერამიკისა და ნაოკომპოზიტების მასალათმცოდნეობის ცენტრი. 0175 თბილისი. კოსტავას 69. საქართველო

E-MAIL: kowsiri@gtu.ge

რეზიუმე: მიზანი. მასალათა მექანიკური სიმტკიცის ან დეფორმაციის სხვადასხვა კონკრეტული სახეობების მიმართ მისი წინაღობის დასახასიათებლად გამოიყენება მოდული. თუ მის უკანასკნელ მნიშვნელობაში განმარტება მოდული გამოიყენება მექანიკური თვისებების

დასახასიათებლად მასალათა ფართო წრისათვის, ჩვენ შემთხვევაში კი კერამიკული მასალებისათვის - მაშინ მასლათა სტაბილურიდან მეტასტაბილურ მდგომარეობაში გადასვლისას, ანუ დაშლის პროცესში, მექანიკური მოდული მნიშვნელოვან როლს უნდა თამაშობდეს. ჩვენი სამუშაოს მიზანია შემუშავდეს კერამიკულ მასალათა მექანიკური მოდულის ფორმულა, რომელიც მოგვცემს ამომწურავ პასუხს მასალათა მაკრო- და მიკრომექნიკური თვისებების, მაკრო- და მიკროსტრუქტურული მდგენელების, როგორიცაა კრისტალური, მინისებური და ფორიანი ფაზების როლის შესახებ მასaლათა სტაბილურიდან მეტასტაბილურ მდგომარეობაში გადასვლის პროცესში.

მეთოდი. კერამიკულ მასალათა მიკრო- და მაკროსტრუქტურული, მიკრო- და მაკრომექანიკური მახასიათებლების შესწავლისა და განზოგადების საფუძველზე შერჩეული იქნა ფორმულის პარამეტრები.

შედეგები. ფორმულა მოიცავს მაკრომექანიკური თვისებებიდან: ძრაობის და ელასტიურობის მოდულს, მექანიკას: ღუნვაზე სამი და ოთხ წერტილიანი დატვირთვით, კუმშვაზე და წყვეტაზე. მიკრომექანიკური მახასიათებლებიდან მოიაზრებს: ბირბაუმის, ბრინელის, შორის, როკველის სამივე პარამეტრს, კნუპის, ვიკერსის და მოოსის სკალის მიხედვით თვისებებს. მორფოლოგიური მახასიათებლებიდან: კრისტალური, მინისებური და ფორიანი ფაზის მასობივი მოცულობითი და ხაზობრივ თვისებებს. დაძაბულობის ინტენსივობის კრიტიკული კოეფიციენტს. შემოტანილია ფორმულაში სრულიად ახალი განსაზღვრება, მატრიცაში ფორიანი ფაზის გადანაწილების ფაქტორი.

დასკვნა. ამდენად, წარმოდგენილი ფორმულა არის კრებსითი ხასიათის და მისი გამოყენება შესაძლებელია ნებისმიერი კერამიკული მასალებისა და კერამიკული კომპოზიტების ტექნოლოგიაში. (საქართველოს ინტელექტუალური საკუთრების ეროვნული ცენტრი-საქპატენტი. დეპონირების დამადასტურებელი მოწმობა 7136. ნაწარმოები: კერამიკულ მასალათა და კომპოზიციების მექანიკური მოდულის ფორმულა. დეპონირებულია 2017. 10. 11.)

საკვანძო სიტყვები: მექანიკური მოდული, კრისტალური ფაზა, მინისებური ფაზა, ფორიანი ფაზის მატრიცაში განაწილების ფაქტორი, მაკრომექანიკა, მიკრომექანიკა, Kic.

UDC 666.762.93

SMART COMPOSITE IN THE SIC-AL_2O_3-SI-SI_2ON_2 SYSTEM

Z. Kovziridze, N. Nizharadze

Georgian Technical University, Institute of Bionanoceramic and Nanocomposite technology. Bionanoceramic and Nanocomposite Materials Science Center , Tbilisi 0175, Kostava str., 69, Georgia

E-mail: kowsiri@gtu.ge

Abstract: **Goal**. The object of the research was to study the composite received in impure nitrogen medium from silicon carbide, silicon and refractory clay mixture.

Method. With X-ray diffraction, petrographic and electron microscope methods the chemical processes happening at burning of the mentioned mixture in technical nitrogen medium and the kind of received binder, phase composition and basic properties are studied.

Results. It is stated that silicon carbide composite with complex binder is received, the main phases being: Si_2ON_2, $3Al_2O_3 \cdot 2SiO_2$ and SiO_2. SiC-Al_2O_3 composite is also received and studied.

Water and acid resistance of composites (H_2SO_4, p-1.84) and resistance to nonferrous metals and slag are studied.

Conclusion. The received composites can be used for production of protective envelope of thermocouple for measuring of temperature of ferrous and nonferrous metals at high temperatures.

Key words: composite, silicon carbide, nitrogen area, silicon oxinitride, resistance.

1. INTRODUCTION

One of the necessary conditions for production of silicon carbide refractory composite with silicon nitride binder is nitrogen clearing from harmful admixtures. This needs a special expensive apparatus to be used. Hence it was interesting to study composite received in impure (technical) nitrogen medium.

At the same time it is evident that nitride and oxynitride [1,2-4] binders are preferred to oxide one [5-7].

Silicon nitride makes binder formation process technological at 1200-1400^{0}C temperature [8-12].

2. MAIN PART

Silicon carbide, black, grade 53 (SS 26327-84), crystalline silicon, grade Kp-1 (SS 2169-69), and Chasov-Yar (Ukraine) refractory clay, grade P-1, [1-3, 13-14) were used as the initial raw material. Their chemical composition is given in Tabl.1-2.

Table 1.

Chemical composition of silicon carbide and silicon, mass%

material	Si	SiC	Admixtures, mass%							
			Fe	Al	Mg	Zr	Ti	Ca	Cr	Cu
SiC	-	96,18	0,05	0,08	0,40	0,20	0,20	0,15	0,03	0,004
Si	98,85	-	0,60	0,50	-	-	-	0,05	-	-

Table 2.

Chemical composition of Chasov-Yar refractory clay, mass%

Oxides amount, mass%									
SiO_2	Al_2O_3	Fe_2O_3	TiO_2	CaO	MgO	SO_3	K_2O	Na_2O	b.l.
51,23	32,81	0,93	0,90	0,52	0,32	0,20	2,83	0,82	9,4

Cylinders of d-15 mm and h-15 mm were burned in technical nitrogen area at 1000; 1100; 1200, 1300, and 1400^{0}C temperatures in furnace with silicon carbide heaters, grade TK 30-200. Nitrogen is supplied to furnace from the tank via rubber pipe, passing drexel in the entrances regulating nitrogen speed coming out of tank. Drexel with water mounted on furnace exit regulates pressure in furnace so that the speed of nitrogen coming out of pipe be less than the speed of nitrogen entered into reaction pipe. Delay time at the final temperature was 1 hours while speed of temperature rise was 250^{0}C/hr.

Technical nitrogen contains definite amount of oxygen - approximately 5-6%. Our purpose was to determine its effect on physical-chemical processes occurring at the production of refractory and to establish, respectively, the type of the received binder.

Investigation of samples was generally done with X-ray phase (DRON 3 device) and microscopic analysis.

The samples burned at 1000-1100^{0}C are characterized with low strength and their surface is clean. According to microscopic description they generally are constructed of silicon carbide high relief grains of 20-50 micron, its compacting combined mass is constructed of crystalline silicon particles and amorphized refractory clay mixture which under double action of microscope beam is characterized with isotropy.

Fig. 1 (1,2) gives the results of X-ray phase analysis of these samples. X-ray clearly show that phase transition processes are more directed to oxidation due to which diffraction maximums are characterized with the following reflection reflexes: α-SiC (silicon carbide) d_{hkl} 2.625-2.627;

2.573; 2.511-2.515; 2.360; 2.180; 1.539 Å. Crystalline silicon d_{hkl} 3.130; 1.909-1.910; 1.635 Å; SiO_2 (quartz) d_{hkl} 3.34; 2.28; 2.45; 1.815 Å. and amorphized clay.

As is seen from the maximums of diffraction reflection the components comprising the samples burned in nitrogen medium at 1000^{0}C are unreactable and unchangeable resulting in clean and easily breakable surface. The maximums of diffraction reflection of the sample burned at 1100^{0}C (Fig.1 (2)) show that there happen oxidation of crystalline silicon due to which with the decrease of intensity of its characteristic line d_{hkl} 3.13 Å there appear a new formation d_{hkl} = 4.09 Å, the intensity of which is still more growing with the increase of burning temperature to 1200^{0}C and equals d_{hkl} = 4.09 Å. (Fig.1,3).

Evidently, oxidation of crystalline silicon with creation of SiO_2 happens on expanse of technical nitrogen containing oxygen. In the sample burned at 1300^{0}C this process is already lessened and there happen the creation of silicon oxynitride, Si_2ON_2,, and as is seen from Fig.1 (3, 4) it begins at 1200^{0}C and at 1300^{0}C there are noticed the reflexes of diffraction reflection: d_{hkl} - 4.70; 4.41-4.43; 3.34-3.35; 2.414-2.420 Å, Which is increased till 1420^{0}C (Fig. 1.5).

This process can be expressed with the following reaction:

$$3Si + SiO_2 + 2N_2 \rightarrow 2Si_2ON_2.$$

According to microscopic description the samples burned at 1200-1300^{0}C are of sufficient strength and on their surface a thin vitreous film is noticed, sometimes with white coarse surface. According to microscope transmitting beam the sample consists of bluish high relief silicon carbide crystals of the same size and number as in samples burned at 1000-1100^{0}C. SiC binder mass is constructed of silicon oxinitride and products received as a result of phase transformation of burned Chasov-Yar clays which at microscopic intercrossing makes aggregately polarized fine grain mass. At 1200-1300^{0}C clay makes vitreous phase and new mullite formations, from diffraction reflection maximums of which d_{hkl} (mullite) - 3.41-3.42; 2.208-2.214; 5.37-5.41 Å are noted.

Thus, at burning of the above mentioned mixture in technical nitrogen area the refractory composite of silicon carbide with complex: oxinitride, alumosilicate and silica binder are received.

Chemical processes happening at binder receipt and the effect of burning regime on the composition of the received binder were studied with introduction of Al_2O_3 nano powder and the above mentioned components into the composition.

Aluminum oxide, grade GT3000SU, is the product of German company “ALCOA”. Its specific surface is BET = 7.1 m^2/g, average size of primary grains D50=0.435 μM. The properties of samples received with variation of Al_2O_3–SiC and Al_2O_3-Si proportions, the type of the received binder and its composition are studied. Mixture compositions at variation of Al_2O_3–SiC proportions and some characteristics are given in Table 3.

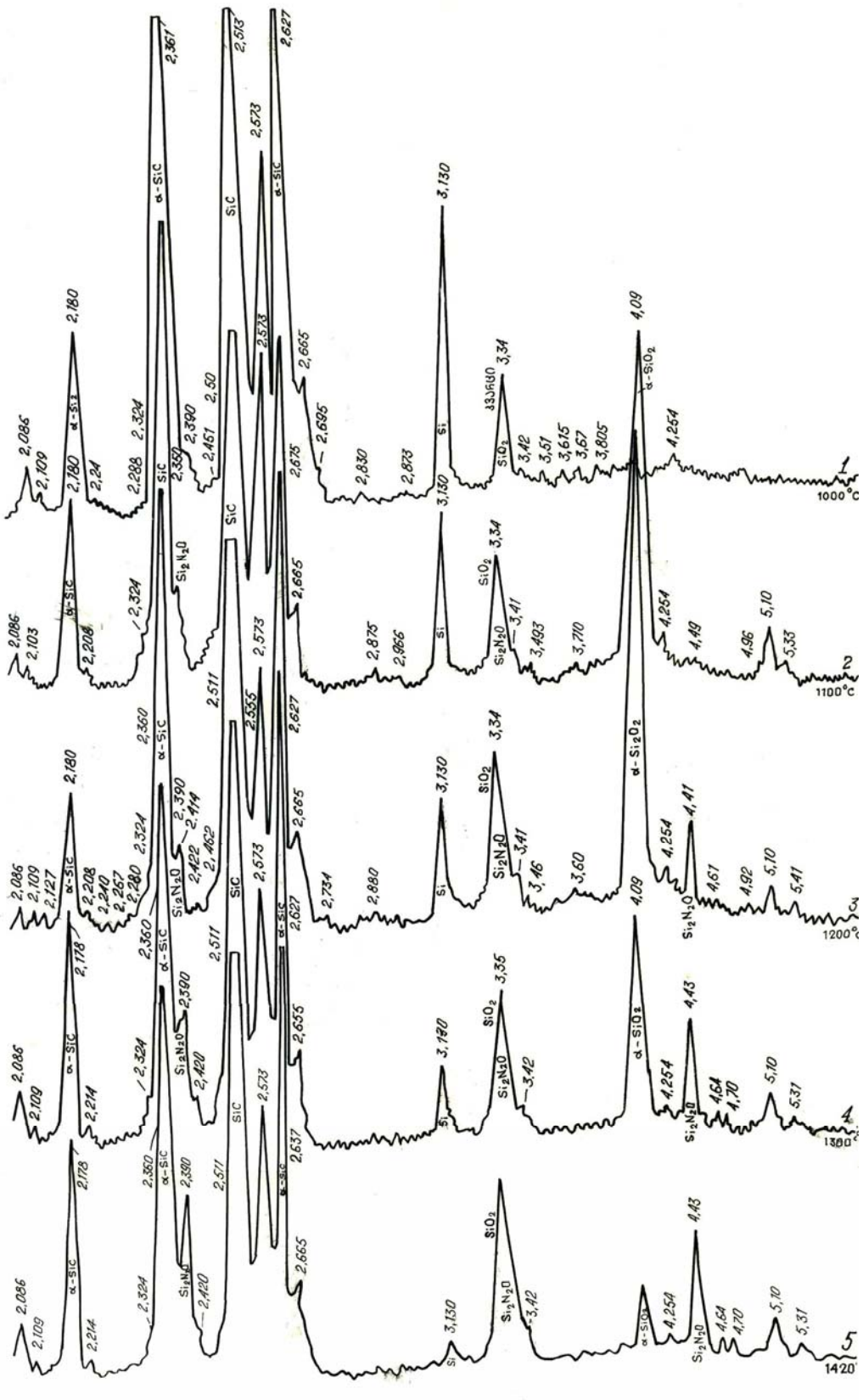

Fig.1. X-ray of silicon carbide, silicon and refractory clay mixture burned in technical nitrogen area at 1000 -1420°C: 1 – 1000°C; 2 – 1100°C; 3 – 1200°C; 4 – 1300°C; 5-1420°C.

Evidently, oxidation of crystalline silicon with creation of SiO_2 happens on expanse of technical nitrogen containing oxygen. In the sample burned at 1300^{0}C this process is already lessened and there happen the creation of silicon oxynitride, Si_2ON_2,, and as is seen from Fig.1 (3, 4) it begins at 1200^{0}C and at 1300^{0}C there are noticed the reflexes of diffraction reflection: d_{hkl} - 4.70; 4.41-4.43; 3.34-3.35; 2.414-2.420 Å,Which is increased till 1420^{0}C (fig. 1.5).

This process can be expressed with the following reaction:

$$3Si + SiO_2 + 2N_2 \rightarrow 2Si_2ON_2.$$

According to microscopic description the samples burned at 1200-1300^{0}C are of sufficient strength and on their surface a thin vitreous film is noticed, sometimes with white coarse surface. According to microscope transmitting beam the sample consists of bluish high relief silicon carbide crystals of the same size and number as in samples burned at 1000-1100^{0}C. SiC binder mass is constructed of silicon oxinitride and products received as a result of phase transformation of burned Chasov-Yar clays which at microscopic intercrossing makes aggregately polarized fine grain mass. At 1200-1300^{0}C clay makes vitreous phase and new mullite formations, from diffraction reflection maximums of which d_{hkl} (mullite) - 3.41-3.42; 2.208-2.214; 5.37-5.41 Å are noted.

Thus, at burning of the above mentioned mixture in technical nitrogen area the refractory composite of silicon carbide with complex: oxi-nitride, alumosilicate and silica binder are received.

Chemical processes happening at binder receipt and the effect of burning regime on the composition of the received binder were studied with introduction of Al_2O_3 nano powder and the above mentioned components into the composition.

The properties of samples received with variation of Al_2O_3–SiC and Al_2O_3-Si proportions, the type of the received binder and its composition are studied. Mixture compositions at variation of Al_2O_3–SiC proportions and some characteristics are given in Table 3.

Table 3.

Mixture compositions and some characteristics

Sample index	Material composition, mass%				Ultimate compression strength, σ, mPa	Open porosity, П, %	Apparent density, σ, g/cm^2
	SiC	Al_2O_3	Si	Chasov-Yar clay			
KA-1	30	45	13	12	146.6	18.50	2.62
KA-2	40	35	13	12	160.5	12.10	2.80
KA-3	50	25	13	12	258.8	3.70	3.36
KA-4	60	15	13	12	120,0	18.80	2.25

It was stated that complex binder has been formed the main composite components of which are mullite ($3Al_2O_32SiO_2$) and silicon oxynitride (Si_2ON_2). By comparison of these data to the received silicon carbide refractory composite which did not contain Al_2O_3 it is clear that SiC with complex binder contained silicon oxynitride, small amount of mullite and SiO_2, i.e. on addition of aluminum oxide to SiC-Al_2O_3 composite SiO_2 phase composition was excluded. Instead, the amount of Si_2ON_2 and mullite has increased. X-ray (Fig.2, 1,2) shows their characteristic lines with higher intensity which undoubtedly has been reflected on the properties of the received composite (Table.3).

In order to determine temperature of components production of SiC-Al_2O_3 binder the samples made of the same mixture were burned at 1000 and 1200^{0}C temperature.

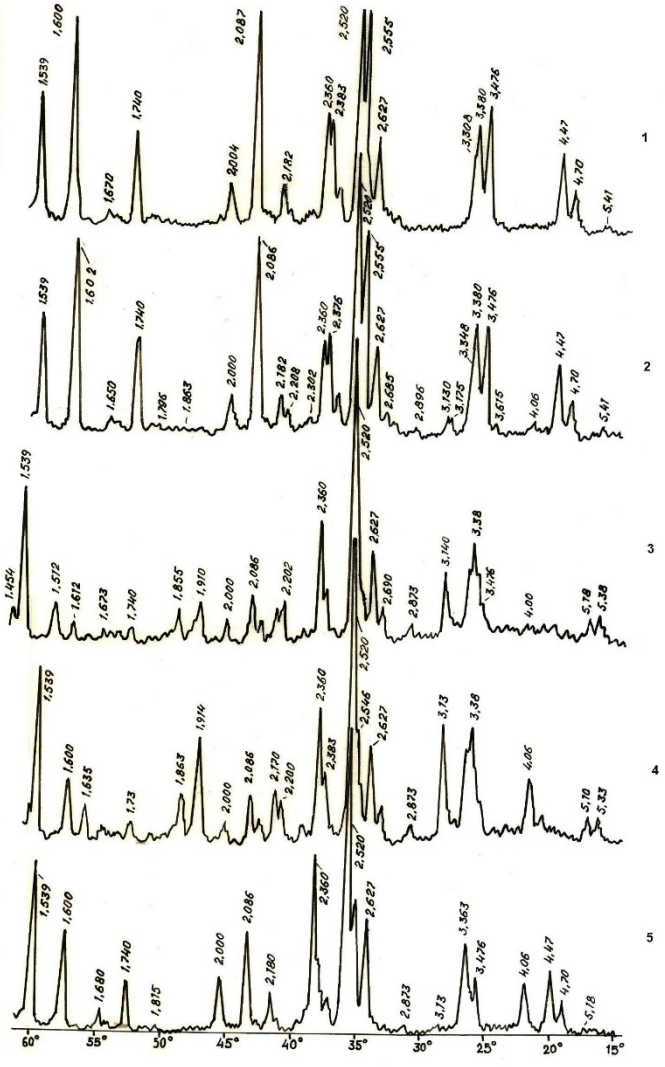

Fig. 2. X-ray of KA-3 composition samples received at thermal treatment at 1420^{0}C with different regimes. Inner layer of the sample received at burning with I regime; 2. Outer layer; 3. With III regime; 4. With V regime; 5. With IV regime.

The X-ray of sample burned at 1000^{0}C (Fig.3) shows the characteristic lines of silicon carbide d_{hkl}, 2.627; 2.52;2.36; 2.182; 2.00; 1.676; 1.54 Å. α - Al_2O_3 d_{hkl}, 3.476; 2.555; 2.376; 2.086; 1.74; 1.60 Å, crystalline silicon - d_{hkl}, 3.132; 1.319; 1.638 Å, quartz (SiO_2) - d_{hkl}, 4.254; 3.348; 2.454; 1.816 Å, while the X-ray of the sample burned at 1200^{0}C shows the peaks of the received silicon oxynitride - d_{hkl}, 4.67; 4.41; 3.348; 2.43; 2.086 Å and mullite - d_{hkl}, 3.43; 2.89; 2.52; 2.21; 1.83 Å.

SiO_2 received at 1000^{0}C is possibly the product of partial oxidation of silicon introduced into the mixture at the expense of technical nitrogen containing oxygen. In our opinion at 1200^{0}C the following reaction has taken place with production of oxynitride:

The analysis of the obtained results shows that on the X-ray of the sample burned with IV regime the main phases are SiC - d_{hkl} 2.627; 2.52; 2.36; 2.18; 1.539 Å, α - Al_2O_3 d_{hkl}, 3.476; 2.547; 2.39; 2.389; 2.086; 1.74; 1.60 Å, silicon oxynitride - d_{hk} 4.70; 4.47; 3.363; 2.422 Å and mullite - d_{hk} 2.685; 2.52; 2.422; 2.208 Å.

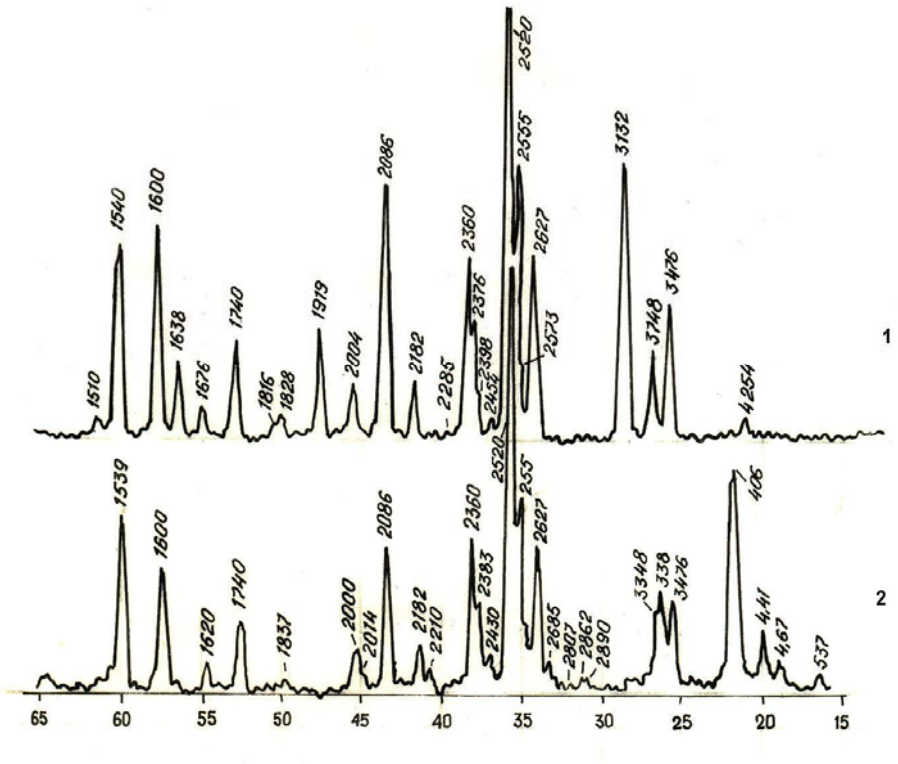

Fig.3. X-ray of KA-3 composition samples burned at 1000 and 1200^{0}C.
1 – 1000^{0}C; 2 – 1200^{0}C

Table 4.

The regime of sample thermal treatment

Regime number	Speed of temperature growth, ^{0}C/min	Burning temperature, ^{0}C	Delay at the final temperature, min	Nitrogen supply
1	5	1420 C	30	Uninterrupted from the beginning to the end
2	5	1000 C	30	From 0^{0}C to 1000^{0}C
3	5	1420 C	20 20 10 10	From 500^{0}C to 600^{0}C From 900^{0}C to 1000^{0}C From 1150^{0}C to 1250^{0}C From 1300^{0}C to 1420^{0}C
4	8 Up to 1200^{0}C in 1200^{0}C-1420^{0}C interval 1.8	Up to 1200^{0}C 1420^{0}C	30	Nitrogen is not supplied 1200^{0}C - 1420^{0}C
5	5	1420^{0}C	30	500^{0}C - 600^{0}C 1200^{0}C - 1420^{0}C

By variation of Al_2O_3–Si proportions for receipt of composites we made up mixtures the material composition of which is given in Table 5. MgO - 1 mass % and Y_2O_3 - 1.5 mass % were added to all mixture above 100%.

From the given components the cylindrical samples were molded by semidry method under 20 MPa pressure. After drying they were burned in furnace in technical nitrogen medium at 1420^{0}C temperature with 1 hour delay.

The main properties of burned samples were checked according the respective State Standards, the results are given in Table 6.

Table 5.

Compositions of Si- Al_2O_3 mixture at proportion variation

Sample index	Material composition , mass%					
	SiC	Si	Al_2O_3	Chasov-Yar clay (Ukraine)	MgO above 100%	Y_2O_3 above 100 %
KN1	40	15	35	10	1.0	1.5
KN2	40	19	31	10	1.0	1.5
KN3	40	23	27	10	1.0	1.5
KN4	40	27	24	10	1.0	1.5

Table 6.

Physical-chemical characteristics of KN1-KN4 composites

Sample index	Ultimate compression strength, σ, MPa	Open porosity, П, %	Apparent density, σ, g/cm²	Thermal resistance, (850⁰C- water) heat exchange	Refracto-riness, ⁰C
KN1	175,00	15,40	2,81	>25	>1770
KN2	120,00	19,80	2,42	>25	1770
KN3	120,00	21,50	2,37	>20	1580
KN4	106,00	20,40	2,32	>20	1620

The samples received with addition of Al_2O_3 are covered with glossy film. The surface of KN4 samples is coarse. Splinters are not glossy.

In order to state phase composition of the received composites X-ray structural analysis was done.

With introduction of Al_2O_3 into SiC-Si mixture and further burning in technical nitrogen area the binder composition has changed. It consists of silicon oxynitride and mullite.

The temperature of binder creation in SiC-Al_2O_3 composite is 1200⁰C.

SiC – Al_2O_3 composite compared to SiC composite is characterized with higher mechanical strength.

Phase composition of the received composite and respectively, its properties vary with changing of thermal treatment regime [15-19].

Nitriding process in SiC- Al_2O_3 composite occurs in the entire layer of the sample.

At variation of SiC - Al_2O_3 proportion the better results are obtained in case of the following proportions: SiC – 50%; Al_2O_3 - 25%; Si – 13%; clay – 12%.

In case of Al_2O_3-Si proportions variation:

SiC – 40%; Al_2O_3 - 35%; Si – 15%; clay – 10%.

i.e. for receiving of SiC- Al_2O_3 composite the optimum composition is:

SiC – 40%; Al_2O_3 - 25-35%; Si – 13-15%;

clay – 10-12%.

For testing water resistance the samples - cylinders with dimensions d – 20 mm and h -15 mm were prepared from the following mixtures: SK, KN1, KN2, KN3, KN4.

Samples were molded with semidry method on hydraulic press under 20 mPa. After drying they were burned in a special stand in nitrogen medium not purified from (technical) oxygen.

Acid resistance was determined in concentrated sulfuric acid (ρ -1.84). For this, samples were prepared (dimensions: d - 20 mm and h – 15 mm) from the following mixtures (Table 8) SK, KN1, KN2, KN3, KN4.

The results of acid resistance of composites are given in Table 8.

Table 7.

Water resistance results

	SK	KN1	KN2	KN3	KN4
Sample mass before test, g	4,98	4,83	4,91	4,77	4,79
Sample mass after test, g	4,98	4,83	4,91	4,77	4,79
Water resistance, %	100	100	100	100	100

Table 8.

The results of composites acid resistance (H_2SO_4, ρ= 1.84 d/cm²)

Sample index	Mass of tested sample, g		Acid resistance , K, %
SK	6,721 6,660	6,635 6,600	98,70 98,19 } 98,44
KN1	6,550 6,910	6,549 6,909	99,98 99,98 } 99,980
KN2	6,060 6,250	6,056 6,245	99,93 99,92 } 99,925
KN3	6,325 6,810	6,324 6,807	99,98 99,95 } 99,970
KN4	3,960 4,110	3,955 4,105	99,97 99,97 } 99,970

Initial, as well as, chemical resistance (water and acid resistance) of composites KN1, KN2 were researched with electron microscopic method at different enlargement (X1000, X3000).

According to electron microscopic pictures the surface of initial samples is not characterized with explicitly formed crystal structure. After treatment in water and, particularly, in sulfuric acid the picture is changed. There appear rather more explicit crystals (Fig.4,a) compared to initial samples, their forms and density increasing from water treated (Fig.4, b) to acid treated (Fig.4, c) ones. This picture is more clear in case of enlargement (X3000; Fig.5).

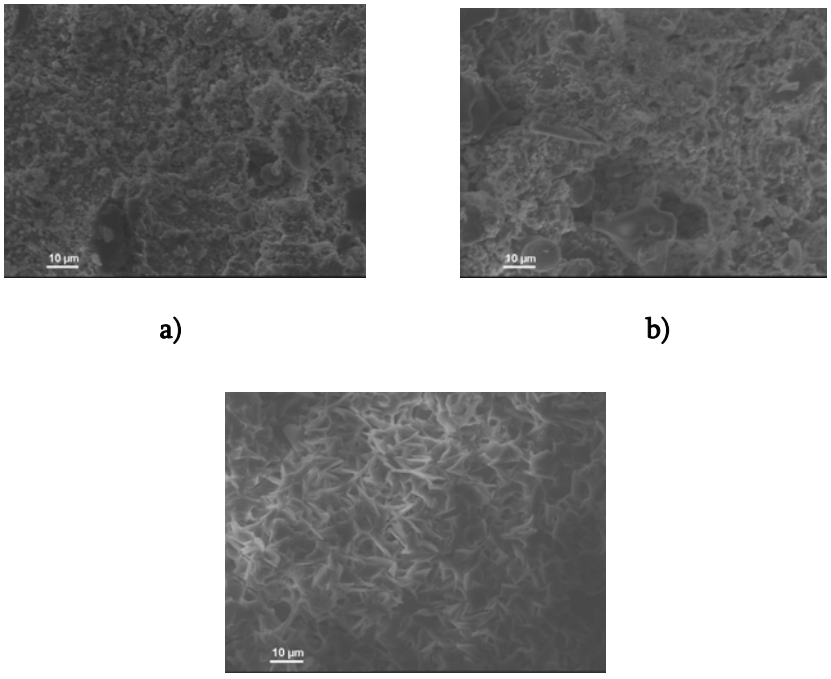

a) b)

c)

Fig. 4. KN1-1000X. a) Initial sample; b) Sample after test for water resistance; c) Sample after test for acid resistance.

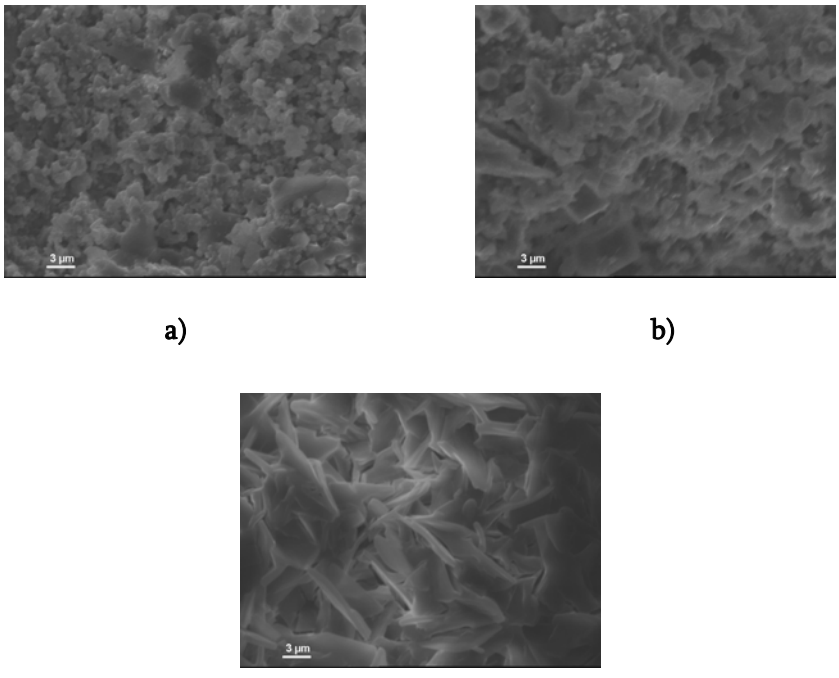

a) b)

c)

Fig. 5. KN1-3000X. a) Initial sample; b) Sample after test for water resistance; c) Sample after test for acid resistance.

This can be explained by the fact that the surface of composites initial samples are covered with thin vitreous film (5-150 nm), which is stronger effected with corrosive media than crystalline part. As a result, in microscope pictures, crystals fixing occurs with vitreous film leaching which being negligible is not expressed in mass losses.

On determination of slag resistance it was considered that metallurgical slags at capillary suction practically do not penetrate into pores with less than 5 mkm radius [15], i.e. refractory materials are not characterized with total porosity. For the structure of porous materials the most important characteristic is pores size.

That's why for determination of slag resistance of the composites received by us it was necessary to determine pore sizes and pore volume of these composites. KN3, KN4 composite samples have been chosen.

We used the instrument: Pascal 240. The tests were held at the ceramic department of Clausthal Technical University, Germany. The results are presented in Fig.6-7.

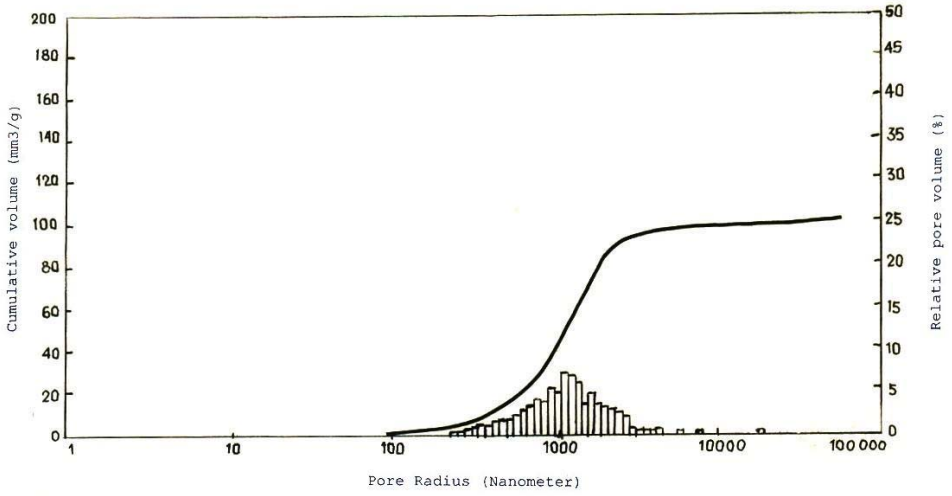

Fig. 6. The relation of volume fraction and total volume of KN3 composite pores to pores radius.

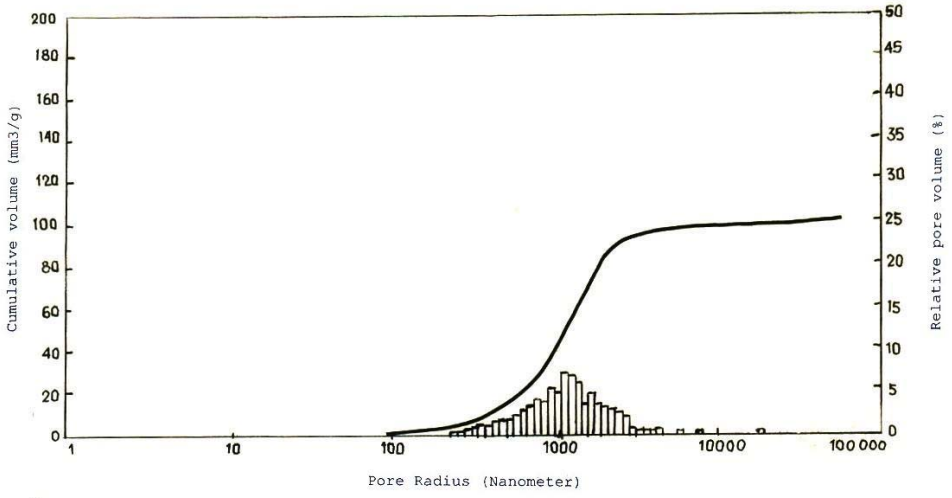

Fig. 7. The relation of volume fraction and total volume of KN4 composite pores to pores radius.

Pore sizes are studied with this method.

As is seen from Fig.6, sample KN3 does not contain pores with radius 100 nm and, of course, in this case its porosity is equal to zero, pore radius growth happens from 100 nm and alongside with radius increase to 1000 nm sample porosity also increases. Pores with radius from 800 nm to 2000 nm are in maximum amount in the sample and, respectively, in this interval porosity sharply increases, it achieves 100 mm^3/g. With further increase of radius their number decreases and in the picture pore volume growth is also slowed down. Then pores of 5000 nm radius practically do not occur and porosity is also unchanged (Fig.6).

The graph in Fig.7 shows that sample KN4 does not contain pores with radius up to 400 nm, with the increase of pore radius from 400 nm to 5000 nm the volume increases. Pore radius increase happens at 5000 nm to 10000 nm but the number of pores with such radius is decreased, therefore volume increase is comparatively negligible. The pores with radius over 10000 nm are also quite insignificant and volume also increases respectively. Total volume of pores achieves 120 mm^3/g, in case of 1000 nm it equals 10 mm^3/g. In case of maximum radius it is 800 mm^3/g.

Unlike sample KN3 in KN4 pores of 1000 nm radius are insignificant and begin to grow from 1000 nm. While in KN3 1000 nm radius pores are in maximum amount and from 15000 nm begin to decrease. Maximum volume in KN3 is 100 mm^3/g and in KN4 -120 mm^3/g.

In refractory materials pores are conventionally divided according size in the following form [16]:

Macro pores 1.7-170 μM

Transient 0.03-1.7 μM

Micro pores <0.03 μM.

The survey of Table 9 and Figs. 6-7 shows that the composites KN3 and KN4 mainly contain transient and macro pores. In these samples maximum size of macro pores is 6000 nm [20]. The most part is from 1000 nm to 5000 nm (Table 10).

Table 9.

Composites porosity and pores total volume

Index	Open porosity, П, %	Apparent density, P, g/cm^2	Maximum total volume, ΣΔV, mm^3/g	ΣΔV, mm^3/g, when pore sizes, nm		
				10-100	100-1000	1000-10000
KN3	26	2.37	102	0	40	100
KN4	29	2.32	119	0	10	115

Slag resistance, in our case, was defined by method of pellets which enables to show well the breaking character of refractory material in relation of the peculiarities of its structure.

For experiment the samples in size d-20 mm and h-15 mm were prepared from mixtures KN3 and KN4, were molded with semidry method under 20 MPa pressure and after drying were burned at 1420^{0}C with one hour delay at the end temperature.

Open-hearth slag pellets were likewise molded with semidry method under 10 MPa pressure and were sited on refractory material samples – cylinders and then thermally treated in furnace at 1450^{0}C with one hour daley at and temperature. The slag treated samples were cut along the axis and then corrosion depth was determined with caliper as the distance from the surface on which samples-tablets were placed to the boundary of slag distribution. The quality of material texture is worse as quickly and as more slag penetrates into refractory. When the surface of refractory-to-slag contact increases rapidly material corrosion and erosion also increase.

Below are given open-hearth slag composition and the results of determination of slag resistance of refractory composites KN3 and KN4.

Table 10.

Open-hearth slag composition

Chemical composition, mass%									
SiO_2	Al_2O_3	FeO	Fe_2O_3	CaO	MgO	MnO	P_2O_5	SO_3	S
18,90	5,63	12,40	4,32	39,20	9,42	8,30	1,11	_	0,32

Table 11.

Slag resistance of refractory composites received on the basis of silicon carbide

Sample title	Mixture composition, mass				Phase composition	Resistance index		
						Cutout diameter, mm	Depth, mm	
	SiC	Si	Chasov-Yar clay	Al_2O_3			Cutout	Penet-ration
KN3	40	23	10	27	α-SiC, mullite, α- Al_2O_3, Si_2ON_2, Si, SiO_2	0	0	2
KN4	40	27	10	23	α-SiC, mullite, α- Al_2O_3, Si_2ON_2, Si, SiO_2	0	0	3

As is seen from the results (Table 11) silicon carbide refractory composites are stable to open-hearth slags. The samples are never etched with slag, saturation diameter of all samples is equal to zero, as to saturation depth for KN3 and KN4 samples they, respectively, are 2 and 3 mm. Pore radii are within 800 - 4000 nm and 1000-6000 nm, respectively (Fig.6-7).

In order to determine crucible metal resistance the following nonferrous metals were chosen: aluminum, tin, lead, brass, bronze and copper. The pieces of these metals were placed in burned crucibles. To avoid oxidation of metals with air oxygen the crucibles heated to metal melting temperature were taken out of sillite furnace and metal surface was covered with friable coke layer. Then crucible was again put into furnace. Test temperature slightly exceeded metal melting temperature. For each test four crucibles were placed in the furnace. Two of them were removed from the furnace after 10 hours and the other two - after 40 hours of testing.

Table 12.

The results of testing of refractory KN1 composite in nonferrous metals

Metal title	Metal melting temperature, ^{0}C	Test temperature, ^{0}C	Test duration, hour	Test results
Aluminum	660,1	900-1000	10 40	No trace of interaction with metal
Tin	231,9	350	10 40	No trace of interaction with metal
Zinc	419,5	550-600	10 40	No trace of interaction with metal
Lead	327,4	550-600	10 40	No trace of interaction with metal
Bronze	1014	1150	10 40	No trace of interaction with metal
Brass	900	1000	10 40	No trace of interaction with metal
Copper	1063	1150	10 40	No trace of interaction with metal

Cooled crucibles were freed from metals and they were visually surveyed. Table 12 gives the results of crucible test which makes clear that as a result of 10 and 40 hours testing refractory crucibles are stable to the above mentioned metals and no metal traces are noticed on crucibles surface [21-31].

3. CONCLUSION

1. Chemical processes having place on burning of silicon carbide, silicon and clay mixture in technical nitrogen medium and the main properties of the received composites are studied.
2. It is stated that on burning in technical nitrogen medium silicon carbide composite with complex binder is received the main phases of which are: Si_2ON_2, $3Al_2O_3 \cdot 2SiO_2$ and SiO_2
3. SiC composites burned in pure and impure (technical) nitrogen medium do not differ in main properties.
4. SiC-Al_2O_3 composite is studied, the type of binder and its composition are stated.
5. SiC-Al_2O_3 composite is received with complex binder. Unlike SiC composite the binder do not contain SiO_2. The increased amount of mullite instead of silica (SiO_2) in binder is conditioned with the fact that the added Al_2O_3 part was connected to SiO_2 forming $3Al_2O_3 \cdot 2SiO_2$. The amount of silicon oxynitride (Si_2ON_2) was also increased. Binder formation begins from 1200^0C.
6. Nitriding process in SiC-Al_2O_3 composite is distributed in the whole layer of sample thickness. It is characterized with high physical-technical indices compared to SiC composite.
7. It is stated that KN1÷KN4 composites are characterized with stability to water (stability 100%), acid (99.97%), nonferrous metals and slag.
8. It is stated that the received composites can be used for preparation of protective envelope of thermocouple for measuring ferrous and nonferrous metals temperature melted at high temperature. For continuous measuring of nonferrous metals and for repeated short-term measuring of ferrous metals.

Acknowledgements

We express our gratitude to Shota Rustaveli Georgian National Science Foundation. The work is done with the grant of the Foundation FR-21-1413 Grant 2022.

REFERENCES

1. Guzman I.Ya., Tumakova E.I., Fedotov A.V. Contrastive researches of some properties of materials on the bases of SiC+Si3N4 and SiC-Si2N2 composites. Moscow, Refractories, 1970, No3, p.44-48.
2. Zabruskova T.N., Guzman I.Ya., Koretnikov H.C. Refractories, 1971, 34, p.55-59.
3. Patrak J. Ber. Deutsch. Keram. Ges., 1972, Bd 47, s. 50.
4. Washburn M.E., Amer. Ceram. Soc. Bull. 1985, v.46, p.553.
5. Kappmeyer K.K. Bull. Amer. Ceram.Soc., 1966, v.45, p.1060.
6. Herbert D.B. Industr. Heat., 1965, v.32, p.925.
7. Washlurn M.E., Lover R.W. Bull. Amer. Ceram. Soc., 1962, v.41, p.447.
8. Samsonov G.V. Nonmetallic nitrides. Moscow, Metallurgia. 1969, p.264.
9. Baumhauer H. Zeit. Kristalogr, 1915, b.5, s.249-259.

10. Collins J., Gerby R.J. Metals, 1955, No 5, p. 612-618.
11. Brokhin I.S., Funke V.F. Receipt and research of some properties of ceramics from silicon nitride, Refractories, 1957, No 12.
12. Rabenau A. Ber.Deutsch. Keram. Ges., 1963, b.40.
13. Kutateladze K.S., Zedginidze E.N., Nizharadze N.S., Vasserman E.M. Nonferrous metals, 1970, No 7, p.5-7.
14. Tickel A., Kramss J. Interceram., 1983, v.32, special issue, p.38-42.
15. W.Kollenberg. Technishe keramik, Vulkan-Verlag, Essen, 2004.
16. Schilm J., Herrmann M., Michael G. Corrosion of silicon nitride in acids J. Eur. Cer. Soc. 23(2003) p. 577-584.
17. Hollstein T., Grass T., Bundschuh K., Schutze M. Das Korrosionsverhalten unterschiedlicher Siliciumnitride in waprigen Loesungen. Keramishe zaitshrift 50 (1998), s. 416-421.
18. Budnikov P., Kharitonov F. Ceramic materials for aggressive media, Moskow, Stroiizdat, 1971.
19. Z. kovziridze, J. Aneli, A. Sarukhanishvili Monograph. Responsiveness of materials to aggressive media. Georgian Technical University. Tbilisi. Georgia. 2008. Pp.129-222
20. Kainarski I.S., Degtyareva E.V. Carborund refractories, Metalurgizdat, Kharkov, 1963, p. 197.
21. Kovziridze Z., Kharitonov F., Medvedovski E., Ceramic electrical insulating materials working in aggressive media, Journal of Georgian Ceramists Association "Ceramics" N 1(9), Tbilisi, 2003, p.3-11.
22. Nickel K.G., Gogotsi Y.G. Corrosion of Hard Materials, in Handbook of Ceramic Hard Materials, Ed.R.Riedel Wiley- VCH, Weinheim. s. 140-182 (2000).
23. G.Ulig. Corrosion of metals (Trans. from German), Moskau. Metallurgy, 1968, 308p. (RUS).
24. K.Kao, V.Huong. Electron transport in solids (Trans. from Engl.), Moskau. MIR, 1984,352 p. (RUS).
25. A.A. Popov, N.Ya. Rapoport, G.E. Zaikov. Corrosion of oriented and stressed polymers. Moskau. Khimia, 1987,232 p.
26. Effect of nuclear radiation on the materials (Ed.J.Herwood), Ship building industry. (Transl. from Engl.), Leningrad, 1962, 300 p. (Rus).
27. Engineering of emale and protector coating, Handbook, ed. L.L.Brogina. Kharkov, KPI, 2003 (Rus).
28. M.Mshvildadze. The production of chemically stable glasses for four components system R20-MnO-B203,-Si02, Dr. dissertation, Georgian Technical University, Tbilisi, 2005. Georgia.
29. A.Sarukhanishvili, T. Cheishvili, Z.Kovziridze. The theoretical principles of composition material obtaining. Georgian Technical Uni¬versity, Tbilisi, 2008.
30. Zviad Kovziridze Physics and kinetics of synthesis. Monograph. Georgian Technical University.Tbilisi Georgia. 2022. Pp.446-488.
31. Zviad Kovziridze, Jimsher aneli, Natela Nijaradze, gulnazi Tabatadze Monograph. Ceramic and Polymer composites. LAP LAMBERT Academic Publishing ISSN: 978-620-2-06984-7 2017. pp. 119-143.,

უაკ 666.762.93

ჭკვიანი კომპოზიტი $SiC-Al_2O_3-Si-Si_2ON_2$ სისტემაში

ზ. კოვზირიძე, ნ. ნიჟარაძე

საქართველოს ტექნიკური უნივერსიტეტი. ბიონანოკერამიკისა და ნანოკომპოზიტების ტექნოლოგიის ინსტიტუტი. ბიონანიკერამიკისა და ნანოკომპოზიტების მასალათმცოდნეობის ცენტრი. 0175 თბილისი. კოსტავას 69. საქართველო

E-MAIL: kowsiri@gtu.ge

რეზიუმე: მიზანი. კვლევის მიზანი იყო სილიციუმის კარბიდის, სილიციუმის და ცეცხლგამძლე თიხის ნარევიდან აზოტის გარემოში მიღებული კომპოზიტის შესწავლა.

მეთოდი. რენტგენოსტრუქტურული, პეტროგრაფიული და ელექტრონული მიკროსკოპის მეთოდებით შესწავლილია აღნიშნული ნარევის ტექნიკური აზოტის გარემოში გამოწვის დროს მიმდინარე პროცესები და მიღებული შემკვრელის სახეობა, ფაზური შედგენილობა და ძირითადი საექსპლოატაციო თვისებები.

შედეგები. მიღებულია სილიციუმის კარბიდის კომპოზიტი კომპლექსური შემკვრელით, ძირითადი ფაზებია: Si_2ON_2, $3Al_2O_3 \cdot 2SiO_2$ და SiO_2. მიღებული და შესწავლილია ასევე $SiC-Al_2O_3$ კომპოზიტი.

შესწავლილია კომპოზიტების წყლისა და მჟავას მიმართ მედეგობა (H_2SO_4, p-1.84) და მედეგობა ფერადი ლითონებისა და წიდის მიმართ.

დასკვნა. მიღებული კომპოზიტები შეიძლება გამოყენებულ იქნას თერმოწყვილის დამცავი გარსაცმების დასამზადებლად მაღალ ტემპერატურებზე სამუშაოდ შავი და ფერადი ლითონებისათვის.

საკვანძო სიტყვები: კომპოზიტი, სილიციუმის კარბიდი, აზოტის გარემო, სილიციუმის ოქსინიტრიდი, მედეგობა.

საკვანძო სიტყვები: კომპოზიტი, სილიციუმის კარბიდი, აზოტის გარემო, სილიციუმის ოქსინიტრიდი, მედეგობა.

UDC 666.762.93

STUDY OF THE EFFECT OF AL_2O_3 NANOPOWDER ON THE PROPERTIES OF SIALON COMPOSITE

Z. Kovziridze, N. Nijaradze, G. Tabatadze, M. Mshvildadze. N. Darakhvelidze

Technical University of Georgia, Institute of Bionanoceramics and Nanocomposite Technology. Bionano-ceramic and Nanocomposite Materials Science Center, 0175, Tbilisi, Kostava Str. 69 Georgia

E-mail: kowsiri@gtu.ge

Resume: ***Objective*** - to obtain a composite in SIAlON-Al_2O_3 system and to study its properties.

Method. Obtaining the composite by metallo thermic and nitrogenation methods. In the present work, the composite containing SIALON is obtained through alum-thermal process, by the reactive sintering method in nitrogen medium, from the mixture of aluminosilicate raw material (Prosyanaya kaolin and Polog refractory clay-Ukraine), nano powder of aluminum oxide (German company "ALCOA"), and metallic silicium with small additives of glass perlite Aragatc (Armenia).

The advantage of this method is that the alumina silicate raw material decomposes during the heat treatment process and the alum-thermal-nitration process takes place at the same time, making it easier to open ALN and AL_2O_3 in the newly formed β-SI_3N_4 crystal lattice, which provides β-Sialon generation at a relatively low temperature, 1250-1300^{0}C.

Result. Corundum-SIALON composite material is obtained by reactive sintering process at a temperature of 1450^{0}C.The corundum and SIALON phases in the composite are confirmed by X-ray phase, spectral and electron-microscopic analyzes. To obtain consolidated samples, the material obtained by reactive sintering was grounded in the attritor and hot pressed at 30 MPa and 1620^{0}C and was kept at the final temperature - 7 minutes. Vacuum – 10^{-3}Pa. The phase composition of the obtained samples remained unchanged after hot pressing, the density increased and the porosity dropped below 0.7%, accordingly the numerical values of the mechanical properties were increased: $\sigma_{press.}$ -1923 MPa; $\sigma_{bend.}$ -470 MPa; HV-19.7 GPa.

Conclusion. obtained corundum - SIALON composite with its physical-technical properties: porosity-0-0.7%; density -3.21g / cm^3; $\sigma_{press.}$ - 1923 MPa; $\sigma_{bend.}$ -470 MPa; HV-19.7 GPa, elasticity modulus -22 GPa; dynamic hardness-3214 N / mm^2; chemical stability to sulfuric acid (density 1.84) - 99.3%, to water -99.9%.

The obtained materials may be recommended in armor engineering, when measuring temperature in metals molten as protective coatings for the thermocouple, as well as in high-temperature furnace linings, as well as in clean processing operations as a metalworking cutting material.

Key words: β-SIALON; corundum; reactive sintering; composite; properties.

1. INTRODUCTION

There are several types of SIALONs: α; β; X; O1; H; R [1-5]. They can be used in oxidizing environments up to 1300^{0}C and in protective environments up to 1800^{0}C [5-7]. Of these diverse types, SIALON exist mainly in the form of three phases: α-, β-SIALON, and also between amorphous or partially crystallized grains. SIALON of α and β categories are characterized by a unique combination, with higher hardnes sand also with high strength usually compared to silicon nitride. The α-SIALON phase is characterized by a higher hardness than the β-SIALON. β-SIALON, like usual silicon nitride, is characterized by a higher impact viscosity. Ceramics are generally characterized by high hardness and abrasion resistance, but are crushable; so, our focus was more on the β-SIALON phase to obtain a composite with relatively high impact viscosity and crack resistance. This is why we have chosen to obtain a composite using alumino silicate raw material by reactive sintering in a nitrogen medium using the alumino thermic method, which ensures the formation of the β-SIALON phase at a lower temperature than when using other methods. [8-24].

2. MAIN PART

Table 1 shows the material composition of the research object.

The chemical composition of Polog clay is as follows (mass %): SiO_2-48.92, Al_2O_3-35.90, Fe_2O_3-1.86, CaO-0.40, MgO-0.30, heat loss - 12.64, refractoriness 1710–1730^{0}C.

Chemical composition of kaolin (wt.%): SiO_2-45.45, TiO_2-O.33, Al_2O_3-38.70, Fe_2O_3-0.46, MgO-trace, CaO-0.36, Na_2O-0.45, K_2O-0.60, heat loss – 13.63. refractoriness– 1770^{0}C.

A detailed description of the composition of the composite is given in the papers [8-24]. The phase analysis of the consolidated sample after hot pressing is shown in Figure 1.

Table 1

Material composition of CN-8 composite, wt.%								
Composite	Geopolymer							
	Prosyanaya kaolin (Ukraine)	Polog clay (Ukraine)	Al	Al_2O_3	Si	Perlite (Armenia)	MgO	Y_2O_3
CN–8	13.9	4.63	23.15	27.78	25.00	2.78	0.92	1.8

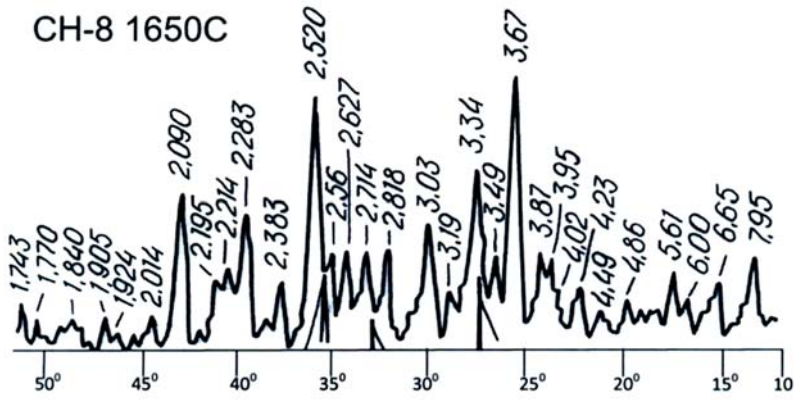

Figure1. X-ray of the hot-pressed composite CN – 8

Figure 1 shows a CN-8 composite radiograph showing SIALON-like reflexes - d_{hkl}: 6,65; 5,45; 3,87; 3,67; 2,520;2,21; the characteristic diffraction peaks of corundum are also observed – d_{hkl}: 3,49; 2,52; 2,36; 2,09, which we introduced into burden to reinforce the SIALON phase.

The physical-technical properties of the obtained samples were studied. The results are presented in Table 2.

The porosity and density of the samples were determined by the hydrostatic weighing method, while the compressive strength and bending strength were determined on a 2054 p5 tensile machine. The results presented in Table 2 allow us to say that the samples of the composite of the selected composition obtained by hot pressing at 1650^0C and pressure of 30 mPa are consolidated and the phase composition corresponds to the set goal, which is confirmed by electron-microscopic examination.

Figure 2 shows the electron microscope image of CN-8 composite fracture obtained at 1650^0C temperature.

As can be seen from Figure 2, the composite consists of two solid phases: the thinnest grains of corundum located in the SIALON matrix, the porous phase is also represented by a small number of thin pores.

From the fracture images it is clear that the material has a decomposing plastic character, a crack is formed in the SIALON phase and its distribution is limited by both the SIALON and the finest nano grains of corundum.

The pores are mostly rounded, the average diameter of the pores is calculated (Table 3). The total volume of the closed pores reaches 1.58% slightly different from the number of pores determined by the hydrostatic method, which should be attributed to the error of porosity measurement by each method. Transverse and semi-transverse pores are not observed in the matrix. Based on the morphological images, the distribution of pores in the material is between equal and unequal. We considered that the distribution factor of the pores in the matrix according to Z. Kovziridze's formula will be: 0.9 [25].

Table 2

Physical-technical properties of CN-8 composite obtained by hot pressing at 1600⁰C and 1650⁰C temperatures

Composite name	Apparent porosity, w%	Total porosity, ∏, %	Density ρ, g/cm³	Compression strength, σpress. MPa	Bending strength, σbend. MPa	Vickers hardness HV,GPa
CN-8 (1600⁰C)	0,7	2,49	3,17	1614	456	16
CN-8 (1650⁰ C)	0,01	0.13	3,21	1923	470	19.7

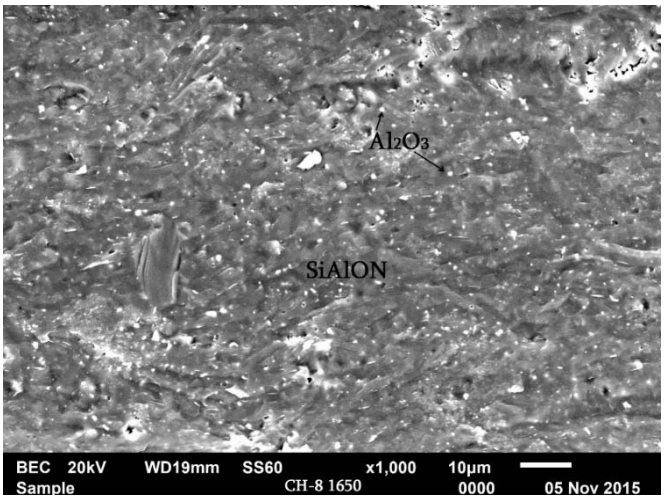

a)

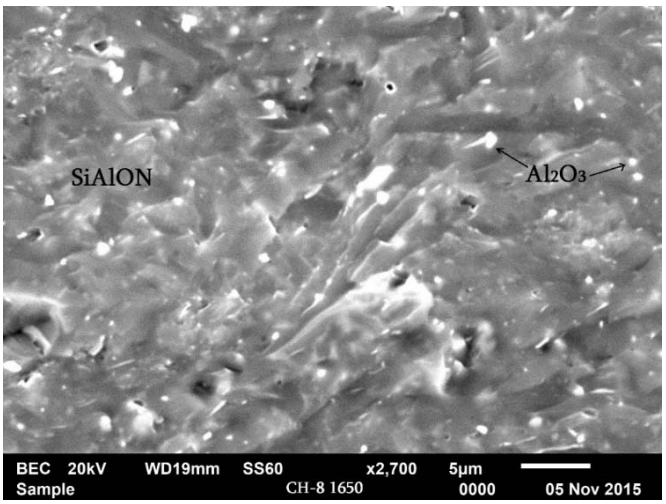

b)

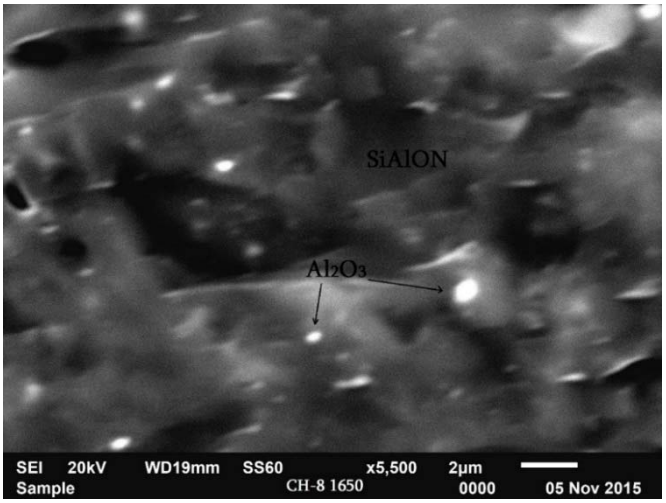

c)

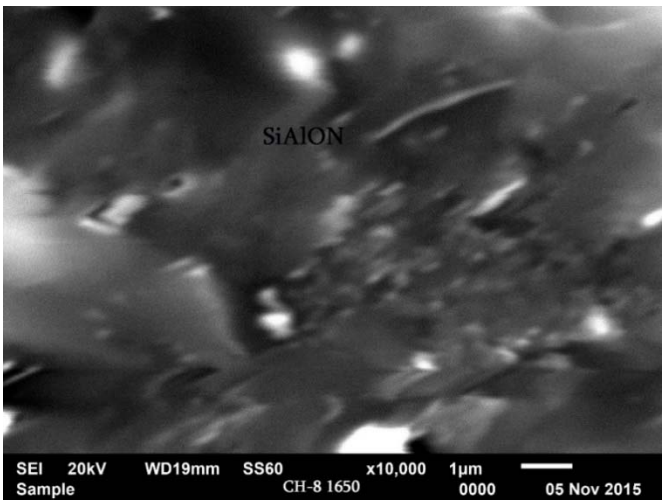

d)

Figure 2. Electron microscope images of CN-8 composite fracture obtained at 1650⁰C temperature

Table 3

Porous phase analysis

Composite CN–8	Vision field S,μM²	Number of the counted pores, n	The biggest pore $D_{max.}$ μM	The smallest pore $D_{min.}$ μM	Pores $D_{mid.}$ μM	Content of pores,%
1600⁰C	345	8	2.0	0.2	0,4	1,98
1650⁰C	345	10	2.0	0.15	0,38	1,17
Average	345	18	2,0	0,15	0,4	1.58

We used Z. Kovziridze's formula for calculating the dependence of macro-mechanical properties of the obtained composite on the porous phase in the matrix:

$$\sigma_{m/p} = \frac{P}{P_m \cdot F_p \cdot P_d \cdot P_{vol}}.$$

Where: P is load, MPa; F_p – shape factor of the pore; P_d – pores distribution factor in the matrix. The mentioned value equals to 1; the evaluation of this parameter depends on the researcher, basing on the morphological picture. Depending on how the pores are distributed in the material and what size they are, the value of the factor can vary from 1 to 0.8. If the pores are evenly distributed in the matrix and they are about the same size, the factor will be equal to 1. The factor is equal to 0.9, if the pore distribution is uneven and finally equal to 0.8, if the pore coalescence[1] process is initiated; $P_{vol.}$ – the volume fraction of the porous phase in the matrix; P_m – the middle size of the pores.

$$\sigma_{m/p} = \frac{470}{0{,}4.0{,}9\ .1\ .0{,}855} = \frac{470}{0{,}308} = \frac{1526MPa}{\mu M}.$$

The middle pore size 0.855, was taken from a sample sintered at an average of 1650^{0}C: 0.13 equal to that obtained by hydrostatic weighing and visual analysis of electron microscopy images - 1.58 wt.%.

Crystalline phase content and average sizes

We determined the dimensions and content of corundum grains in different fields of vision and calculated the phase corundum content in the composite (Table 4). The corundum grain content may actually be higher because the resolution of the finer corundum grains is limited. Since the mixture contained perlite, the composite also contained a certain amount of glassy phase. Aragats perlite is a completely glassy mass (96 mass% is glass, the rest plagioclase, pores and volatiles) that melts at 1240°C. [26].

Presumably, the added 2.78% perlite in the composition produces eutectic melted with the geopolymer ingredients, especially with the alkaline oxides, and, of course, the glassy phase content (Vgp), in the material increases. We got its content equal to 6.5%. Therefore, the number of **crystalline phases** must be equal to:

100-(Vpp[2]+Vgp[3]) =100-(0.8+6.5) =92,7%,

From here the SIALON phase will be 92.7-23.5 = 69.2%. As for the dimensions of the SIALON grains, its structure is presented in the form of leaf packets and in the field of visions seen as a continuous matrix.

---

[1] **Coalescence** - An increase in pores in a solid body, accompanied by the decrease in their total surface area when the total volume does not change. The coalescence process of the pores is observed at the last stages of sintering and is determined by the increase in the size of the large pores due to the vacancy solubility of the small pores.

[2] **Vpp** - volume of the porous phase;

[3] **Vgp**- volume of the glass phase.

Table 4

Content of corundum grains in the composite

Composite CN-8 CN–8	Phase name	Field of vision S, μM²	Number of the counted grains, n	The biggest grain Dmax. μM	The smallest grain Dmin. μM	Dmid. of the grains, μM	Phase content, %
1600⁰C	Al_2O_3	22,22	32	1,00	0,25	0,50	23,1
1650⁰C	Al_2O_3	30,55	39	1,50	0,20	0,49	23,9
	Average	23,88	3,55	1,5	0,20	0.495	23,5

Micro spectral analysis of composite samples was performed, the results of which are consistent with the results of X-ray and electron-microscopic analyzes. The results of micro-X-ray structural analysis are presented in Figure 3a, b, c, d. The correlation[1] dependence of the crystal phase influence on the micro- and macro-canine properties of the materials was calculated according to Kovziridze [27] formula:

$$\sigma_d = \frac{\text{P.Fkd}}{\text{Km Kv Fkf}},,$$

Where P is load; Km – the middle size of the crystals; Kv – volumetric share of crystals in the matrix; F_{kd} – distribution factor of crystals in the matrix, determined by the researcher; in case of even distribution it equals to 1, in case of uneven distribution - 0.9.F_{kf} – crystal shape factor. It is taken as the ratio of the largest characteristic size of the crystal to the smallest, which allows us to characterize the shape of a given set of crystals.

Since the volumetric share of crystals in the matrix is very high - 92.7%, we assumed the F_{kd} distribution factor equal to 1. The average size of crystals for Km aluminum oxide is 0.495 μM. SIALON crystals could not be measured due to the un sharpness of their contours. Visually we assumed the average size of its crystals and aluminum oxide crystals totally equal to 2.5 μM. In this particular case, the shape factor we assumed to be equal to 1 for aluminum oxide crystals having a rounded shape, and 2.5 for SIALON having an elongated shape. In total, we got a form factor equal to 2.5:

$$\sigma_d = \frac{470 \text{ x } 1}{2.5 \text{ x } 92.7 \text{ x } 2.5} = 0.811.$$

[1] **Correlation** – linear connection between random events. The measurement of correlation is the empirical coefficient of correlation.

As can be seen from the result, there is a high correlation and this is understandable, since the content of the crystalline phase is high, the degree of dispersion of the crystals is also high, and the result is achieved by the fact that the phase is evenly distributed in the matrix. The main phase constituent in the matrix is the crystalline phase.

The dynamic hardness and elasticity modulus of the obtained composite were determined on the DUH-211S dynamic ultra-micro dynamic hardness tester in accordance with the requirements of the modern ISO-14577 international standard.

Dynamic hardness (DH) is determined by the magnitude of the load applied to the indenter during the testing process and the depth of its penetration into the material. The advantage of this method over conventional static measurements or diagonal measurements of indentation is that it contains both plastic and elastic components. The measurement results do not depend on indentation size, loads, and heterogeneity of elastic recovery. Dynamic hardness had been determined in a loading-unloading mode before elastic relaxation occurred.

In the scientific literature, correlation implies a statistically significant relationship between the parameters of different processes. Such an explanation of the term is not strict.

Analysis of the indentation of the indenter after the hardness measurement is presented in Figure 5.

As can be seen from Figure 4, the boundaries of the indentations are distinct and no crack is observed even at 1000 mN load, indicating the high cracking resistance of this composite.

Mechanical modulus of materials

For calculating the mechanical modulus of the material, the formula of Kovziridze [28] module was used:

$$M = \frac{Kvol.\,E.\,Kic.\,Pd}{Km.\,Gvol..\,Pvol..\,Pm}\,MPa/\,\mu M2,$$

whereKvol is the volume of the crystalline phase in the material in%; E– elasticity modulus MPa;Kic – critical stress intensity factor;Pd – the pores distribution factor in the matrix, which is taken equal to 1 in the case of even distribution, equal to 0.9 1 in the case of uneven distribution and 0.8 in the case of coalescence of the pores. Km – the middle size of the crystals in the matrix, μM; Gvol – the content of the glassy phase in the matrix, %; Pvol. – pores volume in the matrix, %;Pm – the middle size of the pores in the matrix. Modular dimension is MPa/μM^2. The formula cannot take into account Griffiths [29] cracks, dislocations in crystals, nano-defects in glass, but the formula gives us a complete picture of the resistance to external loading of the material, which is close to the calculated values of the bond strength between atoms. This is exactly why the elasticity modulus is included in the formula:

M=92.7x8,987x40.75x0,9/2,5x6.5x0.855x0.4=

=30184.6/7.6=5.45 GPa/μM^2.

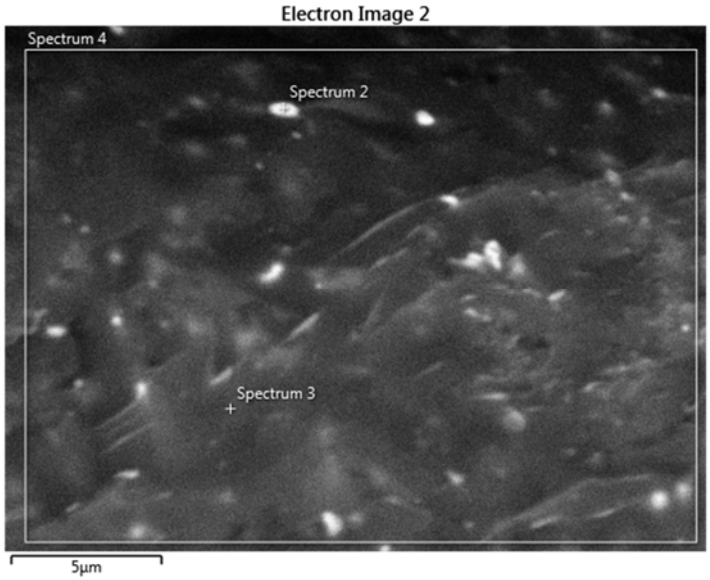
Electron Image 2
Spectrum 4
Spectrum 2
Spectrum 3
5µm

a)

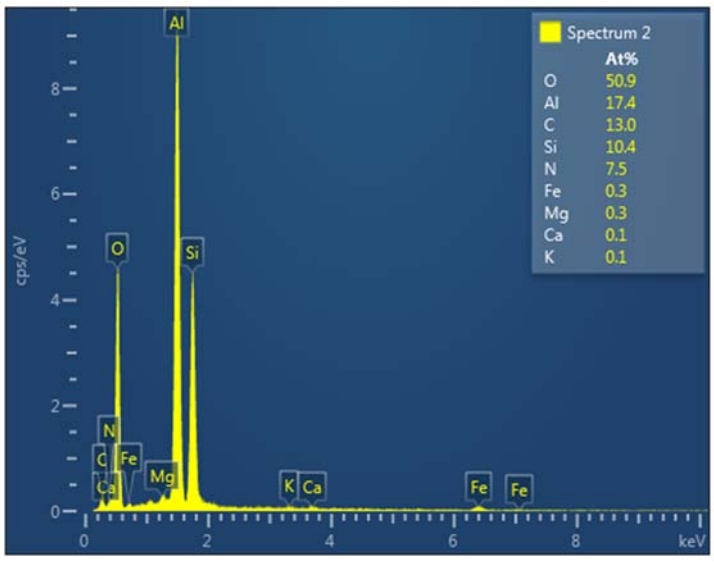
Spectrum 2
At%
O 50.9
Al 17.4
C 13.0
Si 10.4
N 7.5
Fe 0.3
Mg 0.3
Ca 0.1
K 0.1
cps/eV
keV
Al
O
Si
N
C
Ca
Fe
Mg
K
Ca
Fe
Fe

b)

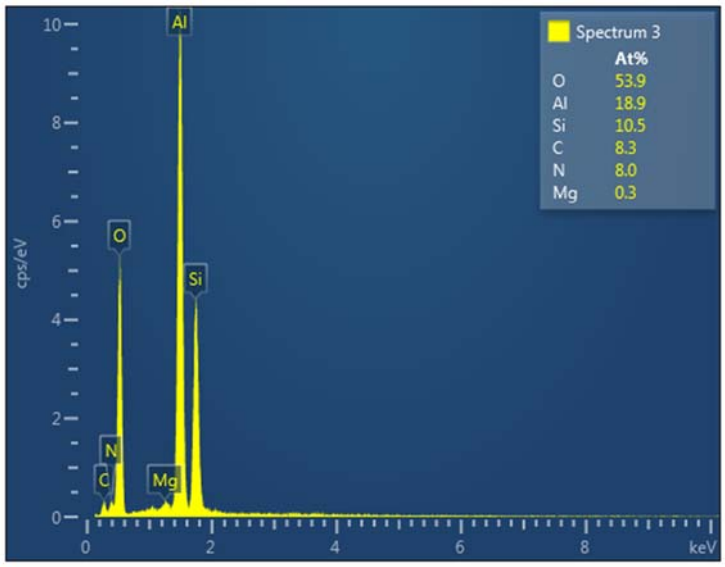

c)

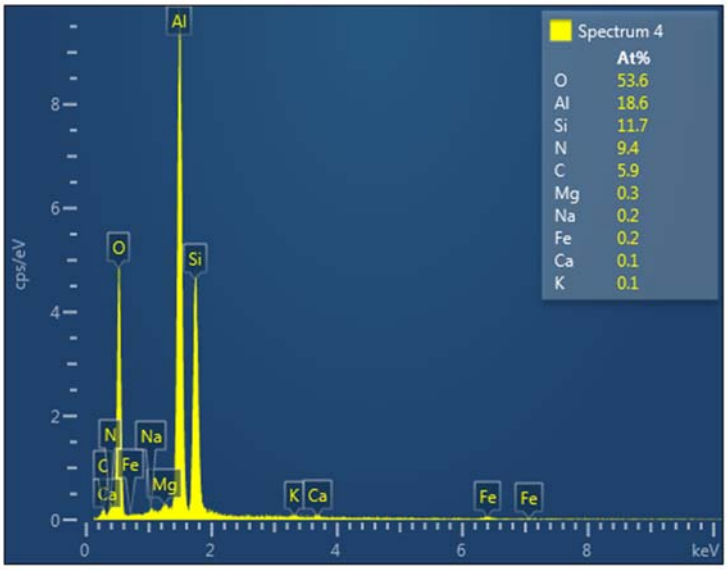

d)

Figure 3. Results of microspectral analysis of CN-8 composite obtained at the temperature of 1650^{0}C

Table 5

Micromechanical characteristics of of CN-8 composite obtained at the temperature of 1650⁰C

<<*** Test condition-CH8-1650 ***>>

Test mode	Load-unload		
Sample name	CH8-1650	Sample No.	CH8-1650
Test force	200.00[mN]	Minimum force	1.96[mN]
Loading speed	1.0(70.0670[mN/sec])	Hold time at load	5[sec]
Hold time at unload	3[sec]	Test count	3
Parameter name		Parameter	20
Comment	24.11.15. .SH8-1650-Tex -Uni-200		
Poisson's ratio	0.250		
Cf-Ap,As Correction	ON	Indenter type	Vickers
Read times	2	Objective lens	50
Indenter elastic	1.140e+006[N/mm2]	Indenter Poisson's ratio	0.070

<<*** Test result ***>>

SEQ	Fmax	hmax	hp	hr	DHV-1	DHV-2	Eit	Length	HV	Data name
	[mN]	[um]	[um]	[um]			[N/mm2]	[um]		
1	206.11	1.2419	0.4801	0.6795	666.193	4435.000	9.252e+004	4.517	1910.017	CH8-1650(1)
2	210.42	1.3860	0.6371	0.8510	546.009	2550.168	8.182e+004	4.517	1949.885	CH8-1650(2)
3	206.11	1.2701	0.6173	0.7663	636.923	2659.186	9.501e+004	4.517	1910.001	CH8-1650(3)
Average	207.55	1.2993	0.5782	0.7656	616.375	3214.785	8.979e+004	4.517	1923.301	
Std. Dev.	2.484	0.076	0.085	0.086	62.672	1058.143	7007.244	0.000	23.023	
CV	1.197	5.879	14.783	11.204	10.168	32.915	7.804	0.000	1.197	

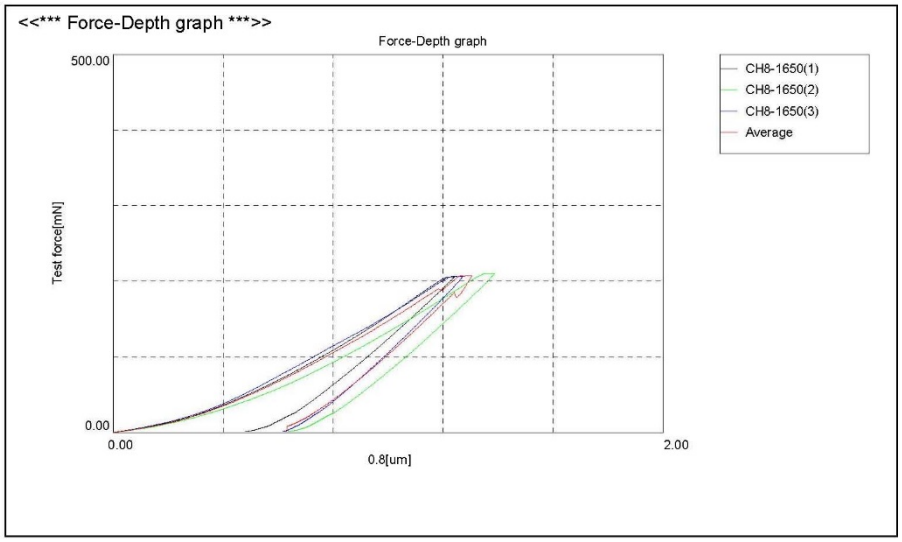

a)

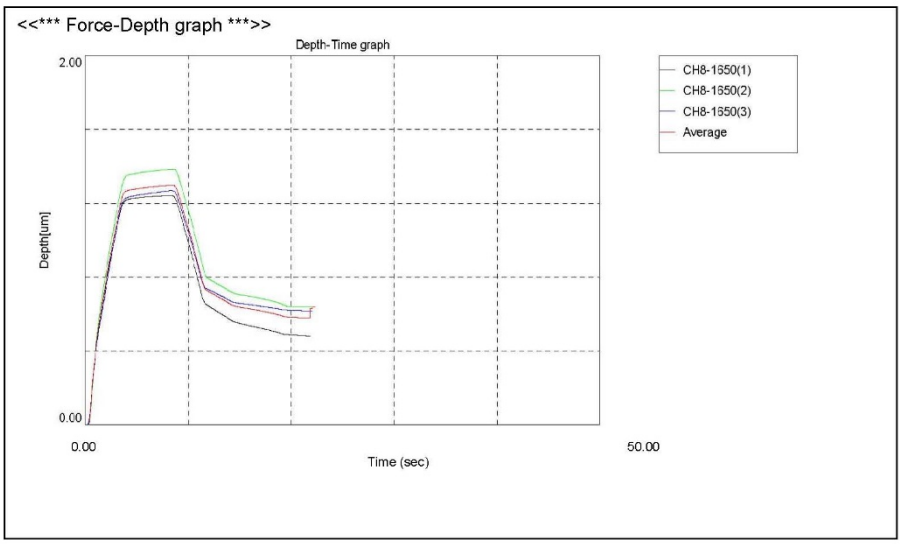

b)

Figure 4. Micromechanical properties of CN-8 composite at a load of 2 mN:
a) the dependence of the deepening in the indentor material on time;
b) the dependence of the indenter load on the indentation depth

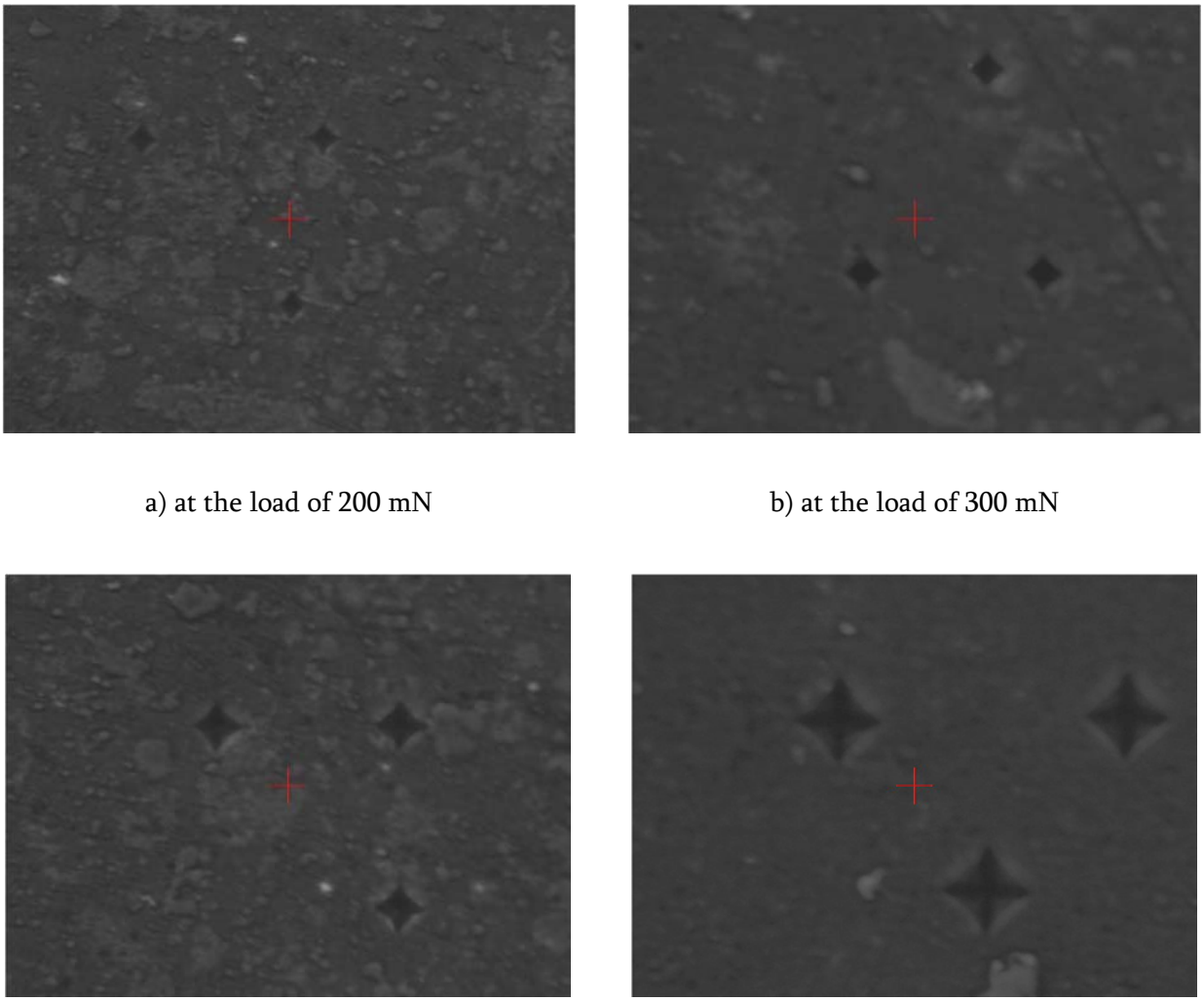

a) at the load of 200 mN

b) at the load of 300 mN

c) at the load of 500mN

Figure 5. Indentation of the indenter at different loads

Table 6

Average sizes of indentations and cracks

# Indentation picture and the value of the load, mN	Penetration depth of the indenter into the material, h, μM	Indentation diagonal length a, μM	Half a length of the indentation diagonal a/2. μM	Average length of crack ℓ, μM	Note
a)100	0.8200	3,546	1.773	The crack is not fixed	The indentation is taken on the matrix
b) 200	1.2993	4,517	2.258	The crack is not fixed	The indentation is taken on the matrix
c) 300	1.8168	6,412	3.206	The crack is not fixed	The indentation is taken on the matrix
d) 500	2.8475	8,452	4.226	The crack is not fixed	The indentation is taken on the matrix

3. CONCLUSION

The composite was synthesized in the Al_2O_3-SiAlON system via the method of metal-thermal and reactive sintering in the nitrogen medium. To obtain a dense material, the porous (13–15%) composite was hot pressed at 1650^0C after being grounded in an attritor, and further studies were performed using both micro- and macro mechanical as well as structural-optical, electron microscopic methods. The porous phase was studied, the percentage content and dimensions were determined, as well as the percentage content of crystalline constituents - SIALON, aluminum oxide - and grain sizes.

The results of the study showed that ß-SIALON was obtained with a silicon nitride structure. This was facilitated by the still newly formed imperfect

crystal lattice of silicon nitride at low temperatures, which, due to its relatively large void, takes in aluminum oxide, aluminum nitride, and then at relatively high temperatures, 1350–1450^{0}C, is formed in the ß-SIALON structure.

The obtained material is characterized by high-performance properties. The mechanics are 470 MPa for bending and 1923 MPa for compression. Micromechanical analysis showed that no cracks were formed in the SIALON matrix during the loading process.

The high properties of the composite were confirmed by calculating the mechanical modulus of Kovziridze, the obtained result exceeded expectations. According to this modulus, there is a real reason for the durability of materials against external loads. The material is obtained by solid phase sintering.

The composite has also been tested according to Kovziridze's formula - dependence of macro-mechanical properties on the content of the porous phase in the matrix.

Kovziridze's formula was also used to determine the micro and macro properties, depending on the crystalline phase content in the matrix. A high correlation (0.811) is obtained.

Acknowledgment

We express our gratitude to Shota Rustaveli Georgian National Science Foundation. The work is done with the grant of the Foundation FR-21-1413 Grant 2022.

REFERENCES

1. Ekstrom T., Kall P.O., Nygren M., Olsson P.O. - Dense Single-Phase Beta-Sialon Ceramics by Glass-Encapsulated Hot Isostatic Pressing. –J. of mat. Sci.- 1989. V.24. p. 1853-1862.
2. Rosenflanz A., I-Wei-Chen. - Phase Relationships and Stability of a-SiALON, -J.Am.Ceram. Soc. 1999. V.82. №4. P. 25-28.
3. Strelov K.K. Theoretical Foundations of the Refractory Materials Technology, textbook for universities/Strelov K.K., Kashcheev I.D. 2nd publication, 1996, p.608.
4. Chukholina, L.N. (2012) Method for Obtaining SiAlON Powder. http://bd.patent.su/2378000 last reviewed - 18. 11.2012.
5. Zhang G, Zhao J., Gao Z., Cao Q., - Cutting performance and wear mechanisms at Sialon-Si3N4 graded nano-composite ceramic cutting tools/ The International Journal of advanced Manufacturing Technology, 2012 V.58, I. 1-4. P. 19-28.
6. Tressler R. E. Theory and Experiment in Corrosion of Advanced Ceramics//Corrosion of Advanced Ceramics/ NATO ASI Series E: Applied Sciences/Ed. K.G.Nickel.-The Netherlands. 1994. N267. p. 3-22.
7. Piekarczyk J., Lis J., Bialoskorski J.- Elastic Properties, Hardness and Indentation Fracture Toughness of beta-Sialons/ Key Engineering Materials.- 1990. V. 89-91, p. 542-546.
8. Z. Kovziridze, N. Nijharadze, N. Darakhvelidze, G. Tabatadze, Z. Mestvirishvili.Carbon and Alum-thermal Processes in the Nitrogen Medium on the Base of Geopolymer.Georgian Ceramics Association Magazine "Ceramics", Vol. 16,N1(31), 2014, pg.32-36
9. Kovziridze Z., Nijaradze N., N. Darakhvelidze, Tabatadze G., Cheishvili T., Mestvirishvili Z.

Mshvildadze M., Nikoleishvili E. Obtaining Sialons byNitro-alum-thermal Processes, Georgian Ceramics Association Magazine "Ceramics", Vol.16 .N2(32), 2014, pg. 23-31.

10. Kovziridze Z., Nijaradze N., Tabatadze G., Cheishvili T.,MestviriSviliZ., Nikoleishvili E., Mshvildadze M., Daraxvelidze N.Obtaining of Nanocomposites in SiC-SiAlON and Al_2O_3-SiAlON System by Alumothermal Processes. Journal of Electronics Cooling and Thermal Control, 2014, 4, *Published Online December 2014 in SciRes. Pp.1- 13
http://www.scirp.org/journal/jectc
USA, DelawareImpact Factor
11. Kovziridze Z., Nijaradze N., Tabatadze G., Daraxvelidze N., MestviriSvili Z.Obtaining of SiAlONs via alum-thermal and nitrogen processes. 14th International Conference of European Ceramic Society, 21-25 June, Toledo, Spein. Poster 2348. 2015
12. Kovziridze Z., Nijaradze N., Tabatadze G., Daraxvelidze N., MestviriSvili Z.Smart Materials in the SiAlON-SiC-Al_2O_3 System. Journal of Material Science and Engineering, International Conference and Expo on Ceramics. August 17-18, 2015 Chicago, USA.
13. Kovziridze Z., Nijaradze N., Daraxvelidze N., Tabatadze G., MestviriSvili Z.Obtaining Sialon-Containing Composite by Nitroaluminothermal Processes, by Reactive Sintering and Hot Pressing. Georgian Ceramics Association Magazine "Ceramics", Vol.18. 1(35). 2016. 83. 9-19.
14. Kovziridze Z., Nijaradze N., Daraxvelidze N., Mestvirisvili Z. Smart Materials in the SiAlON-SiC-Al_2O_3-TiB_2-ZrB_2 System. 2ndAnnual world Congress of Smart Materials (WCSM-2016) 4-6 March, 2016, Singapore
15. Kovziridze Z., Nijaradze N., Daraxvelidze N., Tabatadze G., MestviriSvili Z., Nikoleishvili E., Mshvildadze M., Preparation of Composites by Nitro Aluminothermic Processes, over β–SiAlON Matrix in the SiAlON-SiC-Al_2O3 System. Journal of Electronics Cooling and Thermal Control, Vol.6 No.2, Pub. Date: June 15, 2016, PP. 62-77 Downloads-735. Views-887 (May 2017) Impact Factor.
16. Kovziridze Z., Nijaradze N., Daraxvelidze N., Tabatadze G., MestviriSvili Z.Obtaining of nano composites via alum-thermal and nitrogen processes in the SiC-Si_3N_4-ALN-AL_2O_3-SiO_2. System. 15th Conference&Exhibition of the European Ceramic Society, Ecers 2017, July 9-13,2017/Budapest, Hungary
17. Kovziridze Z., Nijaradze N., Daraxvelidze N., Tabatadze G., Cheishvili T., Mestvirishvili Z., Mshvildadze M. Obtaining the composite by metallothermal and Nitrogenation Processes in Si-SiC-Al Geopolymer Systems, Georgian Ceramics Association Magazine ""Ceramics and Advanced Technologies", V0l.19. 2(38). 2017. Pg. 33-52.
18. Kovziridze Z., Nijaradze N., Tabatadze G., Cheishvili T.,MestviriSvili Z., Mshvildadze M., Daraxvelidze N. Kinkladze V.Obtianing Of SiAlON Composite via Metal-Thermal and Nitrogen Processes in the SiC-Si-Al-Geopolymer System. Journal of Electronics Cooling and Thermal Control, 2017, 7, 103-122,
19. Kovziridze Z., Nijaradze N., Daraxvelidze N., Tabatadze G., MestviriSvili Z. Obtaining of

composite via metallo-thermal and Nitrogenization processes in the SiC-Si-Al-geopolymer System. 7th International Congress on Ceramics – ICC7, Foz de Iguaçu, PR, Brazil, June 17-21, 2018.

20. Kovziridze Z., Nijaradze N., Daraxvelidze N., Taba-tadze G., Balakhashvili M. Obtaining Sialon-Containing Composite in SiC-B4C-Si-Al-Al_2O_3 System by Reactive Sintering Method through Metallothermal and Nitrogenization Processes. Georgian Ceramics Association Magazine "Ceramics and Advanced Technologies", Vol.20. 2(40). 2018. pg.13-17.
21. Kovziridze Z., Nijaradze N., Daraxvelidze N., Taba-tadze G., Mestvirishvili Z.Study of the Phase Composition of Composites in the SiC-B4C-Si-Al-Al_2O_3 System. Georgian Ceramics Association Magazine ""Ceramics and Advanced Technologies",

Vol .21. 1(41). 2019. pg.44-51.

22. Z.Kovziridze, N.Nijaradze, N.Daraxvelidze, G.Tabatadze, Z.MestviriSvili, M.Balakhashvili, M.Mshvildadze. Obtaining of the Composite of β-SiAlON Matrix via Metal-Thermal and Nitrogen Processes in the B_4C-SiC-Al_2O_3-Si-Al-Carbon Fiber-Geopolymer. System. XVI ECERS Conference and Exhibition of the European Ceramic Society. Torino. Italy. 16-20 June 2019. P.680. Abstract Book
23. Kovziridze Z., Nijaradze N., Daraxvelidze N., Tabatadze G., MestviriSvili Z. Ceramic Composite in the SiC-SiAlON System. Euro Global Congress on Tychonix Nanotech. 2019 11-12 November. Valencia, Spain 2019.
24. Kovziridze Z., Nijaradze N., Daraxvelidze N., Tabatadze G., MestviriSvili Z.Composite in the SiC-Al_2O_3-BN-SiAlON System. 8th International Congress on Ceramics. August 23-28. Bexco. Busan. Korea.
25. Kovziridze Z.The Porous Phase Dependence Formula of Macromechanical characteristics. Journal of the Georgian Ceramists Association. "CeramicsandAdvancedTechnologies, Vol.20. 1(39). 2018. Pp.38-44. www.ceramics.gtu.ge
26. Kovziridze Z. D. Development of Scientific Basis and Technologies for the production of Celsianand Aluminosilicate CeramicsUsing Barite and Perlite.Dissertation for the degree of Doctor of Technical Sciences. Tbilisi 1993. pg. 41-50.
27. Kovziridze Z.The Formula of Dependence of Mechanical Characteristics of Materials on Crystalline Phase Composition in the Matrix. Advances in Materials Physics and Chemistry. Vol.10 No.8, August 2020.
    ISSN: 2331-1959.DOI: 10.4236/ampc.2020.108013.
28. Kovziridze Z. Formula of mechanical module of ceramic materials and compositions. Georgian National Intellectual Property Center "Saqpatenti" / Kovziridze Z. / Certificate 7136 2017/10/11.
29. Griffith A.A. Phil. Trans. Roy. Soc. London A221, 1920.

უაკ 666.762.93

Al_2O_3 ნანოფხვნილის გავლენის შესწავლა სიალონური კომპოზიტის თვისებებზე

ზ. კოვზირიძე, ნ. ნიჟარაძე. გ. ტაბატაძე, მ. მშვილ;დაძე, ნ. დარახველიძე

საქართველოს ტექნიკური უნივერსიტეტი. ბიონანოკერამიკისა და ნანოკომპოზიტების ტექნოლოგიის ინსტიტუტი. ბიონანოკერამიკისა და ნანოკომპოზიტების მასალათმცოდნეობის ცენტრი. კოსტავას 69. 0175 თბილისი საქართველო

E-MAIL: kowsiri@gtu.ge

რეზიუმე: მიზანი. SIAlON-Al2O3 სისტემაში კომპოზიტის მიღება და მისი თვისებების შესწავლა.

მეთოდი. კომპოზიტის მიღება მეტალოთერმული და აზოტირებული მეთოდებით. წინამდებარე ნაშრომში SIALON-ის შემცველი კომპოზიტი მიიღება ალუმოთერმული პროცესით, რეაქციული შეცხობის მეთოდით ტექნიკური აზოტის გარემოში, ალუმოსილიკატური ნედლეულის ნარევიდან (პროსიანაიას კაოლინი და პოლოგის ცეცხლგამძლე თიხა-უკრაინა), ალუმინის ოქსიდის ნანო ფხვნილი (გერმანიის კომპანია "ALCOA") და მეტალური სილიციუმი. მინისებური არაგაცის პერლიტის მცირე დანამატებით (სომხეთი). ამ მეთოდის უპირატესობა ის არის, რომ ალუმო- სილიკატური ნედლეული იშლება თერმული დამუშავების პროცესში და ერთდროულად მიმდინარეობს ალუმოთერმული-ნიტრირების პროცესი, რაც აადვილებს ALN და AL_2O_3 გახსნას ახლად წარმოქმნილ β-SI_3N_4-ს კრისტალურ გისოსში, რომელიც უზრუნველყოფს β-სიალონის წარმოქმნას შედარებით დაბალ 1250-1300^{0}C ტემპერატურაზე.

შედეგი. კორუნდი-SIALON კომპოზიციური მასალა მიიღება რეაქციული აგლომერაციის პროცესით 1450^{0}C ტემპერატურაზე. კორუნდის და SIALON ფაზების არსებობა კომპოზიტში დასტურდება რენტგენოსტრუქტურული ფაზური, სპექტრული და ელექტრონულ-მიკროსკოპული ანალიზით. კონსოლიდირებული მასალების მისაღებად რეაქციული შეცხობით მიღებული მასალა გადაიფქვა ატრიტორში და ცხლად დაიწნეხა 30 მპა წნევით, 30 წუთის განმავლობაში 1620^{0}C ტემპერატურაზე. დაყოვნება საბოლოო ტემპერატურაზე - 7 წუთი. გაცივება თავისუფალ რეჟიმში. მიღებული ნიმუშების ფაზური შედგენილობა უცვლელი დარჩა ცხელი წნეხვის შემდეგ, გაიზარდა სიმკვრივე და ღია ფორიანობა შემცირდა და გახდა ნაკლები 1%-ზე.

შესაბამისად გაიზარდა მექანიკური თვისებების რიცხვითი მნიშვნელობები: σკ. -1923 მპა; σღ. -470 მპა; HV-19.7 GPa.

დასკვნა. მიღებულია კომპოზიტი Al_2O_3-SIALON სისტემაში მაღალი ფიზიკურ-ტექნიკური საექსპლოატაციო თვისებებით: ფორიანობა-0.1%; სიმკვრივე -3,21გ/სმ^3; σკ. - 1923 მპა; σღ. -470 მპა; HV-19.7 GPa, ელასტიურობის მოდული -22 GPa; მიკროსისალე-3214 N/mm^2; ქიმიური მედეგობა გოგირდმჟავას მიმართ (სიმკვრივე 1,84) -99,3%, წყლის მიმართ -99,9%.

მიღებული მასალები შეიძლება რეკომენდირებული იყოს ჯავშანტექნიკაში, მაღალტემპერატურულ ღუმელებში თერმოწყვილის დამცავი გარსაცმებისათვის გამღვალი ლითონების ტემპერატურის გასაზომად, ასევე სუფთა დამუშავების ოპერაციებში, როგორც ლითონის დამუშავების მჭრელი მასალა.

საკვანძო სიტყვები: β-SIALON; კორუნდი; რეაქციული შეცხობა; კომპოზიციური; თვისებები.

DOI https://doi.org/10.36073/2960-9534

THE GEORGIAN CERAMISTS ASSOCIATION JOINED THE INTERATIONAL CERAMIC FEDERATION SINCE 2008

THE GEORGIAN CERAMISTS ASSOCIATION HAS BEEN A MEMBER OF THE EUROPEAN CERAMIC SOCIETY SINCE 2002

THE GEORGIAN CERAMIC ASSOCIATION WAS FOUNDED IN 1998
THE MAGAZINE WAS FOUNDED IN 1998

TBILISI, "INTERNATIONAL JOURNAL OF CERAMICS, COMPOSITES, SCIENCE AND ADVANCED TECHNOLOGIES", Vol. 26. 1(51). 2024

Reference of magazine is obligatory on reprinting

Print circulation 5. Contract amount 50. Printed A4 format.

GEORGIAN CERAMISTS ASSOCIATION. Tbilisi. Str. Kostava 69. Phone: +995 599 151957
E-mail: kowsiri@gtu.ge, Zviad Kovziridze

http://ceramics.gtu.ge